PHDG

Professor Heinemanns
Doktorandengruppe
Verein zur Förderung
von wissenschaftlichen Arbeiten
in Reservoircharakterisierung und -simulation

TEXTBOOK SERIES

VOLUME 1

FLUID FLOW IN POROUS MEDIA

by

Zoltán E. HEINEMANN
Professor for Reservoir Engineering
Leoben, October 2005

actualized
by
Dr. Georg Mittermeir
Tehran, February 2013

For kind Attention

The Textbook series of the PHDG is an aid for PhD students accepted by the Association or those applying for support from it. These scripts have the objective to stabilize and homogenize the knowledge of the candidates, not necessarily studied petroleum engineering and originating from different countries and universities.

The textbooks are subject to continuous update and improvement. PHDG suggests to download them in yearly sequence. In some cases they are provided on different levels of knowledge making it easier to enter the subjects. Therefore there is also some overlapping between the volumes. It is expected that the users will suggest improvements for both, the contents and the formulations.

PHDG's Textbooks available at 1.1.2015:

1. Fluid Flow in Porous Medium
2. Well Testing
3. Systematic of the Reservoir Flow Equations
4. Introduction to Reservoir Simulation
5. Natural Fractured Reservoir Engineering

***PHDG Textbooks in preparation, intended to be issued during 2015*:**

1. Discretization and Gridding in Reservoir Simulation
2. Advanced Reservoir Simulation
3. Reservoir Fluid Characterisation

Supplementary scripts *used at the Montanuniversität up to the retirement of Professor Zoltán E. Heinemann in July 2006.*

1. Reservoir Fluids
2. Petroleum Recovery

Table of Contents

List of Figures

1 Fundamental Properties of Porous Media

A porous medium is a solid containing void spaces (pores), either connected or unconnected, dispersed within it in either a regular or random manner. These so called pores may contain a variety of fluids such as air, water, oil etc. If the pores represent a certain portion of the bulk volume, a complex network can be formed which is able to carry fluids. Only these permeable and porous media are taken into consideration in this volume.

Various examples can be named where porous media play an important role or where the technology requires them as a tool.

- In Soil Science:
  The porous medium (soil) contains and transports water and nutrients to plants.

- In Hydrology:
  The porous medium is a water bearing and sealing layer.

- In Chemical Engineering:
  Porous medium is applied as filter or catalyst bed.

- In **Petroleum Engineering**:
  Porous medium (reservoir rock) stores crude oil and natural gas.

1.1 Porosity

1.1.1 General Aspects and Definition

Basically two groups of porous media can be distinguished:

- intergranular-intragranular
- fractured.

Materials having both, fractured and intergranular porosity, are called dual (double) porous media. On the other hand, concerning the mechanical properties, one should distinguish between:

- consolidated
- unconsolidated

porous media. In a consolidated porous medium the particles (grains) are held together by a cementing material, in an unconsolidated porous medium the grains are loose. A typical characteristic of a consolidated medium is the possibility to form shape-retaining samples.

Definition of Porosity

The porosity of porous media is defined as the ratio of the volume of the pores to the total bulk volume of the media (usually expressed as fraction or percent). Let us select any point of the porous media and its environment with a sufficiently large volume V_T, where:

$$V_T = V_p + V_s \quad , \tag{1.1}$$

where

V_p is the void volume (pore volume) and

V_s is the volume of the solid material.

Porosity is defined as the ratio of pore volume to total volume, which can be expressed as:

$$\phi = \frac{V_p}{V_T} = \frac{V_T - V_s}{V_T} . \tag{1.2}$$

Basically one must distinguish between two kinds of porosities:

- Total porosity (isolated pores are considered also) and
- Effective porosity ϕ_{eff} (effective in the sense of fluid transport).

The storage capacity of a reservoir rock always depends on the effective porosity, since it contains the reservoir fluids.

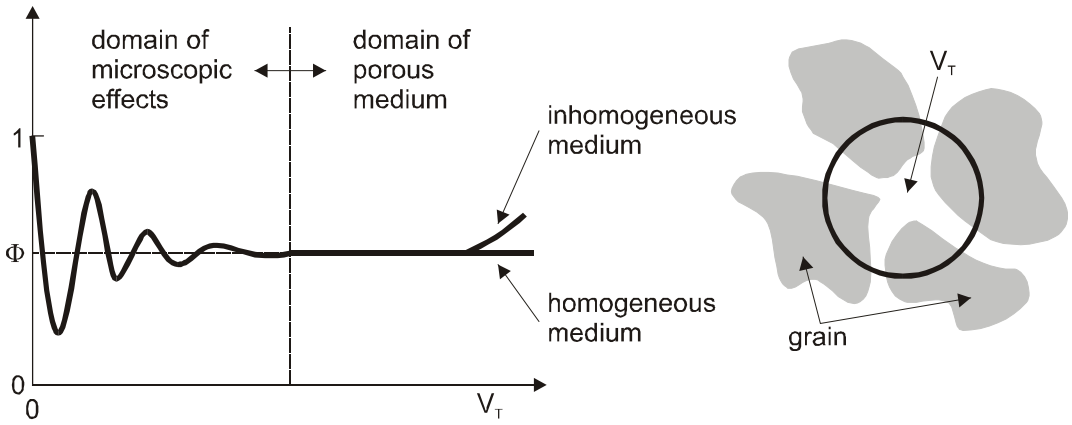

Figure 1.1: Definition of representative control volume for porosity measurements

Porosity is a statistical quantity which depends on the magnitude of the total volume taken into consideration (see Figure 1.1). If the selected volume is too small (e.g.: $V_T = 10^{-9}m^3$) the calculated porosity can deviate greatly from the true value, therefore the volume V_T should be large enough in order to obtain the statistical average of porosity.

On the other side if the volume is too large the porosity may deviate from the real value due to the influence of heterogeneity.

1.1.2 Determination of Porosity

The determination of the porosity with sufficient accuracy is not a trivial issue, especially for small samples. If the errors in measuring V_T and V_P are ΔV_T and ΔV_P then Eq. 1.2 will lead to:

$$\frac{\Delta\phi}{\phi} = \frac{\Delta V_p}{V_p} + \frac{\Delta V_T}{V_T} \tag{1.3}$$

where $\Delta\phi$ is the error in calculating the porosity.

Assuming that $\Delta V_p = \Delta V_T = \Delta V$ Eq. 1.3 can be written as:

$$\frac{\Delta\phi}{\phi} = \frac{\Delta V}{V_T}\left(1+\frac{1}{\phi}\right) . \tag{1.4}$$

According to Eq. 1.4, the relative error of the porosity measurement depends on V_T and ϕ. Assuming an error $\Delta V=10^{-9}$ m^3 for the values of V, this error can be up to 50% as shown in Table 1.1.

Table 1.1: Relative errors in measuring porosity $(\Delta V_T = \pm 10^{-9}[m^3])$

ϕ[%]	1	4	12	20
$V_T[m^3]$				
2.10^{-9}	50.50	13.00	4.25	3.00
4	25.20	6.50	2.10	1.50
8	12.60	3.25	1.10	0.70
16	6.30	1.60	0.50	0.37
32	0.30	0.80	0.26	0.18
64	0.16	0.40	0.13	0.09

The following quantities are necessary in order to calculate the porosity based on Eq. 1.2:

- the total volume (V_T),
- the solid volume (V_s),
- the void volume (V_p).

Example 1.1:

*A core plug has a radius of 1.25*10^{-2} [m] and a length of 5.0*10^{-2} [m]. It is completely saturated with brine having a density of 1200 [kg/m^3]. The dry core plug weighted 5.1*10^{-3} [kg], and 10.4*10^{-3} [kg] when it was saturated with brine. Calculate the effective porosity of the core plug.*

Solution:

Weight of brine in the plug $\quad w = 10.4\times10^{-3} - 5.1\times10^{-3} = 5.3\times10^{-3}[kg]$

Volume of brine (pore volume) $\quad V_p = \frac{w}{\rho_w} = \frac{5.3\times10^{-3}}{1.2\times10^{3}} = 4.42\times10^{-6}[m^3]$

Bulk Volume of plug $V_T = r^2 \pi h = 24.5 \times 10^{-6} [m^3]$

Porosity of plug $\phi = \frac{V_p}{V_T} = 18[\%]$

1.1.3 Compaction

Figure 1.2 shows porous media built with spheres of equal size. The spheres are arranged in three different ways to illustrate the effect of compaction on the porosity of a pack. However, no characteristic factor has been introduced yet to describe the compaction as a property.

Compaction - and thus porosity - of a sediment depends on the greatest depth a rock reached during its genesis. Figure 1.3 shows the porosity of clay and sandstone as a function of depth. The compaction - in contrast to the compressibility - is irreversible.

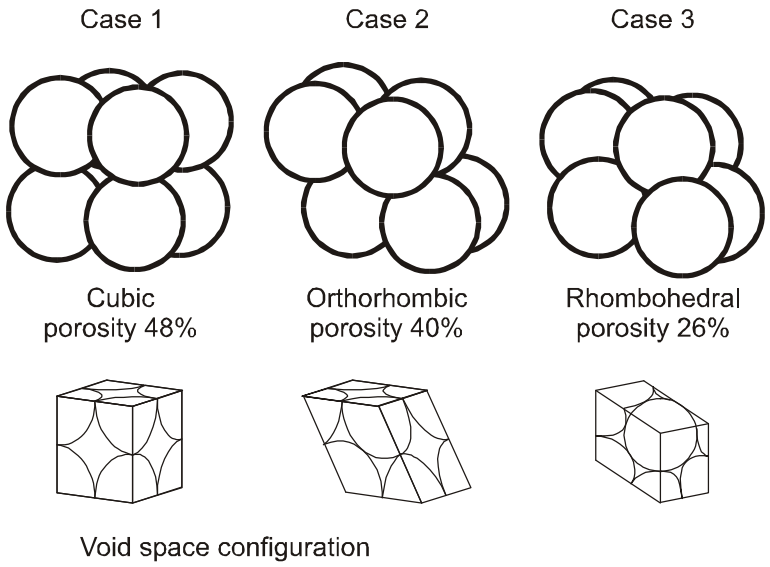

Figure 1.2: Packing of spheres and porosity (after *P.K.Link*[1.12])

1.1.4 Compressibility of Porous Media

Reservoir rock is not considered to be a rigid system but as a - only minor though - elastic and thus compressible medium. Change of pressure inside the pore space during production also affects the porosity.

The isothermal compressibility of porosity is defined as:

$$c_\phi = \frac{1}{\phi}\left(\frac{\partial \phi}{\partial p}\right)_T . \tag{1.5}$$

Integration of the preceding equation leads to:

$$\phi = \phi_0 e^{c_\phi (p - p_0)} \approx \phi_0 [1 + c_\phi (p - p_0)] . \tag{1.6}$$

where ϕ_0 is the porosity at the pressure p_0.

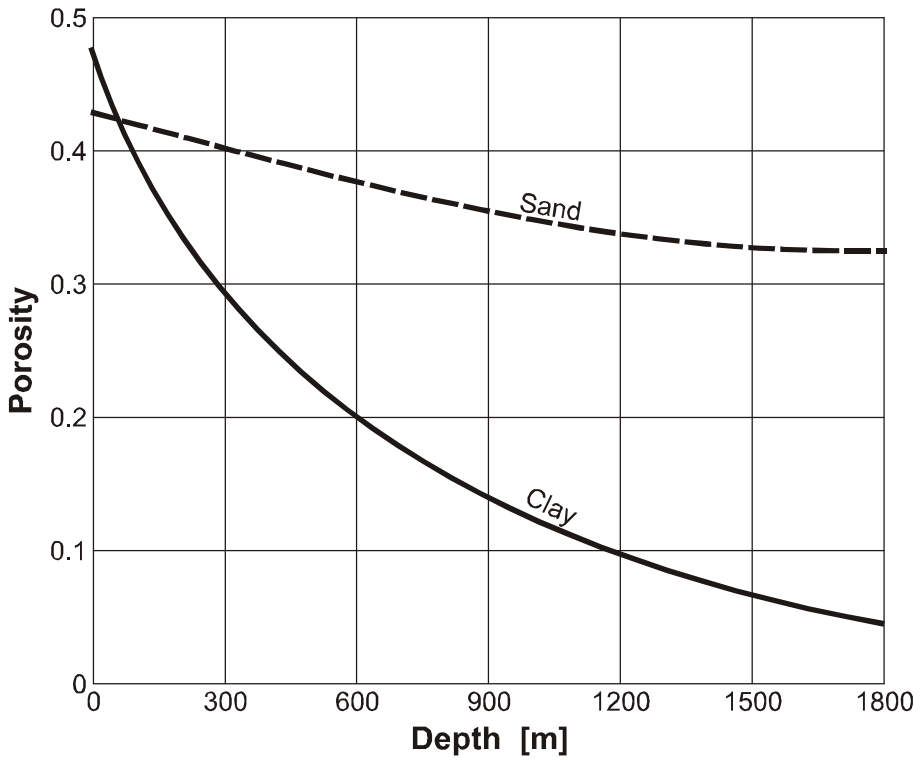

Figure 1.3: Sediment compaction and porosity (from *Krumberlain* and *Sloss*[1.9])

However, c_ϕ is small and normally regarded as a constant. The pore volume alteration during the pressure drop in the reservoir has its source in the elasticity of the solid. Therefore c_ϕ will be a function of porosity. Figure 1.4 illustrates this relation.

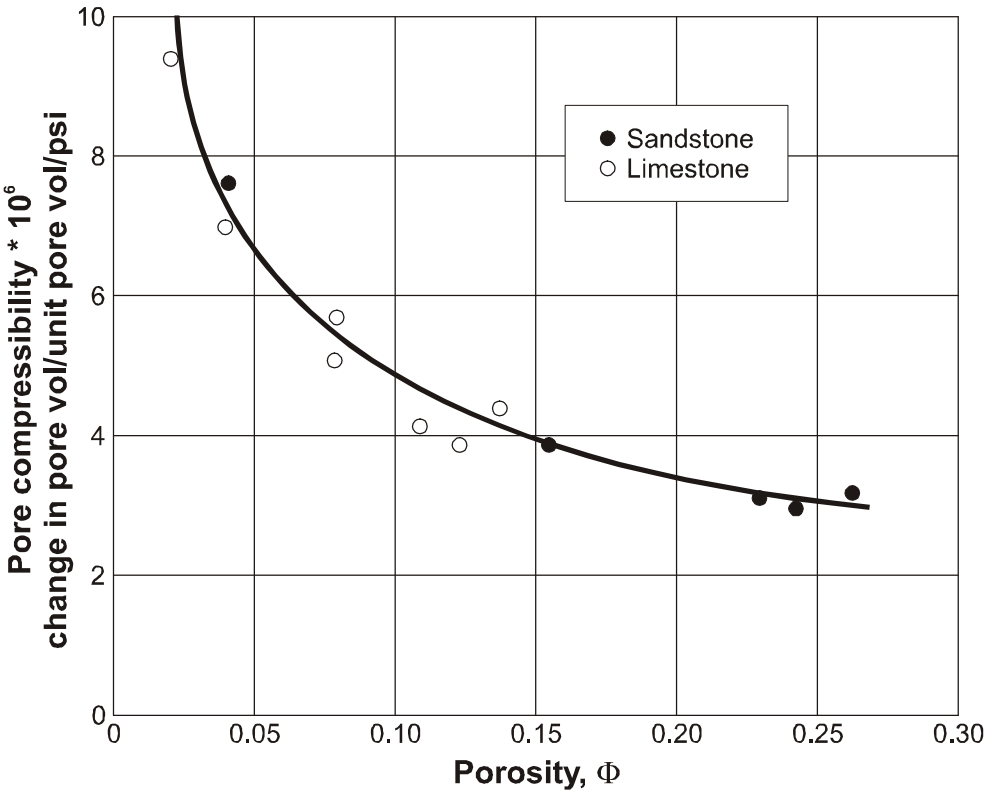

Figure 1.4: Pore compressibilities of rocks (after *H.N.Hall*[1.7])

The compressibility of the pore space is influenced by overburden pressure too, which is illustrated in Figure 1.5.

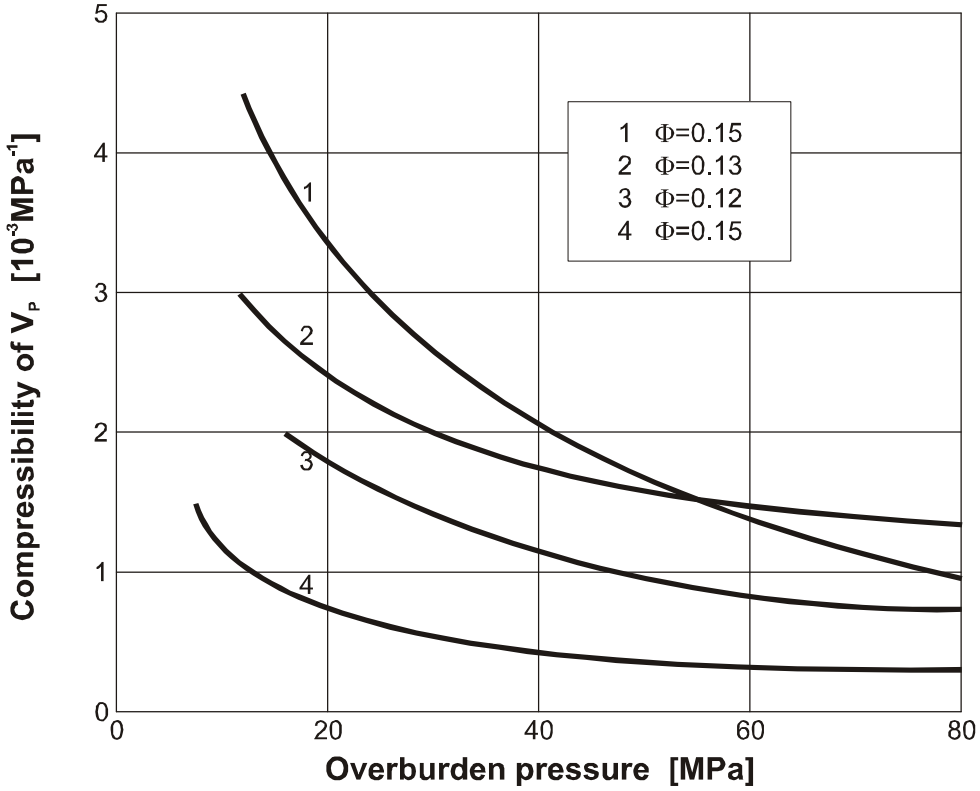

Figure 1.5: Pore volume compressibility factor in terms of overburden pressure (after *I.Fatt*[1.6])

1.1.5 Classification of Porosity

Porosity can be classified as primary or secondary. Primary porosity forms during deposition of sediments and includes interparticle and intraparticle porosities. Secondary porosity forms after deposition and develops during diagenesis by dissolution, dolomitization and through production of fractures in the rock.

Intergranular porosity (also interparticle porosity) is formed between grains during deposition and is the amount of pore space between grains or particles. Intraparticle porosity occurs within individual particles or grains. It is abundant in carbonate sediments and can be an important part of the preserved porosity in carbonate rocks. Internal chambers or other openings within individual or colonial skeletal organisms are the most commonly recognized form of intraparticle pores.

One can distinguish between fabric and non-fabric selective porosity. Fabric selective porosity includes primary (interparticle and intraparticle porosity) and secondary (e.g. intercrystalline or moldic porosity). Secondary non-fabric selective porosity includes vuggy porosity and fracture porosity.

Intercrystalline porosity occurs between crystals of similar size and is restricted to crystals

that have grown in place, for example dolomites, evaporates and recrystallized carbonates. The sizes of pores is generally controlled by the size of crystals. Intercrystalline porosity may either be primary or secondary in origin.

Vuggy porosity is a non-fabric selective porosity caused by selective removal (solution) of grains in a rock. Depending on the extent of solution, the resulting pores are classified as molds, solution enlarged molds or vugs. Recovery efficiency in reservoirs with moldic porosity is strongly controlled by the size and number of connections between the molds.

Fracture porosity generally refers to porosity that occurs along breaks in a sediment or rock body where there has been little mutual displacement along the fracture. Natural fractures occur in all subsurface formations. Fracture porosity grades into breccia porosity with increasing dislocation. In carbonate rocks, fracture porosity may originate from collapse related to solution, slumping, or tectonic deformation.

Fractures can be observed on cores, and can be characterized as filled, semi-filled and open fractures. Filled fractures do not contribute to the porosity. The fractures are described by their orientation as horizontal, vertical or oblique fractures.

1.2 Capillary Properties

1.2.1 Saturation

Basically pore space may contain several phases. The saturation of a certain phase is defined as:

$$S_i = \frac{\text{Volume of phase i in the porous media}}{\text{Effective pore volume of the porous media}}. \tag{1.7}$$

Summation of the saturations results in:

$$\sum_i S_i = 1 . \tag{1.8}$$

1.2.2 Wettability

Wettability of a reservoir-rock fluid system is the ability of one fluid in the presence of another to spread on the surface of the rock. Wettability plays an important role in the production of oil and gas as it not only determines the initial fluid distributions, but also it is a major factor in the flow processes in the reservoir rock. The degree of wetting of solids by liquids is usually measured by the contact angle that a liquid-liquid interface makes with a solid.

A fluid drop on a plane solid surface can take various shapes. The respective shape (either flat or shaped like a pearl) depends on the wettability of the considered solid. Figure 1.6 illustrates that property. In case of air and water the water is the wetting phase, for air and mercury the air is the wetting fluid.

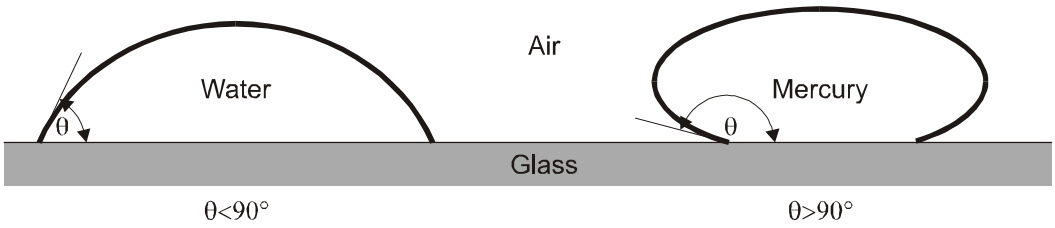

Figure 1.6: Comparison of wetting to non-wetting fluid

The contact angle is used as a measure of wettability. In the case of a wetting fluid, the contact angle is smaller than 90°. If the contact angle is larger than 90°, then the fluid is referred to as non-wetting.

150 years ago *Young* defined the contact angle as a consequence of the static equilibrium, between a drop of liquid and a plane of a solid surface. The drop of liquid will take a certain shape due to the interfacial tensions acting on it, which are:

σ_{12} the interfacial tension between fluid 1 and 2,

σ_{s1} and σ_{s2} the interfacial tensions between solid and fluids.

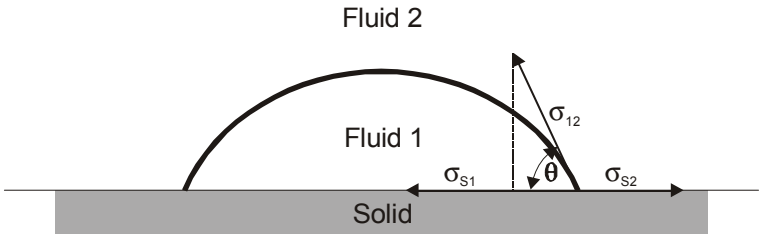

Figure 1.7: Definition of the contact angle by *Young*

From Figure 1.7, Eq. 1.9 and Eq. 1.10 will result:

$$\cos\theta = \frac{\sigma_{s2} - \sigma_{s1}}{\sigma_{12}} \tag{1.9}$$

$$\sigma_{s1} + \sigma_{12}\cos\theta = \sigma_{s2} \tag{1.10}$$

Interfacial tensions σ, and thus θ, are regarded as temperature-dependent. At room temperature the interfacial tension between water and air is 0.073 [N/m] and between oil and water about [0.03 N/m].

1.2.2.1 Classification of Reservoir Rocks based on Wettability

The wettability of a reservoir rock system depends on many factors:

- reservoir rock material
- pore geometry
- geological mechanisms
- composition and amount of oil and brine
- pressure and temperature
- changes in saturation, pressure and composition during production.

When regarding oil reservoirs it is necessary to consider the specific rock and fluid properties in order to determine whether the reservoir rock is *water* or *oil wet*. Rocks which are neither water nor oil wet al called *intermediate or neutral wet*. The data published by Treiber *et al.*[1.19] (Table 1.2) show that most of the carbonate reservoirs are oil wet, while the sandstone reservoirs can be equally water or oil wet.

Table 1.2: Reservoir wettability based on contact angle messurements (after Treiber *et al.*[1.19])

Wettability	Contact Angle [°]	Number of Reservoir Investigated		
		Sand	Carbonate	Total
water wet	0-75	13	2	15
intermediate wet	75-105	2	1	3
oil wet	105-180	15	22	37

The internal surface of reservoir rock is composed of many minerals with different surface chemistry and adsorption properties, which may lead to variations in wettability. The concept of *fractional wettability,* also called heterogeneous or *spotted wettability*, was proposed by many authors. Note that the fractional wettability conceptually differes from the intermediate wettability, which assumes that all portions of the rock surface have a slight but equal preference to being wetted by water or oil.

Mixed wettability is a special type of fractional wettability in where the oil-wet surface forms continuous paths through the larger pores. The smaller pores remain water-wet and contain no oil. *Salathiel* explained the situation when oil invades an originally water-wet reservoir it displaces water from the larger pores, while the smaller pores remain water-filled. A mixed-wettability condition occurs if in the oil deposits a film of oil-wet organic material only on those solid surfaces that are in direct contact with the oil but not on the surfaces covered by water.

1.2.2.2 Measurement of Wettability

The wettability measured in the laboratory strongly depends on the core handling. To obtain representative information on the wetting preferences in the reservoir from laboratory experiments the following conditions should be fulfilled:

- surface properties of the rock should be preserved,
- method should enable differentiation of the entire range of wettability,
- result should not depend on rock permeability and fluid viscosity,
- result should be reproducible.

Cores in three different states of preservation are used in core analysis:

- native state,
- cleaned state and
- restored state.

The term *native-state* is used for any core that was obtained and stored by methods that preserve the wettability of the reservoir. The best way is to drill the core with a suitable

oil-filtrate-type drilling mud, which maintains the original connate water saturation. The original wettability can also be maintained using a water-based drilling mud that contains no compounds that can alter core wettability.

From a *cleaned core* all original and infiltrated fluids were removed. Cleaned cores are usually strongly water-wet and should only be used for measurements such as porosity and gas permeability where the wettability will not affect the results.

The third type of core is the *restored-state* core. In this case the native wettability is restored by a three-step process. The core is cleaned and then saturated with brine, followed by crude oil. Finally the core is aged at reservoir temperature for about 1000 hours.

Native-state cores yield the best results for multi-phase properties (wettability, capillary pressure, relative permeabilities) because alterations of the wettability of the undisturbed reservoir rock are minimized.

Different methods have been used for the categorization of the wettability. A detailed discussion of all methods has been published by *Anderson*[1.2,1.3]. Two groups of methods are distinguished:

1. *Quantitative methods:*

    • determination of the contact angle
    • Amott
    • Amott-Harvey
    • USBM wettability indices (centrifuge method)

2. *Qualitative methods*:

    • imbibition rate
    • microscopic examination
    • capillary pressure curves
    • relative permeability/saturation relationship

Unfortunately none of the methods is generally accepted which leads to ambiguities while comparing data from different sources and from different dates. Many wettability measurements are also imprecise, particularly near neutral wettability, therefore one should be cautious using literature data and conclusions.

1.2.2.2.1 Contact Angle Measurement

The contact angle measurement is based on the principles demonstrated in Figure 1.7 and is called sessible drop method. The basic method uses a single polished mineral crystal. *Leach at al.*[1.10] modified the sessile drop method using two crystal plates. The oil drop is placed between the two crystal plates so that it contacts a large area of each plate.

Sandstones are composed primary of quartz and limestones of calcite, therefore quartz or calcite crystals can be used to simulate the pore surfaces of the reservoir rock. Obviously, the wettability of clays in the reservoir cannot examined with this method.

1.2.2.2.2 Amott Method[1.19]

The Amott method combines imbibition and forced displacement to measure the average wettability of a core. Both reservoir core and fluids can be used in the test.

A core sample is chosen and saturated with oil. The oil sample is then placed in an imbibition cell surrounded by water. The water is allowed to imbibe into the core sample displacing oil out of the sample until equilibrium is reached. The volume of water imbibed is measured after 20 hours.

Afterwards the core sample is removed and the remaining oil in the sample is forced down to residual saturation by displacement with water. This could be achieved by centrifuging under brine. The volume of oil displaced is measured directly or by weight measurements.

The core, which is now saturated with water, is placed in an imbibition cell and surrounded by oil. The oil is allowed to imbibe into the core displacing water out of the sample. The volume of water displaced is measured (equal to the volume of oil imbibed). after 20 hours. After equilibrium is reached the core is removed from the cell and the remaining water is forced out by displacement in a centrifuge.

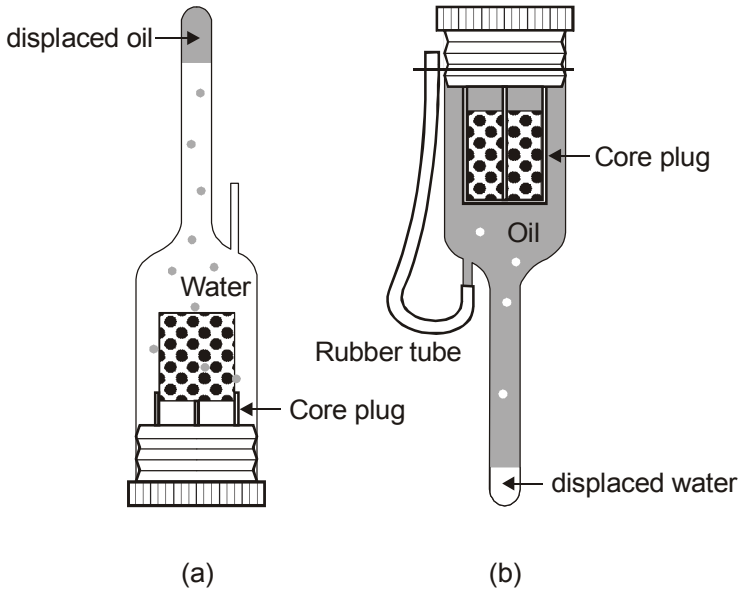

Figure 1.8: Imbibition cell with oil saturated sample surrounded by water (a), water saturated core sample surrounded by oil (b) (after *Torsaeter*[1.20])

The results are expressed by the displacement-with-oil-ratio:

$$\delta_O = \text{displacement-with-oil-ratio} = \frac{\text{spontaneous displaced water}}{\text{total displaced water}} \tag{1.11}$$

and the displacement-with-water-ratio:

$$\delta_W = \text{displacement-with -water -ratio} = \frac{\text{spontaneous displaced oil}}{\text{total displaced oil}} \tag{1.12}$$

δ_W approaches 1 as the water wetness increases. Similarly, oil wet cores manifest $\delta_O \to 1$ and $\delta_w = 0$. Both ratios are zero for neutrally wet cores. *Amott* chose an arbitrary time of 20 hours for the spontaneous oil and water imbibition steps. The period of time for imbibition to take place could last from several hours up to months. If the imibition is stopped after a short period of time, then the measured spontaneous imbibition volume will be lower than the equilibrium value for low permeability samples. This results in underestimation of δ_W and δ_O. The main shortcoming of the *Amott* wettability test and its modifications is that they are insensitive near neutral wettability.

The *Amott-Harvey* relative displacement index combines the two ratios into a single wettability index that varies from +1 for complete water wetness to -1 for complete oil wetness. Recording all volumes during the measurement allows to calculate the wettability index *WI*:

$$WI = \frac{V_{O1}}{V_{O1} + V_{O2}} - \frac{V_{W1}}{V_{W1} - V_{W2}} = \delta_W - \delta_O \tag{1.13}$$

where

V_{O1}.....volume of oil produced during water imbibtion

V_{O2}.....volume of oil produced during water flooding

V_{W1}.....volume of water produced during oil "imbibition"

V_{W2}.....volume of water produced during oil flooding

The system is regarded as water wet when $0.3 \le WI \le 1$, intermediate wet when $-0.3 < WI < 0.3$, and oil-wet when $-1 \le WI < -0.3$.

1.2.2.2.3 USBM Wettability Index

The USBM (U.S. Bureau of Mines) method is a test developed by *Donaldson*[1.5].

It is based on measuring two capillary pressure curves:

1. Displacement of the oil by brine, starting at the irreducible water saturation and end up with the residual oil saturation

2. Displacement of oil in the reverse direction.

The capillary pressure will defined in Section 1.2.3 therefore switch there at the first read and return afterwards.

The USBM test compares the work necessary for one fluid to displace the other. The work required for the wetting fluid to displace the non-wetting fluid from the core is less than the work required in the opposite direction. The work required is proportional to the area under the capillary pressure curve. In other words, when a core is water-wet, the area under the brine-drive capillary pressure curve (when the water displaces the oil) is smaller than the area under the capillary pressure curve for the reverse displacement.

Before the test is run the plug is prepared be centrifugation under oil at high speed to achieved irreducible water saturation (maximum oil saturation). In the first step of the measurement the core is placed in brine and centrifuged at incrementally increasing speeds until a capillary pressure of -10 psi. This step is called the brine drive because brine displaces oil from the core. At each incremental capillary pressure the average saturation of the plug is calculated from the volume of expelled oil.

In the second step the core is placed in oil and centrifuged. During this oil drive step oil displaces brine from the core. The capillary pressures and average saturations are measured until a capillary pressure of 10 psi is reached.

The USBM method uses the ratio of areas under the two capillary pressure curves to calculate a wettability index:

$$W = \log\left(\frac{A_1}{A_2}\right) \tag{1.14}$$

where A_1 and A_2 are the areas under the oil- and brine-drive curves, respectively. Examples of water-wet, oil-wet and intermediate-wet are shown in Figure 1.9.

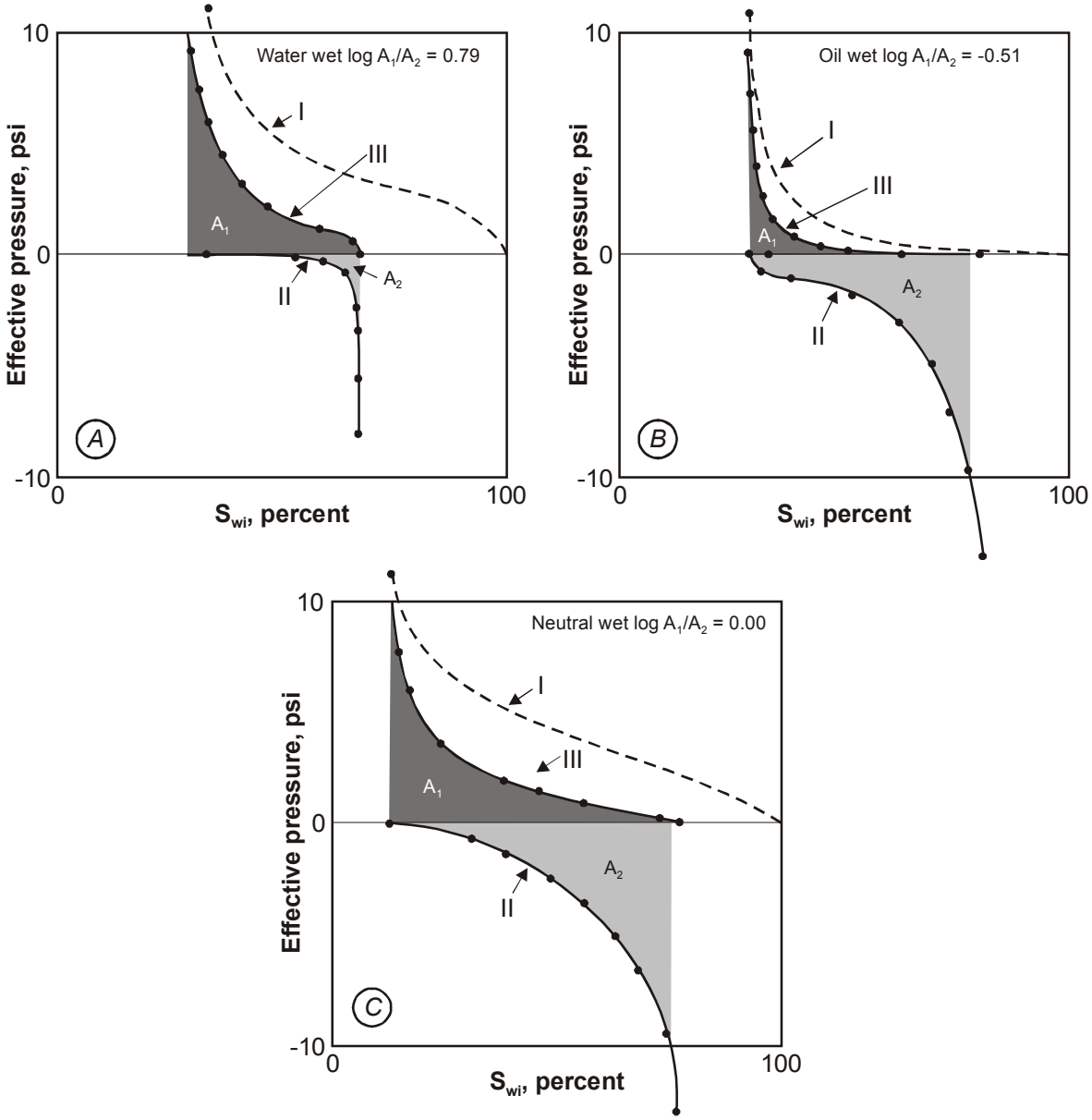

Figure 1.9: USBM wettability measurement on water-wet, oil-wet and intermediate-wet core samples (after *Donaldson at al.*[1.5] and *Anderson*[1.3])

Table 1.3: Approximate relationship between contact angle, USBM and Amott wettability indexes (after Anderson[1.3])

	water wet	neutrally wet	oil wet
Contact angle Minimum Maximum	 0° 60 to 75°	 60 to 75° 105 to 120°	 105 to 120° 180°
USBM wettability index	W near 1	W near 0	W near -1
Amott wettability index Displacement-by-water ratio Displacement-by-oil ratio	 Positive Zero	 Zero Zero	 Zero Positive
Amott-Harvey wettability index	$0.3 \le I \le 1.0$	$-(0.3 < I < 0.3)$	$-(1.0 \le I \le -0.3)$

The USBM test is a relatively rapid measurement and measures, similar to the *Amott* test, the average wettability of the core. Its major advantage over the Amott method is the sensitivity near neutral wettability. A minor disadvantage is that the USBM wettability index can only be measured on plug-size samples because the samples must be spun in a centrifuge. Additionally the USBM test cannot determine wheter a system has fractional or mixed wettability, while the *Amott* test is sometimes sensitive.

In many cases none of the wettability indices are available and the wettability will be characterized by one or more qualitative methods: microscopic examination, imbibition rates, relative permeability curves, permeability/saturation relationships, capillary pressure curves, etc. The most commonly used qualitative wettability measurement is the imbibition method because it gives a quick but rough idea of the wettability without requiring any complicated equipment. Some values used for characterization are given in Table 1.4.

Table 1.4: Properties characterizing the wettability

Parameter	water wet	oil wet
S_{wir}	>0.2	<0.15
S_w at $k_{rw}=k_{ro}$	>0.5	<0.5
k_{rw} at $1-S_{or}$	<0.3	>0.5

1.2.3 Capillary Pressure

1.2.3.1 Definition

For any two immiscible fluids (e.g. oil and water), the pressures at both sides of the fluid interface are not equal. This pressure difference, called capillary pressure P_c, can be calculate by the *Laplace* equation:

$$P_c = \sigma_{12}\left(\frac{1}{r_1} + \frac{1}{r_2}\right) = p_{nw} - p_w \tag{1.15}$$

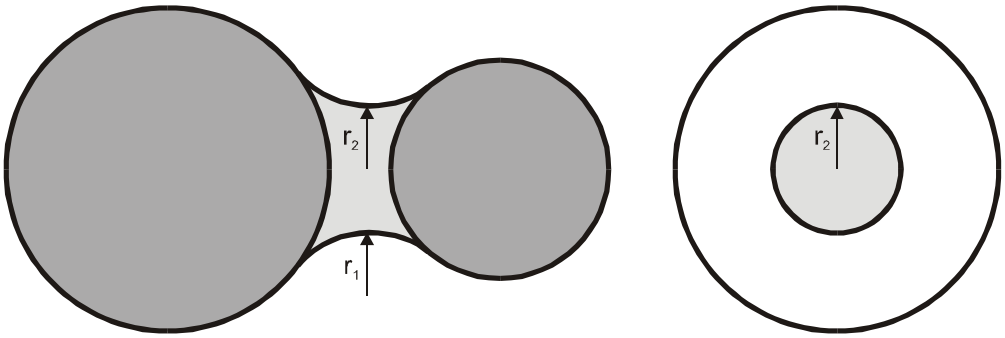

Figure 1.10: Illustration of the principal radii of the curvatures

Figure 1.10 illustrates the principle curvatures radii r_1 and r_2 which are elements of the *Laplace* equation.

If a porous medium is completely (100%) saturated with the non-wetting Fluid 2 and contacted by the wetting Fluid 1, then Fluid 1 spontaneously intrudes into the pore space. Fluid 1 will displace Fluid 2, until equilibrium is achieved. This is called *imbibition*. Equilibrium is achieved when Fluid 1 uniformly occupies the pore spaces with greatest possible interfacial curvature.

Thus, in the case of imbibition, Fluid 1 will occupy the smaller pore spaces first. In order to illustrate this capillary equilibrium in a simplified manner, one could imagine the porous medium as a bundle of infinitely long glass rods with uniform radius R (Figure 1.11).

If air is the non-wetting and water is the wetting fluid, then $\sigma_{s2} = 0$ and thus $\sigma_{s1} = \sigma_{12}$ and $\cos\theta = 1$.

Since one of the two principle radii of curvature (r_2) is infinite, it is easy to calculate the porosity and water saturation of the wetting fluid as follows:

$$\phi = 1 - \frac{\pi}{4} \tag{1.16}$$

and the water saturation can be calculated from:

$$S_1 = \frac{4}{4-\pi}\left[\sqrt{\left(\frac{r}{R}\right)^2 + 2\left(\frac{r}{R}\right)} - \operatorname{acos}\left(\frac{R}{r+R}\right) - \left(\frac{r}{R}\right)^2 \operatorname{asin}\left(\frac{R}{r+R}\right)\right]. \tag{1.17}$$

Based on the geometry of the cylindrical rods Figure 1.11 the capillary pressure can be calculated from Eq. 1.15 as:

$$P_c = \frac{\sigma_{12}}{r} \tag{1.18}$$

where $r = r_1$ which is the radius of the water air interface.

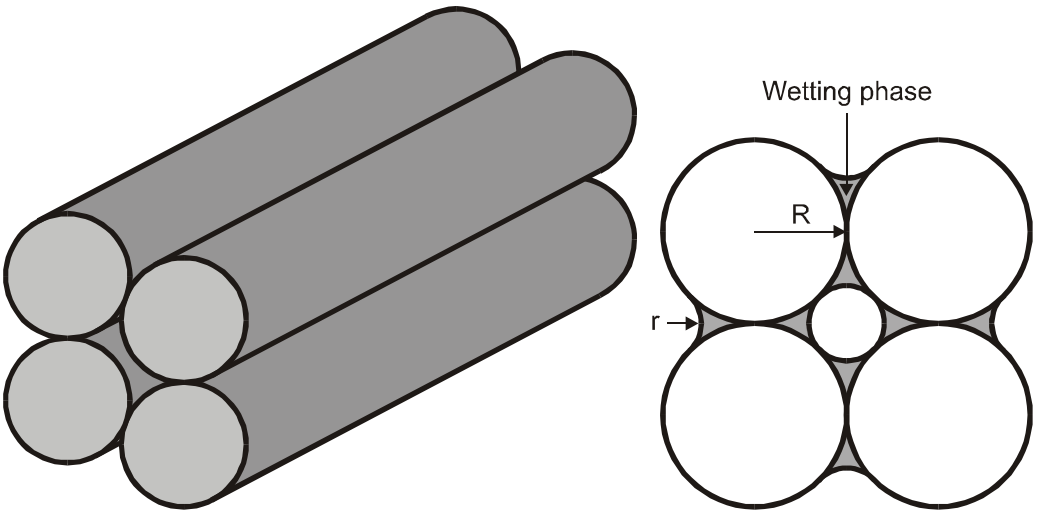

Figure 1.11: Modeling the porous medium as a bundle of cylindrical rods

Since S_1 and P_c are functions of r, the following is also valid:

$$P_c = P_c(S_1) \tag{1.19}$$

For a bundle of rods having a radius of $R = 7.3\ 10^{-5}$ [m] and $\sigma_{12} = 0.037$ [N/m] the relationship between the capillary pressure and S_1 is shown in Figure 1.12.

Let p_w be the pressure in the wetting phase and p_{nw} in the non-wetting phase, then the capillary pressure is defined as follows:

$$p_{nw} - p_w = P_c(S_w) \tag{1.20}$$

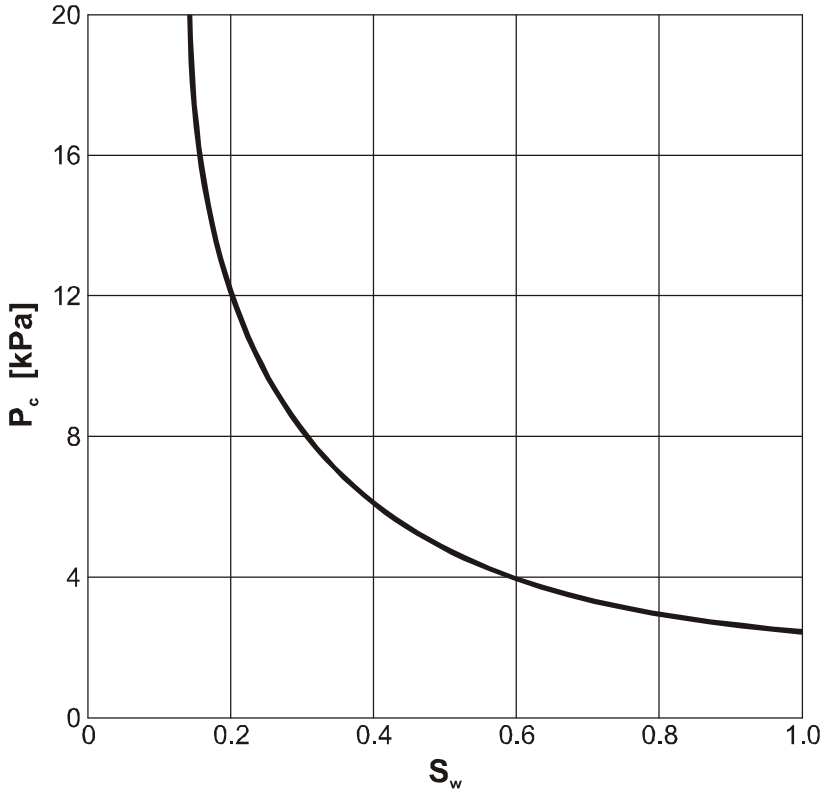

Figure 1.12: Capillary pressure versus saturation of the wetting phase for the model in Figure 1.11

1.2.3.2 Measurement of Capillary Pressure in a Porous Medium

The various kinds of measurement methods are all based on the same principle: A constant pressure is exerted on the porous medium, until capillary equilibrium has generated a constant saturation. Consequently this applied pressure equals capillary pressure which corresponds to the given saturations. The saturation can be calculated with the help of material balance.

One of the devices used for measurement of the capillary pressure curve is illustrated in Figure 1.13. The upper and lower cells are separated by a diaphragm, which is impermeable to the non-wetting fluid. The sample (core), which is placed into the upper chamber, and the diaphragm are both saturated with the wetting fluid. The non-wetting fluid surrounding the core, e.g. air, is then set under constant pressure and is thus pressed into the pore-space of the core.

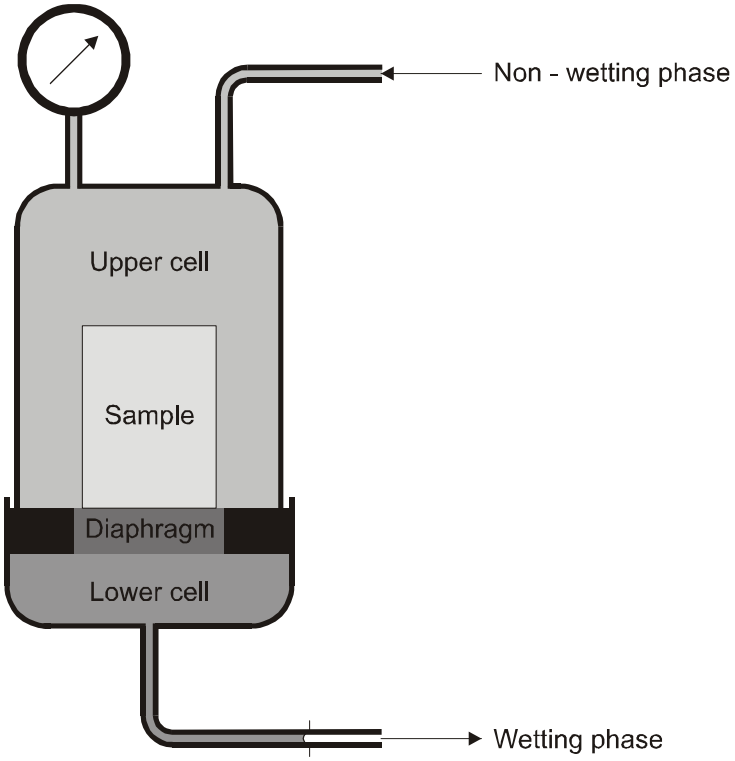

Figure 1.13: Schematic diagram of a diaphragm device for capillary pressure determination by drainage (after *Welge* and *Bruce*)

The wetting fluid, displaced by the non wetting fluid, flows through the diaphragm into a graduated pipette to be measured. This procedure is then repeated several times at higher pressures. It is essential to pay attention to the fact that capillary equilibrium should be achieved at every pressure step so the displaced volume is no longer a function of time. However, it will never come to a complete displacement of the wetting fluid. The so called *connate water saturation* always stays behind. After completing the described drainage and measurement procedure, it is possible to establish the capillary pressure curve for imbibition by reducing the pressure stepwise inside the upper chamber.

Figure 1.14 shows a typical capillary pressure curve. If the core is saturated completely with the wetting phase (e.g. water) at the beginning of the measurement, then a certain pressure must be applied to enable the non-wetting phase to intrude the pore space. This pressure is the threshold pressure which depends on the largest pore diameter.

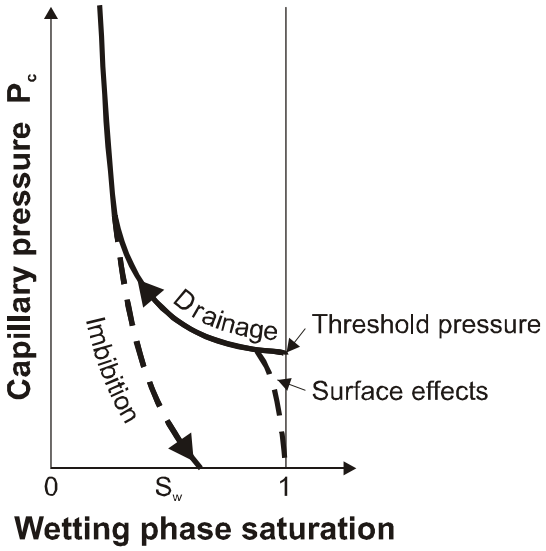

Figure 1.14: Hysteresis of the capillary pressure curve

The capillary pressure curve will be asymptotic to a certain limit value of saturation - the so called *connate water saturation.* This procedure of a wetting fluid being displaced by a non-wetting fluid is called *drainage.*

On the other hand, in case of *imbibition* the non-wetting fluid, with which the core is initially saturated, will be displaced spontaneously by the wetting fluid. This means that the porous medium is imbibing the wetting fluid immediately. Thus the capillary pressure curve appears as a hysteresis (Figure 1.14).

1.2.3.2.1 Method of Centrifuge

A column of sand, saturated with wetting fluid (e.g. water) at atmospheric pressure, comes to equilibrium by gravity drainage. The saturation distribution in the column can be meassured by cutting it into sections. The pressure gradient in the wetting fluid is determined by the density of the liquid and the acceleration due to gravity. If the level of the free liquid surface, where the capillary pressure is zero, is known, the relation P_c versus S at any point in the column can be calculated by measuring the saturation at this point.

The spontaneous gravity drainage cannot be applied to oil-field rocks due to the low value of g at the earth's surface. Centrifuging a liquid bearing porous medium of small sample size produces a stronger gravitational field and, therefore, increases the drainage rate and the establishment of the equilibrium, and minimizes capillary end effects. *Hassler and Brunner*[1.8] proposed the centrifuge method in 1945.

The pressure applicable with the diaphragm method is limited to 4 to 5 bars. Using the centrifuge method, capillary pressure curves can be messuered up to 21 bars (300 psia). Therefore, this method is suitable to investigate tight, low permeable samples too.

Currently, the centrifuge method is widely applied throughout oil industry.

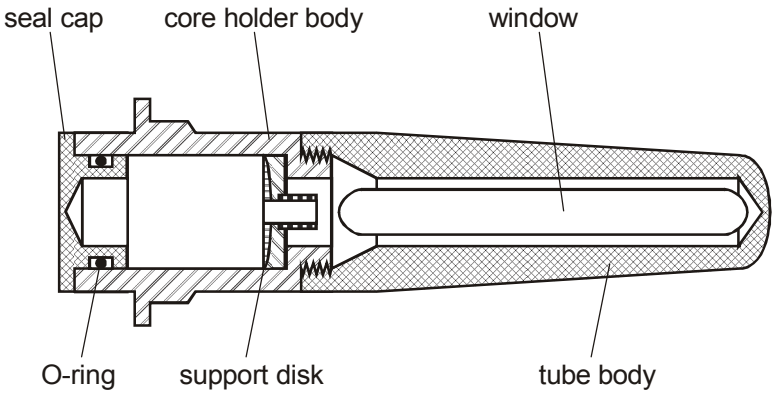

Figure 1.15: Core holder for capillary-pressure determination in centrifuge. (See *Slobod*[1.18])

Considering the laboratory handbook published by *Torsaeter and Abtahi*[1.20], the USBM(United States Bureau of Mines) procedure is as follows:

1. A core sample is saturated with brine (100 % saturation).
2. The sample is then placed in a centrifuge core holder (see Figure 1.15) which seals the side walls and has been filled with oil before.
3. The sample is spun at a particular speed, and the heaver fluid brine is displaced into the tube which originally was filled with oil.
4. The displaced brine is measured using a stroboscope while the centrifuge continues spinning. The average saturation of the sample at the given rotational speed is calculated from the amount of fluid displaced and the known pore volume. After fluid displacement appears to stop, the rotational speed is increased, and the fluid produced at the higher speed is measured. In this manner a set of data (typically 6 data points) of average saturation versus rotational speed is generated.
5. The procedure given by the Items 1-4 is called *primary drainage*.
6. Then the core is placed in an inverted core holder filled with brine. The brine is allowed to spontaneously imbibe into the core sample. Then the sample is centrifuged at incremental steps corresponding to the procedure described by Item 4. This process is called *imbibition*.
7. Then the core is placed again in a core holder filled with oil. The centrifugation corresponding to Item 4 is called *secondary drainage*.

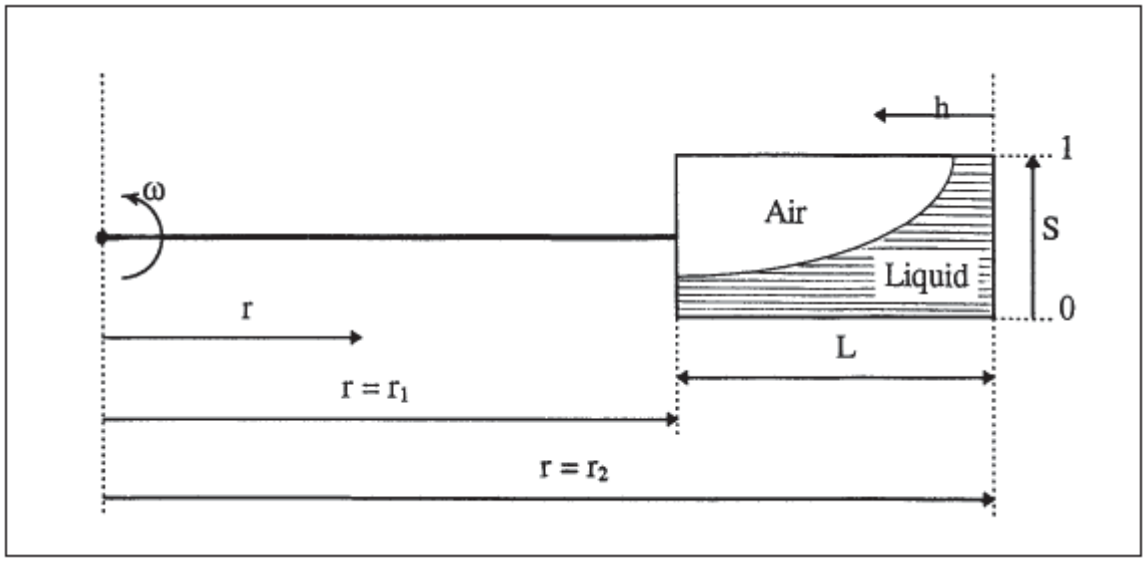

Figure 1.16: Schematic diagram of a core in a centrifuge and its boundary conditions

The raw material from the centrifuge experiments must be converted into a relationship between saturation and capillary pressure. *Hassler and Brunner*[1.8] proposed a method which has become widely accepted:

$$P_c(r_1) = \frac{1}{2}\Delta\rho\omega^2\left(r_2^2 - r_1^2\right) \tag{1.21}$$

where

$P_c(r_1)$ capillary pressure at the top of the sample (top refers to the face closest to the axis of rotation)

$\Delta\rho$ density difference, e.g. air-brine

r_1, r_2 radial distances of the axis of rotation to the top and the bottom of the sample

ω angular velocity of the centrifuge [revolutions per second]

Replacing the centrifugal acceleration term $\frac{1}{2}\omega^2(r_1 + r_2)$ in Eq. 1.21 with the gravitational acceleration *g* makes the analogy with the determination of the capillary pressure by gravity drainage evident. A key assumption in the derivation of Eq. 1.21 is a zero capillary pressure at the bottom of the sample (r_2) at all rotation speeds.

The second step is to calculate the saturation at the top of the core sample. *Hassler and Brunner*[1.8] derived the following expression:

$$S(r_1) = \frac{d}{dP_c(r_1)}[\bar{S}P_c(r_1)] \tag{1.22}$$

where $\overline{S}$ is the average saturation. In practice, Eq. 1.22 is applied by plotting the product of capillary pressure and average saturation versus capillary pressure and calculating graphically or numerically the tangent of the curve.

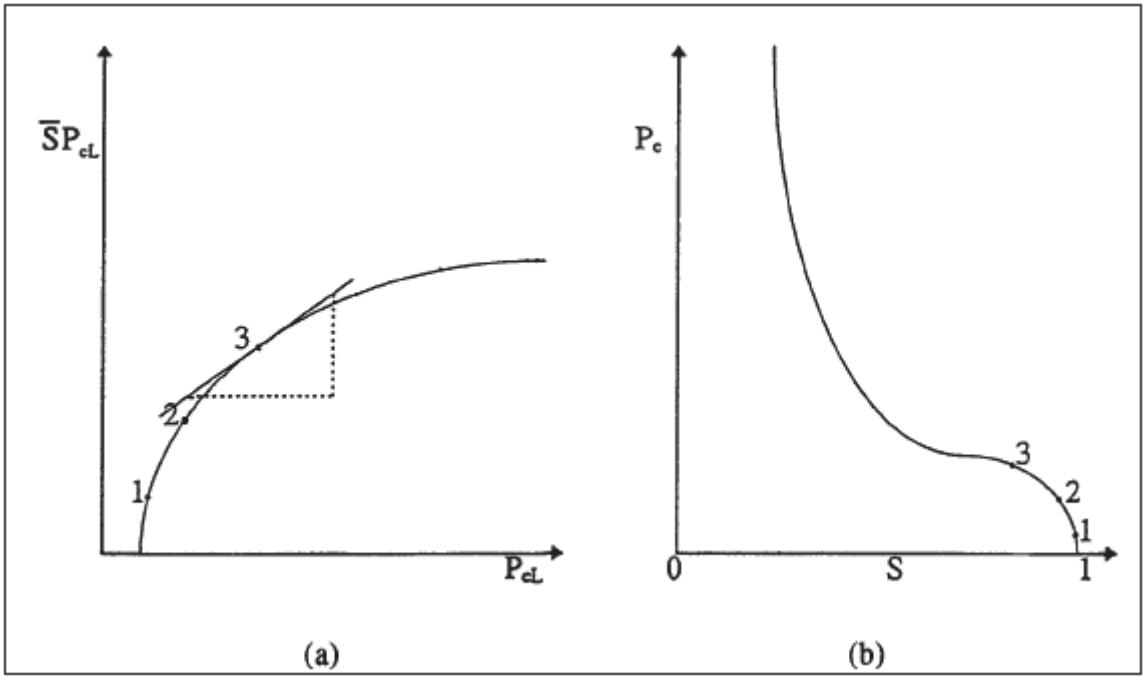

Figure 1.17: Graphical differentiation of $\overline{S}P_c$-P_c curve (a) to determine S-P_c curve (b)

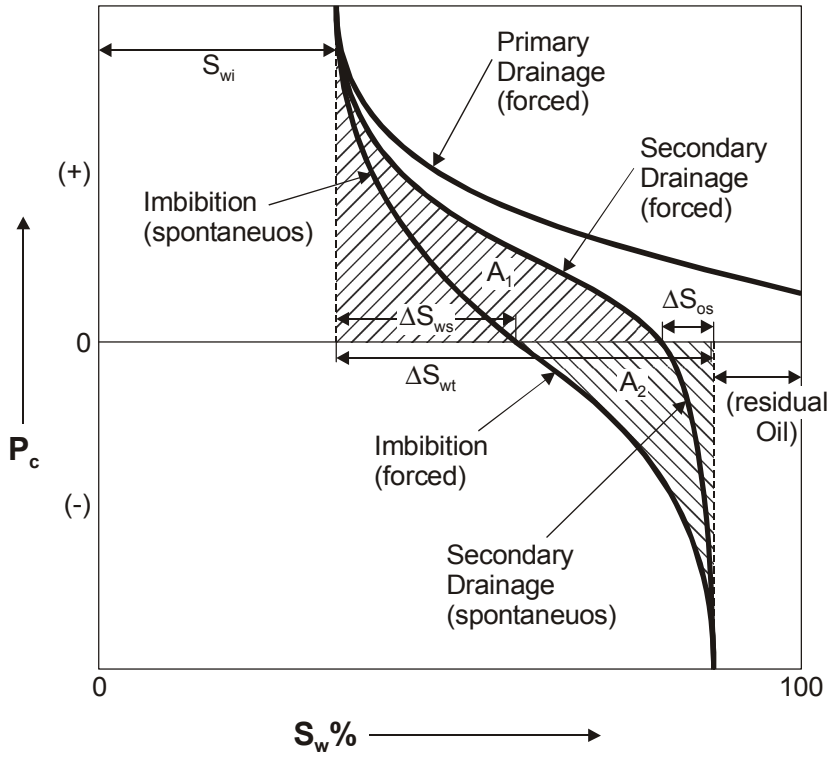

Figure 1.18: Typical capillary pressure curves and the relationships of wettability measurements by

Amott and USBM tests to P_c (see *Torsaeter*[1.20])

Figure 1.18 shows typical capillary pressure curves and relationships of wettability measurements by USBM tests. The relative wetting tendencies of oil and brine in a porous medium, which is given by $WI = log(A_1/A_2)$ and the distribution of pore sizes determine the shape of the capillary pressure curves. In general, water-wet systems should have a larger area in the brine-displaced-by oil curves (area A_1 of Figure 1.18) than the area under the oil-displaced-by-brine curves (area A_2 of Figure 1.18). Therefore, $log(A_1/A_2)$ for water-wet systems is greater than zero. Conversely, the area ratio is less than unity for oil-wet systems and $log(A_1/A_2)$ is negative.

Based on publications critical for the approach of *Hassler and Brunner*[1.8], the conventional centrifuge method may suffer from at least two uncertainties regarding the basic assumptions:

- **Zero capillary pressure at the bottom of the sample**: *Wunderlich*[1.21] cites personal communication with *Korringa* that he has demonstrated that the *Hassler-Brunner* key assumption cannot be correct if the system reaches thermodynamic equilibrium. Anyway, the general success of the method at low capillary pressures suggests that many systems do not reach a complete thermodynamic equilibrium during the usual time scale, rather a hydraulic equilibrium.

- **Time scale of measurement:** An elemental question for an experimentalist is "How long does it take before equilibrium is reasonably approached at each speed?" Some of the earliest investigators, e.g. *Slobod et al.*[1.18], provide time estimates based on the absolute permeability of the sample. *O'Meara et al.*[1.13] are convinced that such estimates are incomplete because equilibrium times certainly depend on relative as well as absolute permeabilities: as wetting phase saturation decreases with increasing speed, it becomes more difficult for the wetting phase to flow which certainly draws out the equilibrium time. Consequently, a typical service laboratory "rule of thumb", which suggests changing centrifuge speed after some fixed amount of time or after some period throughout which there is no "significant" production, may frequently result in a wrong prediction of the saturation distribution.

1.2.3.2.2 Mercury Injection (Purcell Method)

The original devise used by *Purcell* is shown in Figure 1.19. The non-wetting fluid is mercury. The method can be applied on cleaned cores only using the following procedure:

1. The core is placed and evacuated inside the cell.
2. The cell is filled with *Hg* up to the level indicator (non-wetting fluid *Hg* will not be imbibed into the pore space of the core), then the volume indicator of the pump is set to zero.
3. Nitrogen is used for applying a constant pressure to force *Hg* into the core. A constant *Hg* level is held by the pump.

4. Step 3 will be repeated by stepwise increasing the pressure. At each pressure step the *Hg*-volume is measured which has to be pumped into the cell in order to maintain the level. Due to the necessity of capillary equilibrium for a correct reading of the injected volume, each step may take some hours.
5. Final pressures may range from 1 to 100 MPa. At the end of the measurement the empty cell should be calibrated for the applied pressure range.

This procedure enables the capillary pressure to be determined as a function of the *Hg*-saturation.

The mercury injection method offers two advantages. Firstly the time for the determination of a complete curve is less than one hour and secondly the range of pressure is increased compared with other methods. However, the transformation of the results to reservoir conditions is difficult due to the unrealistic fluid system.

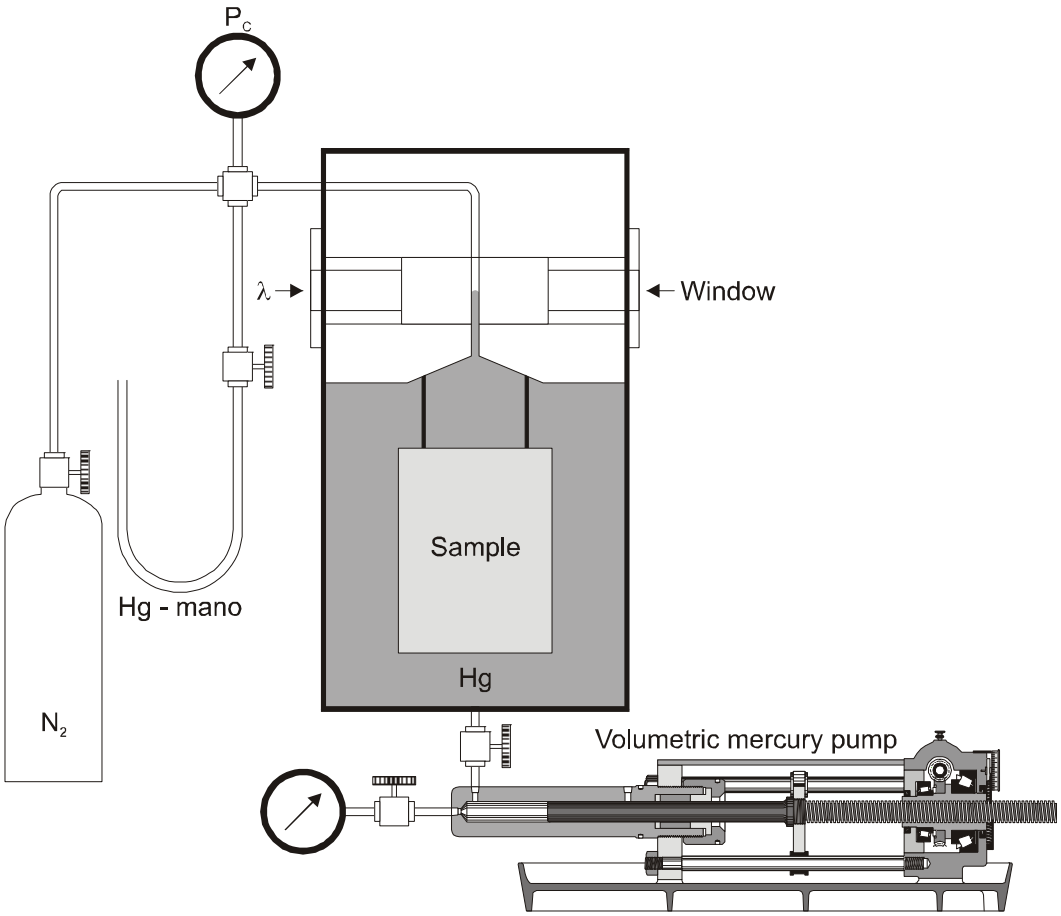

Figure 1.19: Assembly with mercury pump for capillary pressure measurement (*Purcell*-method)

1.2.3.3 Conversion of Laboratory Data

In Order to use capillary pressure data measured in the laboratory for capillary pressure

determination under reservoir conditions, a proper conversion of this data should be done at first. The conversion is based on Eq. 1.23

$$P_{cR} = \frac{\cos\theta_R \sigma_R}{\cos\theta_L \sigma_L} \cdot P_{cL} \tag{1.23}$$

where

P_{cR} is the capillary pressure under reservoir conditions,
P_{cL} is the capillary pressure measured under laboratory conditions,
σ_R is the interfacial tension under reservoir conditions,
σ_L is the interfacial tension measured under laboratory conditions,
θ_R is the contact angle measured under reservoir conditions,
θ_L is the contact angle measured under laboratory conditions.

Table 1.5 shows some interfacial tension values measured in the laboratory and estimated values in reservoir.

Table 1.5: Interfacial tension and contact analyses

In the Laboratory	*In the Reservoir*
$\sigma_{w/a}$ = 0.07 N/m	$\sigma_{w/o}$ = 0.028N/m
$\theta_{w/a}$ = 0	$\theta_{w/o}$ = 33° to 55°
$\sigma_{Hg/a}$ = 0.48	
$\theta_{Hg/a}$ = 140°	

1.2.4 The *Leverett* Function

According to *Leverett* the capillary pressure curves of core plugs - obtained from samples of the same formation - may be correlated with other properties. These investigations resulted in the dimensionless *J*-function (see Figure 1.20) which is given by:

$$J(S_w) = \frac{P_c}{\sigma_{12}\cos\theta}\sqrt{\frac{k}{\phi}}, \tag{1.24}$$

where

Pc is the capillary pressure,

σ_{12} is the interfacial tension between fluid 1 and 2,

θ is the contact angle,

k is the permeability,

ϕ is the porosity.

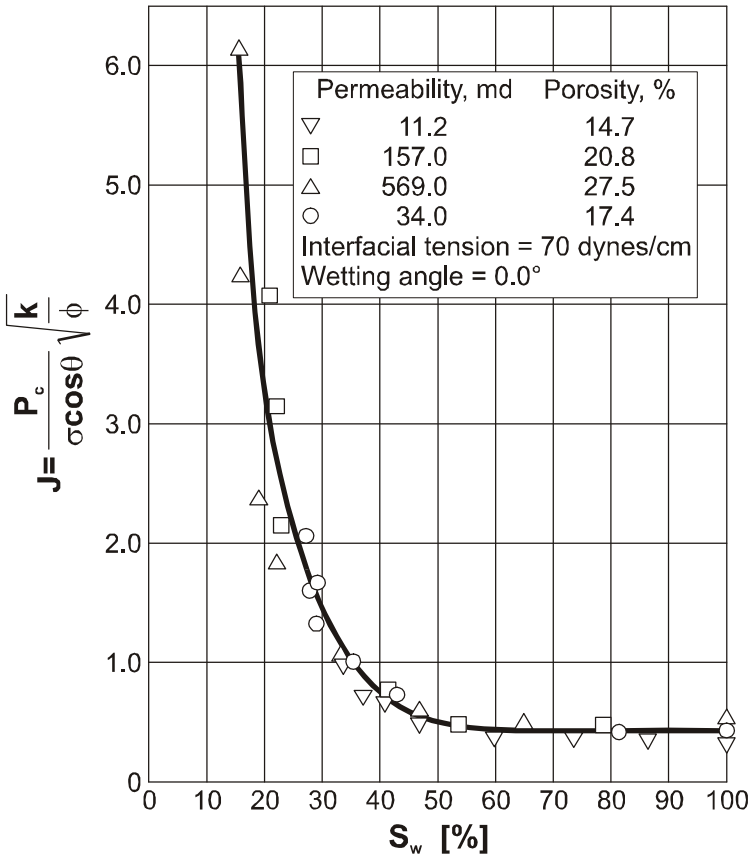

Figure 1.20: The dimensionless capillary *J* function curve (after *Leverett*)

1.2.5 Pore Size Distribution

Eq. 1.26 indicates that each capillary pressure value can be related to a certain radius, which corresponds to a specific saturation as indicated by Eq. 1.19. Again consider a bundle of equally long capillary tubes, so the circular cross-sections of the capillary tubes correspond to a certain partition function, then it is possible to set up a $V_i = V_i(r_e)$-function using the *Purcell*-method:

$$P_c(r) = \frac{2\sigma\cos\theta}{r} = P_c(S_{Hg}) \tag{1.25}$$

Where r is defined as the smallest radius which has to be filled with the non-wetting fluid in order to reach a certain part of the pore space. It is customary to use the terms r_e (pore entry radius) and S_e (effective saturation). This function is a distinctive property of reservoir rocks and is therefore very often used to characterize a porous medium. Figure 1.21 shows the measured non wetting fluid saturation $S_e(P_c)$ versus the effective pore size $r_e(P_c)$ calculated from Eq. 1.25. The function shown is similar to the function of cumulative frequency distribution in statistics.

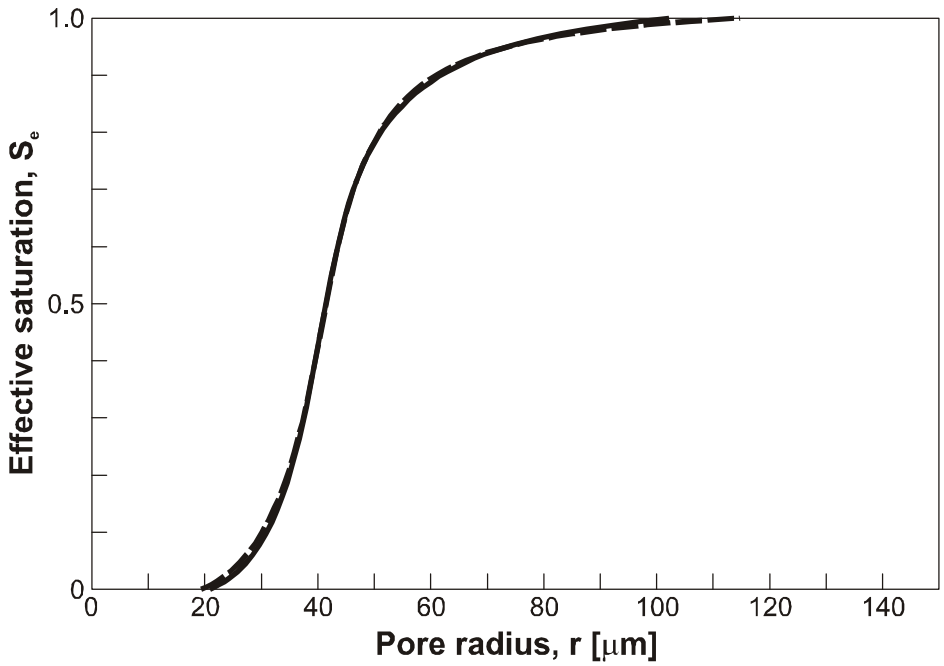

Figure 1.21: Non wetting fluid saturation versus the effective pore size distribution

Another way to determine the pore-radii distribution is by means of statistical methods (e.g. from thin ground sections). Characteristic for this method is the fact that the pore radius is measured directly. The extent to which the distribution curves of the two methods diverge is illustrated in Figure 1.22, which shows the pore volume distribution function determined by the centrifuge method (the curve with sharp peak), and the other one determined by photography of thin sections.

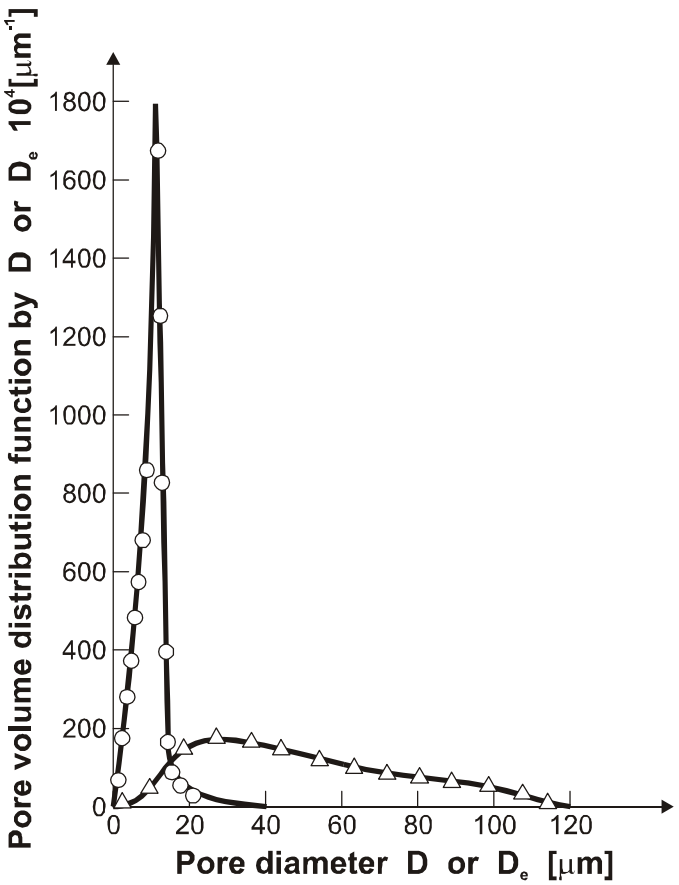

Figure 1.22: Bivariant pore radii distribution (from *Dullien* and *Mehta*)

1.2.6 Vertical Equilibrium

If - as graphically illustrated in Figure 1.23 - empty capillary tubes are placed into a tub filled with a wetting fluid, the menisci will rise against gravity until equilibrium between gravity and capillary force is reached. Regarding a single capillary tube, the position (height *h)* of the meniscus is determined by the equilibrium of the gravitational and capillary forces:

$$P_c = h(\rho_w - \rho_{nw})g = \frac{2\sigma\cos\theta}{r}. \tag{1.26}$$

In addition, Figure 1.23 illustrates that S_w is a function of height h if the porous medium is regarded as a bundle of capillary tubes with equal length, but different diameters. The wetting fluid saturation of the bundle can be defined as ratio of the wetting fluid filled cross section over all capillary tubes. Correspondingly the capillary pressure function may be expressed in terms of $h = h(S_w)$. Therefore the saturation may be determined as a function of the vertical distance from the $P_c = 0$ plane:

$$P_c(S_w) = h(S_w)(\rho_w - \rho_{nw})g, \tag{1.27}$$

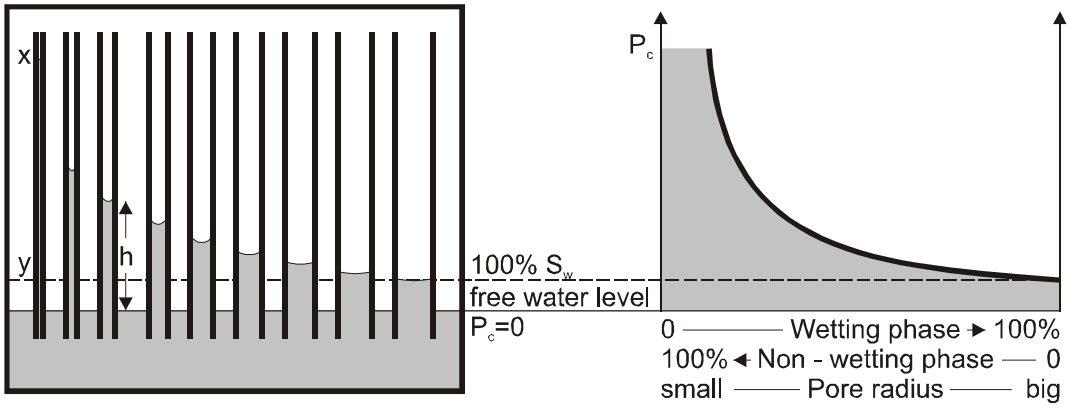

Figure 1.23: Equilibrium between gravity and capillary forces

$$h(S_w) = \frac{P_c(S_w)}{(\rho_w - \rho_{nw})g}, \tag{1.28}$$

where

ρ_w is the density of the wetting phase,

ρ_{nw} is the density of the non-wetting phase,

$P_c(S_w)$ is the capillary pressure of the wetting phase (e.g. water),

g is the gravitational constant.

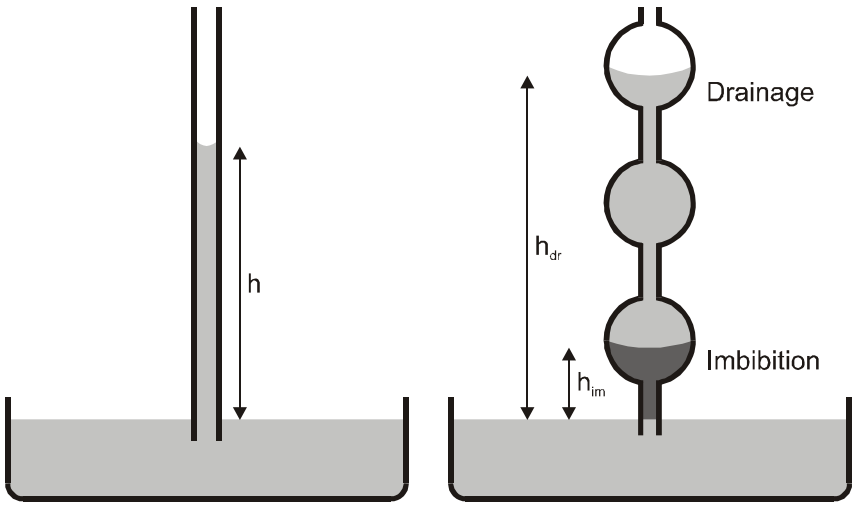

Figure 1.24: Drainage and imbibition in capillary tubes

This appearance of hysteresis may also be explained using capillary tubes. In the case of an uniform radius of the capillary tube (see Figure 1.24a), the height of the meniscus of a

wetting phase above the contact level will be independent of the displacement process. It makes no difference in the measurement of P_c if (i) the capillary tube is filled first with the wetting fluid and placed in the tub (drainage), or (ii) an empty tube is placed in the tub and the wetting fluid enters the tube (imbibition). If this procedure is repeated with capillary tubes having sequentially different diameters, then the height of the meniscus will depend on the saturation process as shown in Figure 1.24b.

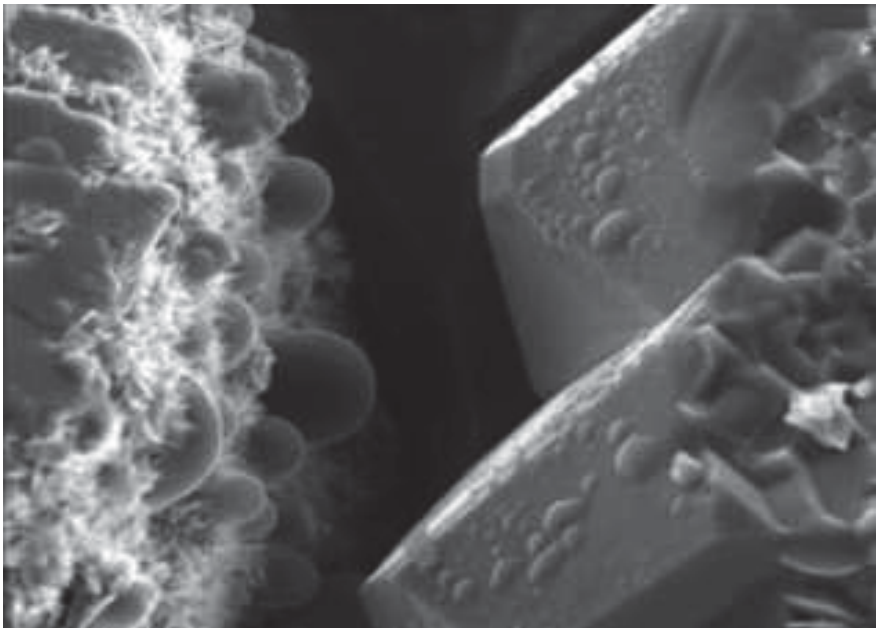

Figure 1.25: Microscopic view of non-wetting (left side) and wetting fluid on mineral surfaces

Example 1.2:

Calculate the height of the transition zone at S_w = 0.7 above the level of P_c = 0, if the laboratory measurement of P_c using air/water system is 20600 [N/m²] at S_w = 0.7. Use Table 1.2 and the following data:

ρ_o = 800 [kgm^{-3}]

ρ_w = 1100 [kgm^{-3}]

θ_R = 45°

Solution:

$$P_{cR} = \frac{\cos\theta_R \sigma_R}{\cos\theta_L \sigma_L} \cdot P_{cL} = \frac{0.71 \cdot 0.028}{0.07} \cdot 20600 = 5850[Nm^2]$$

$$h = \frac{P_{cR}}{(\rho_w - \rho_o)g} = \frac{5850}{(1100 - 800)(9.81)} = 2[m]$$

1.3 Permeability

It is important to distinguish between mass flow and filtration:

In the case of *mass flow* all particles in the field of flow are in motion, whereas in the case of *filtration*, only a portion of the mass particles flows and the remaining part forms the flooded framework.

First investigations regarding filtration date back to the year 1825. *Chaumont* had the idea of diging a trench parallel to the river Garonne (in Southern France) and then to dewater this trench using an Archimedian screw. He measured the time elapsed until the water level had resumed a certain height. Results of this experiment were unfortunately lost.

1.3.1 *Darcy*'s Law

In the year 1854 *Dupuit* made experiments with urban water filters in London. Velocity of filtration had been 5 [m^3m^{-2}] per day. From the results he deduced that the pressure drop caused by the filter was proportional to the velocity of filtration.

Henry Darcy proved this hypothesis in the year 1856 using the equipment illustrated in Figure 1.26. Investigations were made with various sand gravel packs. *Darcy* found that the flow through the sand filter corresponded to the following formula:

$$Q = K \cdot \frac{S}{L} \cdot h, \tag{1.29}$$

where

K is the permeability coefficient,

S is the cross-section of the packing,

L is the length of the packing,

h is the difference in piezometric head.

At the first World Oil Congress in 1933 the permeability was defined by *Fancher*, *Lewis*, and *Barnes*. In the same year *Wyckoff, Botset, Muskat* and *Reed* suggested to give the unit of permeability the name *Darcy.*

From that time on the equation is called *Darcy*'s Law:

$$q = A \cdot \frac{k}{\mu} \cdot \frac{\Delta p}{L}, \tag{1.30}$$

where:

A is the cross-section of the porous medium perpendicular to the direction of flow

k is the permeability as a material property of the porous medium

L is the length of the porous media in direction of flow

Δp is the pressure difference along the porous medium

μ is the viscosity of the flowing fluid

Darcy's-law in Eq. 1.26 is only valid for a laminar and steady-state on-phase flow through a porous medium. Moreover, the fluid has to be largely incompressible.

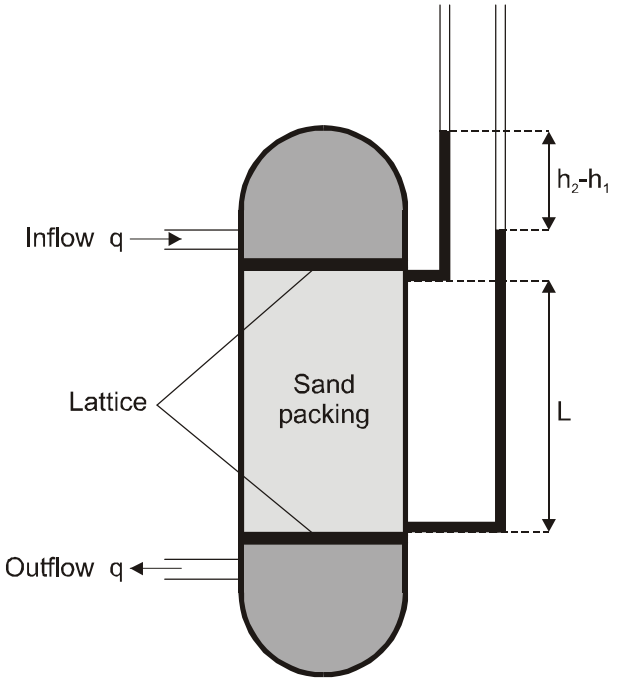

Figure 1.26: Schematic diagram of DARCY's experiment

1.3.2 Definition and Units of Permeability

Even today it is customary to use DARCY [D] as a unit of permeability. The permeability of a porous media will be 1 [Darcy], if at a 1 [cm^2] cross-section a fluid with 1 [cP] viscosity flowing with a rate of 1 [cm^3/s] will cause a pressure drop of 1 [atm/cm]:

$$k = \frac{\mu q}{A} / \frac{\Delta P}{L} = \frac{[cp][cm^3/s]}{[cm^2]} / \frac{[atm]}{[cm]} = 1 Darcy. \tag{1.31}$$

By using the *SI*-units

$$\frac{[Nsm^{-2}][m^3 s^{-1}]}{[m^2]} / \frac{[Nm^{-2}]}{[m]} = [m^2]$$

The relationship between the two units is:

1 Darcy = 0.987 x 10^{-12} [m^2]

Example 1.3:

A cylindrical core having a radius 2.54 10^{-2} [m] and length of 0.3 [m], was flooded with brine at a steady rate of 1.10^{-6} [$m^3 s^{-1}$], the differential pressure across the core was 10 [bar]. Calculate the absolute permeability of the core. Assume brine viscosity 0.001 [Pa.s].

Solution:

From Darcy's law

$$q = A\frac{k}{\mu}\frac{\Delta p}{L}$$

$$k = q\frac{\mu}{A}\frac{L}{\Delta p}$$

$$k = \frac{1\times10^{-6}[m^3]}{s} \times \frac{0.001[Pas]}{20.3\times10^{-4}[m^2]} \times \frac{0.3[m]}{10[bar]}$$

$$k = 1.48\times10^{-13}[m^2] = 0.148[D]$$

Exercise:

Calculate the permeability of a core plug from the following test:

- *Flow rate = 2.10^{-6} [$m^3 s^{-1}$]*
- *Inlet pressure = 5 [bar]*
- *Outlet pressure = 1 [bar]*
- *Length of core = 0.1 [m]*
- *Area = 1.10^{-4} [m^2]*
- *Viscosity = 0.002 [Pa.s]*

1.3.3 Measurements of Permeability

The method depends on the following factors:

- consolidation of the medium
- core size
- fluid properties
- the applied pressure.

Samples from a consolidated media can be shaped as regular geometrical forms:
- cylinders with a diameter ranging from 0.02 to 0.05 [m]
- cubes with 0.02 [m] length of the side.

The rock sample - mostly formed cylindrically (core) - is fixed in the device with a sealing rubber gaiter. Usually gas is used to measure permeability of core samples instead of liquids. Since gas is the non-wetting fluid it does not alter the original state of the core and the measurements can be repeated. It can also be used for low permeability cores where a higher pressure difference is required.

By applying constant pressure, the gas commences to flow through the sample, and thus permeability may be calculated using Darcy's law for ideal gas as follows:

$$q = -\frac{kA}{\mu L}(p_1 - p_2), \tag{1.32}$$

where:

p_1 is the inlet pressure,

p_2 is the outlet pressure,

k is the permeability of the core,

q is the flow rate of gas at average pressure $\bar{p} = \frac{p_1 + p_2}{2}$,

μ is the dynamic viscosity of gas at the average pressure $\bar{p}$

To convert the flow rate $\bar{q}$ to a flow rate measured under atmospheric pressure p_a, while ideal gas behavior is assumed, then:

$$\overline{qp} = q_a p_a, \tag{1.33}$$

where:

q_a is the flow rate of gas at atmospheric pressure p_a.

From Eq. 1.33 the flow rate q can be written as:

$$\bar{q} = \frac{q_a p_a}{\bar{p}}. \tag{1.34}$$

Substituting Eq. 1.34 into yields:

$$q_a = \frac{-k_a A}{\mu L p_a}(p_1 - p_2)\left(\frac{p_1 + p_2}{2}\right). \tag{1.35}$$

From Eq. 1.35 the permeability k_a can be written as:

$$k_a = \frac{-2 q_a \mu L}{A} \frac{p_a}{(p_1^{\,2} - p_2^{\,2})}, \tag{1.36}$$

where

q_a is the flow rate at atmospheric pressure p_a.

The prearrangement for unconsolidated media is very similar to the equipment of *Darcy* (see Figure 1.26). The device may be described as a cylinder inside which a porous medium is positioned between two lattices see Figure 1.28.

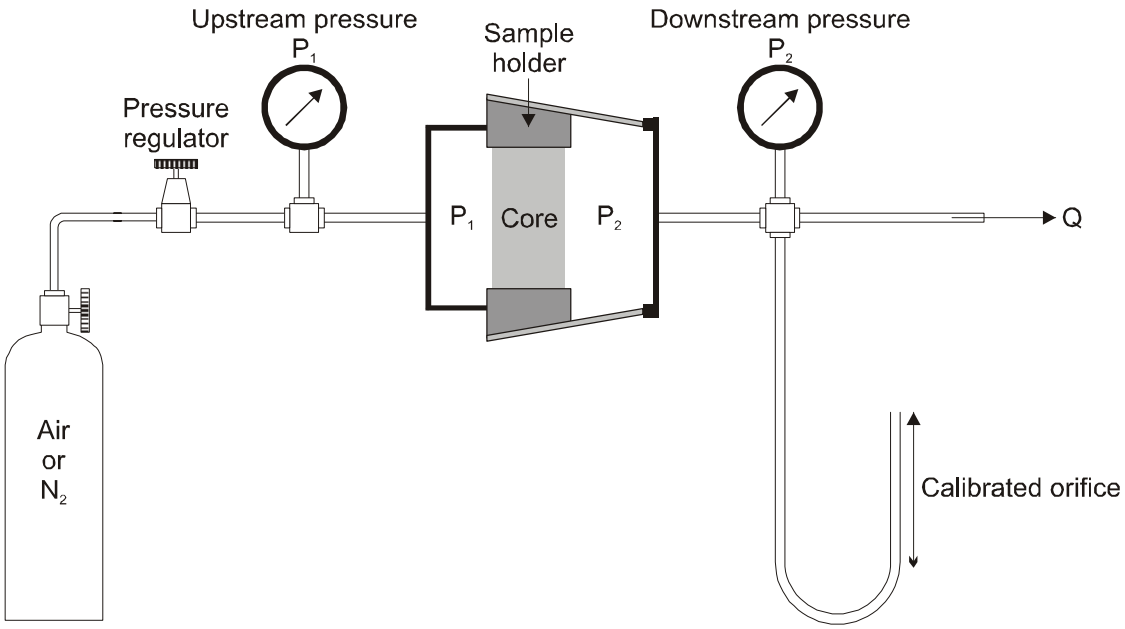

Figure 1.27: Air permeameter: Schematic Flow diagram (after *Monicard*)

In order to measure the permeability of very compact media using a liquid, high pressure gradients must be applied. The liquid is either injected with constant gas pressure or by use of a micropump. The *Hassler* core holder is a common device. Hereby the permeability measurement is possible both in horizontal and vertical direction (see Figure 1.29). Permeability measurement in a vertical direction presupposes the casing of the core by an impermeable rubber gaiter. In doing so air, water or oil can be pressed through the core in an axial direction.

Horizontal measurement makes a sealing of the top surfaces of the core necessary. Then the area of the cylindrical surface is covered both at the inflow and outflow opening to one quarter with a lattice. This enables the core to remain permeable in these areas when cased by the rubber gaiter. The fluid is then pressed horizontally through the lattice and the core.

Advantages of the *Hassler* core holder are:

- excellent sealing,
- optimal selection of core length,
- compatibility of large pressure gradients,
- permeability measurement in two directions,
- independency from the fluid used.

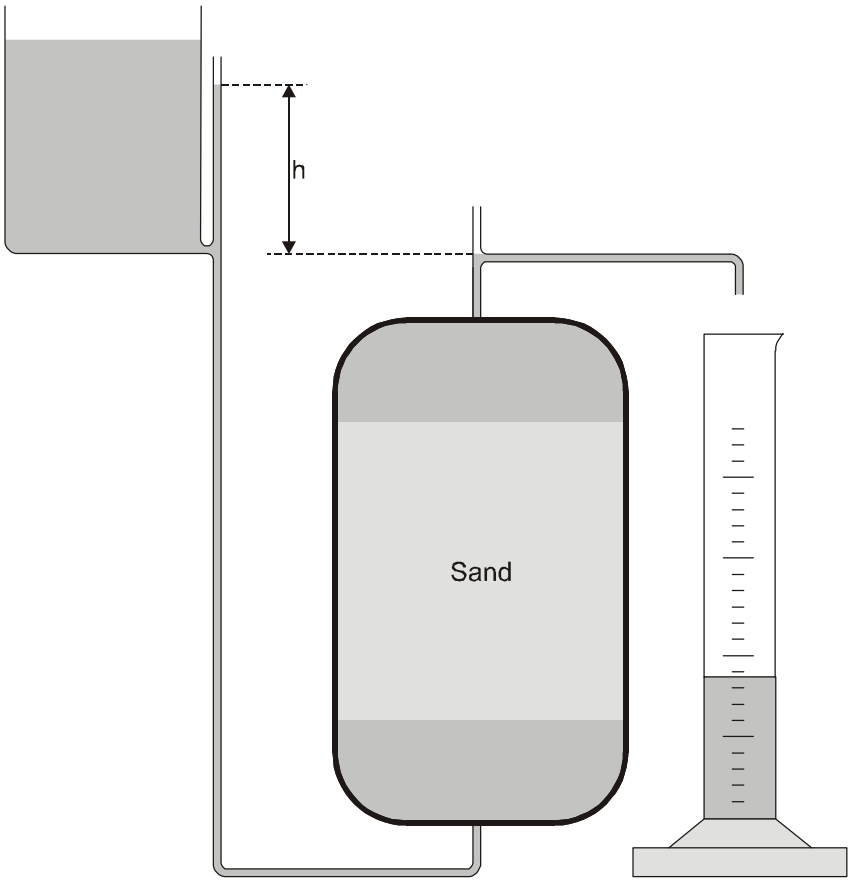

Figure 1.28: Schema of permeability measurement for unconsolidated media (from *Monicard*)

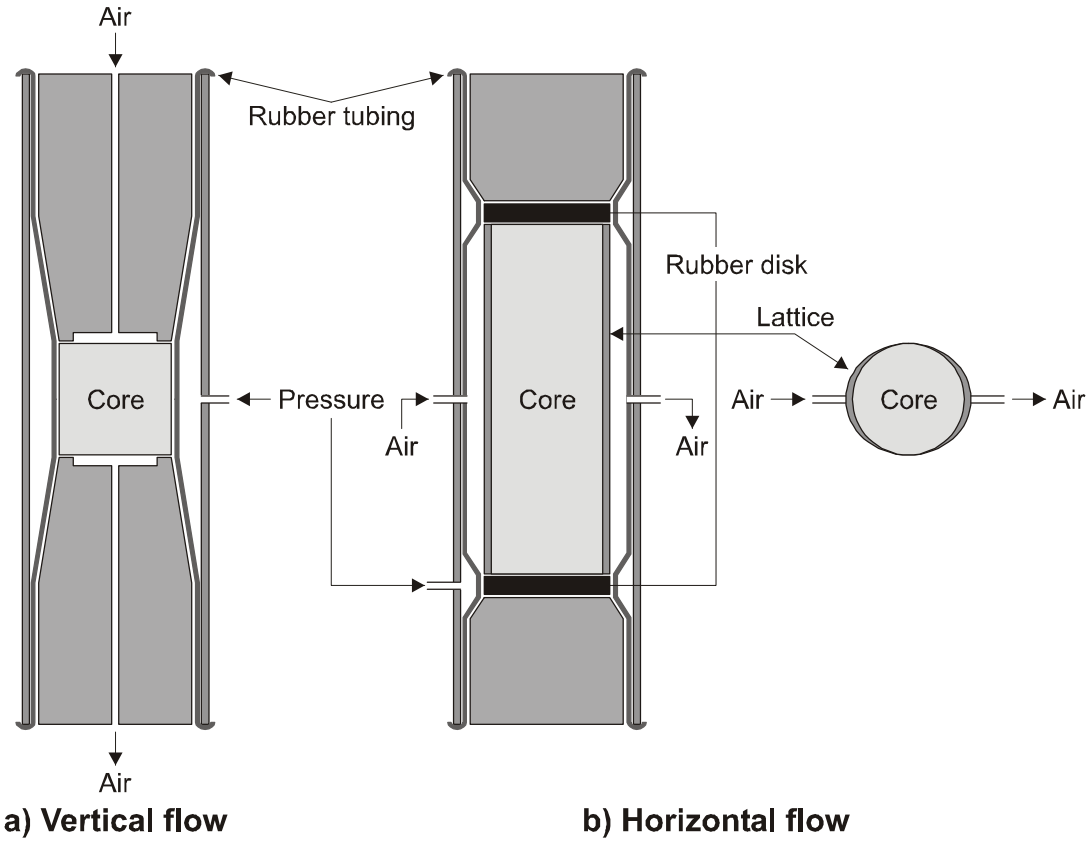

Figure 1.29: *Hassler* type core holder (from *Monicard*)

1.3.4 *Klinkenberg* Effect

Klinkenberg noticed that the permeability of gas is not the same as for liquids and in addition the gas permeability depends on pressure. The correlation between gas permeability k_a, liquid permeability k_l and mean pressure inside the core p_m, is given by Eq. 1.37. The parameter b depends on the gas used.

$$k_a = k_l\left(1 + \frac{b}{p_m}\right) \tag{1.37}$$

(1.38)

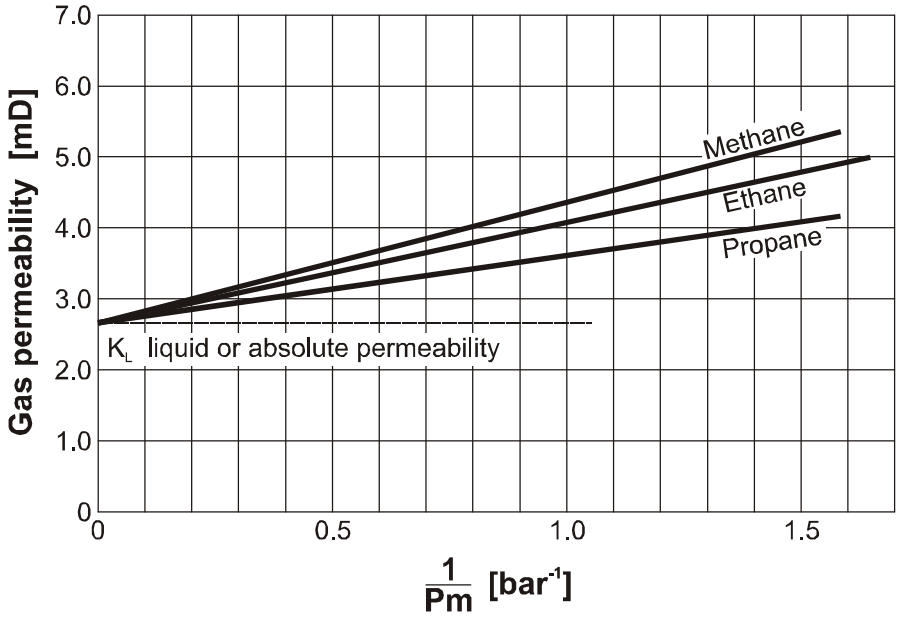

Figure 1.30: Variation in gas permeability with mean pressure and type of gas (from *Klinkenberg*)

Physically the *Klinkenberg*-effect may be explained by the phenomenon of surface slipping of gases caused by the *Brown* motion. This surface slipping decreases with increasing pressure. However, at low pressure this effect is responsible for the deviation of the gas permeabilities.

1.3.5 Analogies between the Laws of *Darcy*, *Ohm* and *Fourier*

The following is a comparison of different laws which have a similar form to *DARCY*'s law:

Darcy's law

$$q = A\frac{k}{\mu}\frac{\Delta p}{L} \tag{1.39}$$

Ohm's law of electrical current:

$$J = A\frac{1}{\rho}\frac{U}{L} \tag{1.40}$$

Fourier's law of heat conduction:

$$Q = A\lambda\frac{\Delta T}{L}, \tag{1.41}$$

where:

A	is the cross section [m^2]
J	is the amperage [A]
k	is the permeability [m^2]
L	is the length [m]
Q	is the rate of heat [Js^{-1}]
q	is the flow rate [m^3s^{-1}]
U	is the voltage [V]
Δp	is the difference in pressure [Pa]
ΔT	is the difference in temperature [°C]
μ	is the dynamic viscosity [Pa.s]
λ	is the thermal conductivity [Wm^{-1} °K]
ρ	is the electrical resistance [Ωm]

The form of Eq. 1.39, Eq. 1.40 and Eq. 1.41 is similar.

These analogies enable a simulation of filtration processes with the help of electrical models and the adoption of mathematical solutions obtained from heat flow problems.

Table 1.6: Comparison between the laws of *Darcy*, *Ohm*, and *Fourier*

Darcy	**Ohm**	**Fourier**
Flow Rate $u[m^3 s^{-1}]$	Amperage $J[A]$	Heat conduction rate $Q[Js^{-1}]$
Permeability coefficent $K = \frac{k}{\mu}$ $[m^2 Pa^{-1} s^{-1}]$	Electrical conductivity $\gamma = \frac{1}{\rho}$ $\left[\frac{1}{\Omega m}\right]$	Thermal conductivity λ $\left[\frac{W}{mK}\right]$
Pressure difference $\Delta p[Pa]$	Voltage $U[V]$	Temperature difference $\Delta T[K]$

1.3.6 Filtration Velocity

The velocity of filtration is defined as a fluid volume q flowing through the surface A of a porous medium within unit time:

$$u = \frac{q}{A}[ms^{-1}]. \tag{1.42}$$

u is an arithmetical quantity. In comparison to the actual velocity of flow in pore channels, great differences can be recognized. However a statistical average is easily calculated as follows:

$$v = \frac{q}{A\phi} = \frac{u}{\phi}, \tag{1.43}$$

where ϕ is the porosity and v the displacement velocity.

If a fluid at a velocity of $u = 1$ [mday^{-1}] is injected into a porous medium with a porosity of 0.1, a specific fluid particle will be transported within a distance of 10 [m] in one day.

1.3.7 Quadratic Equation of Filtration

Darcy's law is only an approximation of the general equation of filtration given by:

$$\frac{dp}{dx} = \alpha u + bu^2 . \tag{1.44}$$

If bu^2 is small - in comparison to the term of first order - then Eq. 1.44 will be reduced to the *Darcy* formula and α can be calculated by:

$$\alpha = -\frac{\mu}{k} . \tag{1.45}$$

In consequence of experiments, b can be defined as:

$$b = -b'\rho = -\frac{\beta\rho}{k} , \tag{1.46}$$

where b, respectively β, is independent of the fluid properties. The unit of ß is [m] and is considered as a characteristic length of the porous medium. Further the velocity of mass filtration Q_m may be introduced as the product of filtration velocity and density:

$$\rho u = Q_m / A , \tag{1.47}$$

where A is the cross-section.

Then Eq. 1.44 can be written as:

$$\rho dp = -\frac{\mu Q_m}{Ak}\left(1 + \frac{\beta Q_m}{\mu A}\right) dx \tag{1.48}$$

The order of magnitude of β ranges at 10^{-5}[m]. Therefore the correction factor:

$$\frac{\beta Q_m}{\mu A} \tag{1.49}$$

becomes negligible in oil reservoirs, where Q_m is not too large. However, in gas reservoirs Q_m is large in the vicinity of wells. Therefore the correction factor may often be significant.

1.4 Relative Permeabilities

It was not until 1917 that *Lewis* discovered the coexistence of water, oil and gas in a hydrocarbon reservoir. In 1926 *Becker* and *Parkhurst* had the idea to consider oil and gas in a reservoir as liquid and gaseous phases of the hydrocarbon system being under thermodynamic equilibrium.

The knowledge that finally led to a systematic research of multiphase filtration in porous media originally referred to the gas/oil ratio. In the year 1927 *Uren* conducted experiments, in which he simulated an oil reservoir with gas drive by using a tank filled with sand and gas-saturated oil at a pressure of several bars. From the results of this experiment, *Uren* recognized that on one side the detached gas reduces the permeability, but on the other side provides the energy needed to mobilize the oil.

In the same year *Power* made experiments with a sand-filled pipe *2.20* [m] long and *0.06* [m] in diameter. He injected saturated oil slightly above bubble point pressure into the pipe. In doing so, he observed that at a constant rate the pressure gradient is larger in cases of gas liberation. Thus a two phase flow causes an additional pressure drop for the flowing system. *Power* concluded that the additional pressure loss was due to separated gas bubbles caused by the JAMIN-effect.

An overestimation of the JAMIN-effect led *Herold* to the opinion that a given pressure gradient can only set a certain number of oil-gas interfaces (gas bubbles) in motion. However, this would mean that the drainage area of a well was limited. Though this theory was greatly contested - especially by *Versluy*'s and *Lewis*-; the slogan "more wells, more oil" was accepted in practice. It lasted until the year 1945 when this phenomenon was understood. *Hassler*, *Brunner* and *Deahl* were convicted that a gas bubble was not able to plug a porous medium due to the existence of various cross linkings between the pore channels and the possibility of the gas molecules diffusing through the oil.

In the year 1936 *Hassler* made experiments which contributed greatly to the solution of multiphase problems. The so called *Hassler* core holder was already described in Figure 1.29. First the cores were saturated with oil derivates which were then displaced by air. *Hassler* measured the permeability of air and determined the saturation by weight control of the core. This was possible due to the advantage of a quick demount and mount of the core.

Hassler observed that it is essential to determine the permeability not only for dry cores but for cores with any saturation. The retention of the wetting phase at the outlet is called *end effect* and was also discovered by *Hassler*.

Wyckoff and *Botset* conducted research work with brine and carbon dioxide in the same year as *Hassler* made his investigations. Brine was used to ensure measurability of the electrical conductivity as shown in Figure 1.32.

The model used by *Wyckoff* and *Botset* was 3 [m] long and 0.05 [m] in diameter. They

measured the pressure at 10 equidistant points determining the permeability both of the wetting (k_w) and non-wetting (k_{nw}) phase as a function of saturation. The variation of viscosity and saturation of the samples, at steady-state flow, is determined by the gas/oil ratio. They made the observation that saturation may be independent of the absolute permeability at a given gas/oil ratio.

1.4.1 Definition of Relative Permeability

As the historical review showed, all efforts were made to extend the validity of the *Darcy*-law to multiphase filtration. If this is possible, then the following formulas may be set up:

$$q_w = -A\frac{kk_{rw}}{\mu_w}\frac{\Delta p}{L} \tag{1.50}$$

$$q_{nw} = -A\frac{kk_{rnw}}{\mu_{nw}}\frac{\Delta p}{L} \tag{1.51}$$

where:

k_{rw} is the relative permeability of the wetting phase

k_{rnw} is the relative permeability of the nonwetting phase.

The same indices are also valid for the flow rate q and the viscosity μ. The relative permeability of the wetting phase is defined as:

$$k_{rw}(S_w) = \frac{k_w(S_w)}{k}; \qquad 0 \le k_{rw}(S_w) \le 1\,, \tag{1.52}$$

where k_w is the effective permeability of the wetting phase. This definition is valid for k_{rnw}, also.

Finally, *Leverett* had conducted several experiments concerning the relative permeability in case of a fluid/fluid system and then extended these to three-phase water-oil-gas-systems. He introduced not only the capillary pressure into the equations of multiphase filtration, but together with *Buckley* he also set up the theory of frontal displacement which will be covered in Chapter 4.

1.4.2 Definitions of End-Point Saturations

A relative permeability is zero at a given saturation. For the displacing phases these saturations are called *critical water saturation* (S_{wc}) and *critical gas saturation* (S_{gc}),

respectively. They are the saturations at which the displacing water or gas phase begins to flow.

For the displaced phase the minimum saturation is residual saturation: for oil displaced by water (S_{orw}) or displaced by gas (S_{org}), for gas (S_{gr}) and for water (S_{wr}). They are the saturations which can be achived in laboratory, under reservoir conditions, by infinite long displacement.

The *irreducible water saturation* (S_{wir}) is the pore volume occupied by water in the reservoir at maximum hydrocarbon saturation. In water-wet rock it represents the layer of adsorbed water coating solid surfaces and the pendular water around grain contacts and at pore throats. Irreducible water saturation is an equilibrium situation. It differs from "residual water saturation," and from "critical water saturation" measured by core analysis, as well.

1.4.3 Relative Permeability Measurements

The following three methods can be applied:

- The *Hassler*-method: The principle behind this method is the ability to adjust the phase pressures and the filtration velocity independently by the use of one or two diaphragms.
- The PENN-STATE method: Two fluids are injected simultaneously at constant rates.
- The *Welge* method: The principle is the calculation of the relative permeability using the results received from the displacement experiments.

1.4.3.1 The HASSLER method

Leas, *Jenks* and *Russel* used the *Hassler* device in their instrumentation as shown in Figure 1.31.

Hassler-core holder contains a core *(C)* placed on a diaphragm *(D)*. The diaphragm is an artificial porous medium exhibiting a relatively large capillary threshold pressure. It is fully saturated with the wetting phase to prevent the flow of the non wetting phase downstream. Since the diaphragm is completely impermeable to the non wetting phase, it is perforated in order to inject gas into the system.

The wetting phase can be considered as static under equilibrium conditions. This equilibrium will be achieved if the pressure drop along the core keeps balance to gravity. The pressure can be regulated, so the saturation distribution can be regarded as homogeneous.

The pressure drop is measured along the core, and the wetting phase pressure is regulated by a mercury flask. The saturations are directly marked by the meniscus m. In doing so the relative permeability of gases is determined. The wetting phase remains immobile being in capillary equilibrium with the flowing non-wetting phase.

Using the device by *Rappoport* and *Leas* (see Figure 1.32) it is possible to measure the relative permeability of the wetting phase. A significant distinction from the method described above is the use of two diaphragms between which the core is positioned. The desired pressure of the non-wetting phase can be fixed. The wetting phase circulates from top to bottom. In order to obtain a homogeneous saturation distribution in the core, it is essential to regulate the flow velocity so that the pressure drop approximately becomes equal to the hydrostatic pressure difference.

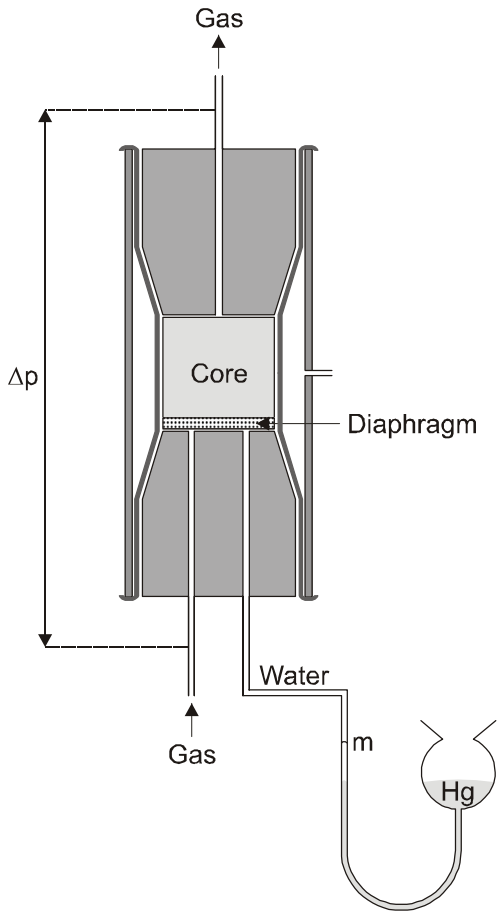

Figure 1.31: Schematic diagram of a device for measuring relative permeabilities of the non-wetting phase (after *Leas, Jenks*, and *Rassel*)

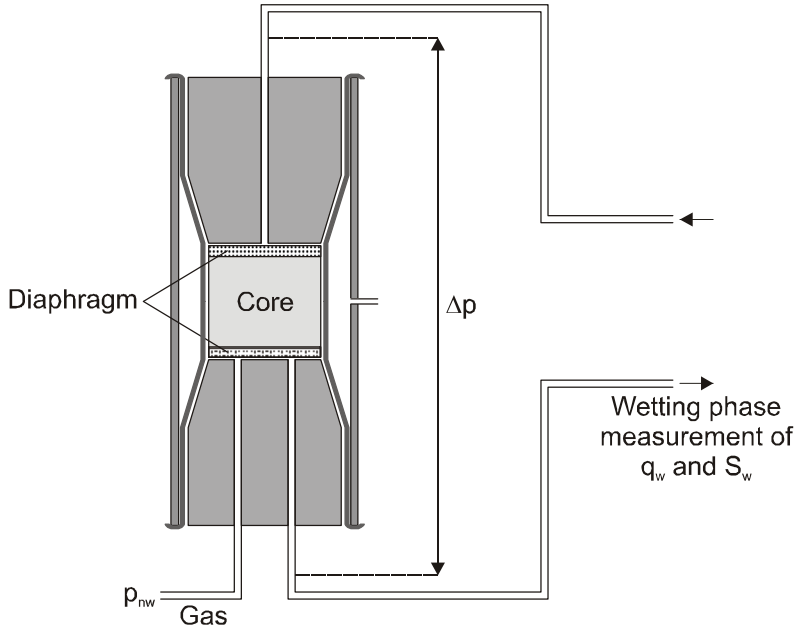

Figure 1.32: Schematic diagram of a device for measuring relative permeabilities of the wetting phase (after Rappoport and Leas)

The *Hassler* method is considered theoretically adequate and efficiently reproducible.

Summarized, the essence of this method is that only the relative permeability of the wetting phase will be measured, whereas the non-wetting phase is immobile.

As an example of the efforts of many scientific groups to develop a modification of the *Hassler*-method - in order to measure the relative permeability of both phases some efforts were made by *Osoba* as shown in Figure 1.33. The method used by *Hafford* as shown in Figure 1.34 which can be considered as a simplification of the instrumentation of *Osoba*.

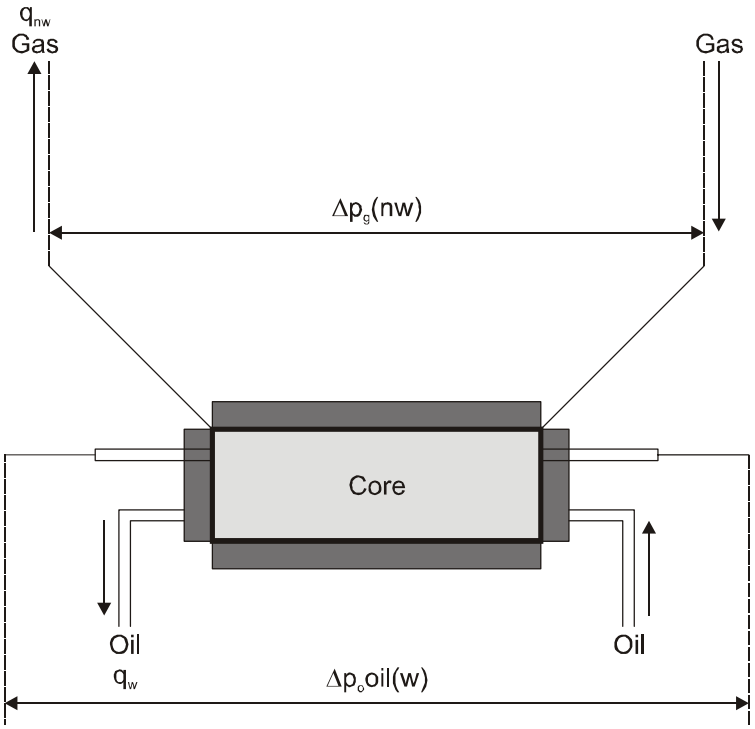

Figure 1.33: Schematic diagram of a device for relative permeability measurements (after *Osoba*)

If the flow rate is high enough to prevent capillary-end-effects (explained in Chapter 4), it is possible to run the experiment without a diaphragm on the outlet side.

Although *Hafford* measured the saturation by weighing, the accuracy of this experiment is questionable, since demounting the core for weighing (being under high pressure during the measurement of relative permeability) causes the expansion of the fluids. Therefore it may be possible that certain fluid quantities will be displaced from the core. *Loomis*, *Crowell* and *Richardson* investigated this problem and verified the reproducibility of the *Hassler* method by neglecting the amount of fluids displaced from the core during demounting.

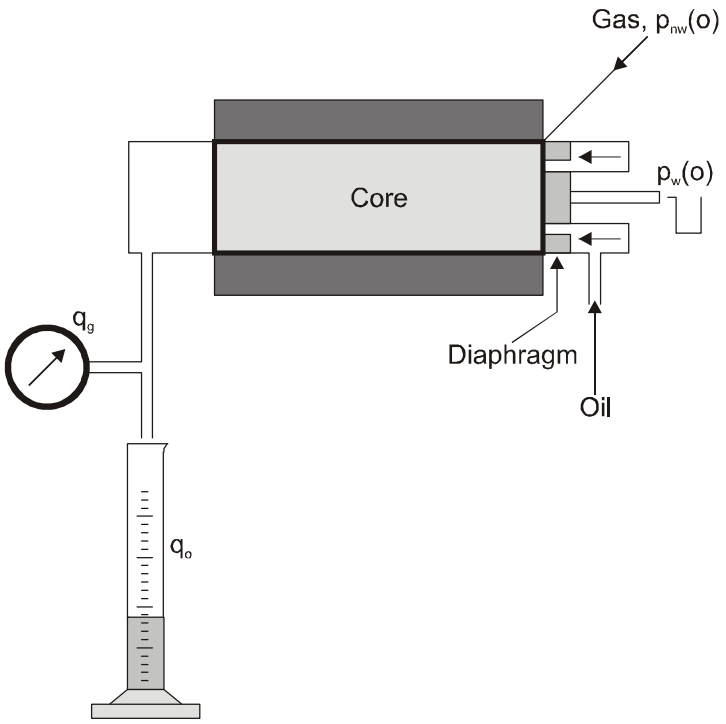

Figure 1.34: Schematic diagram of a device for relative permeability measurements (after *Hafford*)

1.4.3.2 PENN-STATE-Method

This method was developed by *Yuster* and colleagues at Pennsylvania State University, therefore the name PENN-STATE. In many cases it is referred to as the dynamic steady-state displacement method. Figure 1.35 presents the instrumentation used by *Morse*, *Terwilliger* and *Yuster* to measure relative permeability. The basic principle behind this method is the following:

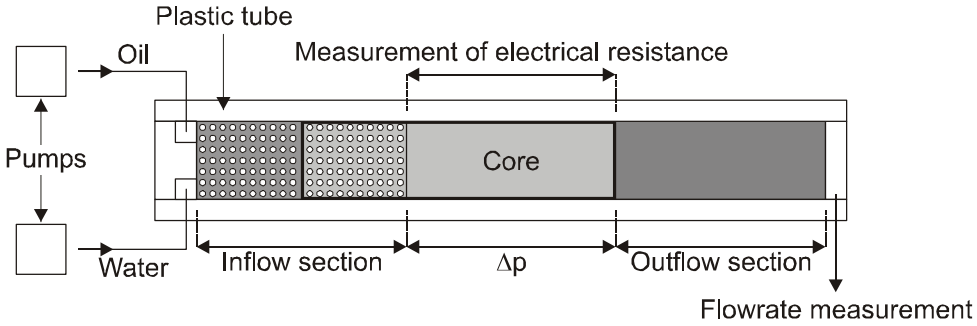

Figure 1.35: Schematic diagram of the PENN-STATE device for relative permeability measurements (after *Morse, Terwilliger*, and *Yuster*)

At first the core is embedded in a plastic tube in order to achieve the indispensable sealing. The core placed inside the holder has been fitted between two porous packings which should provide both satisfactory mixing of fluids and the prevention of capillary end effects at the inlet and outlet of the core. The fluids are injected at a constant rate by two micropumps.

Likewise *Yuster* determined the saturation by weighing. Determination in terms of measuring the electrical conductivity has not been very successful, since conductivity not only depends on saturation but also on the fluid distribution.

Problems arise concerning the application of this method in connection with the development of capillary contact between the core and the two packings. It is also difficult to guarantee the homogeneous distribution of the phases.

1.4.3.3 *Welge*-Method

This method was at first developed by *Welge* and it is based on the evaluation a continuous two phase displacement.

1.4.4 Saturation Distribution and Relative Permeability

The main difference between the *Hassler* method and the PENN-STATE principle is the fact that the *Hassler* method considers the movement of only one fluid. Therefore it is evident that the mobile phase forms continuous paths, called channels, through the porous medium. But in case of dynamical methods both phases are in motion. The filtration processes will only coincide with the results of the *Hassler*-method, if each phase individually forms some channel system of its own and maintains this. In consequence the fluids should not flow alternately through the same channels as small drops or larger filaments.

In 1949 and 1950, two experiments were conducted in order to analyse the nature of phase distribution in porous media. The so called API-research project 47B was carried out at the University of Oklahoma. Between two transparent slices, little spheres were packed to simulate a porous medium. The water and oil filtrated simultaneously through this artificial medium. The motion of the fluids had been filmed and magnified.

The film verified that water and oil form their own flow channel systems in which the wetting fluid occupies the smaller pores. Increasing oil saturation affected a growing number of oil channels and a decrease of water channels. Further it was noticed that these channels maintain their position. The flow has been laminar and - in spite of great tortuosity - free of turbulences.

Simultaneously the distribution of the residual oil saturation after water displacement has been investigated. It was noticed that the residual oil is distributed in few oil filaments occupying the relatively larger pores.

AMOCO also made experiments on sand packing as a porous medium. As the wetting fluid, Wood-metal was used. The non-wetting fluid was colored synthetic resin. After transforming the fluids into a solid state, the saturation distribution due to the relative permeabilities was made observable. The preparation of the sample by grinding off progressively, a great amount of photographs, enable a journey through the porous medium. The method also proved the theory of separated flow through the pore channels.

Basically it must be distinguished between two kinds of displacement:

- the wetting phase is the displacing fluid (imbibition)
- the wetting phase is the displaced fluid (drainage)

The phase whose saturation has been increased after displacement is always considered the displacing phase. Differences between imbibition and drainage are illustrated in Figure 1.36. Just as supposed the relative permeability is not only a function of saturation, but also depends on the saturation distribution (in consequence of the structure of the pore channels and the wettability of the porous medium).

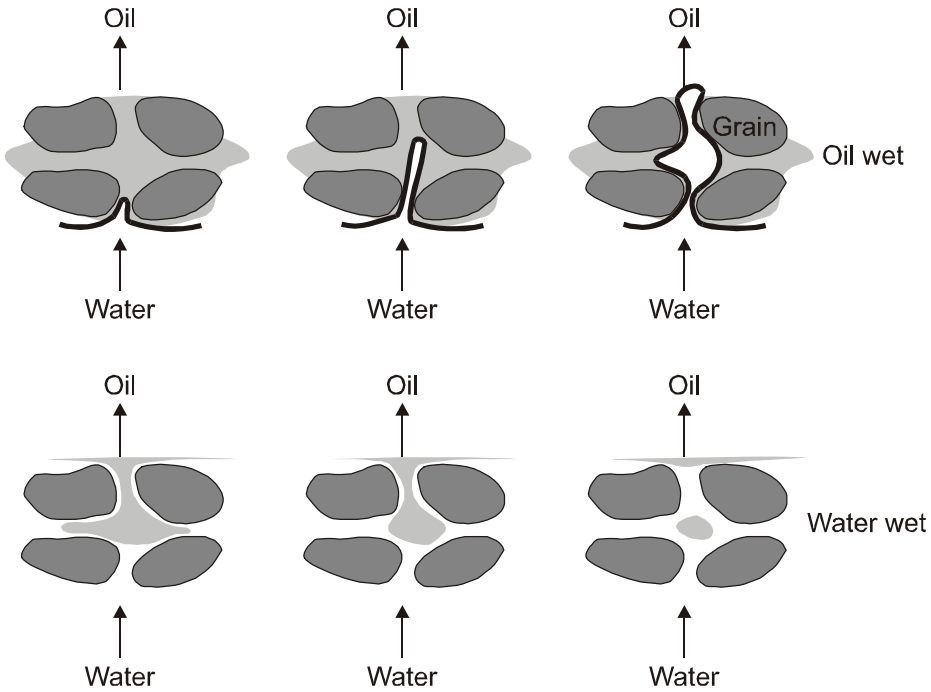

Figure 1.36: Schematic diagram of water invasion into porous media permeabilities of the wetting phase (after *Craig*)

The distribution of the non-wetting phase at drainage differs from the one at imbibition. Figure 1.37 illustrates this aspect. The deviation of the curve in the direction of displacement is referred to as the hysteresis of relative permeability. In addition Figure 1.38 shows two oil/water permeability function pairs to indicate the role of wettability.

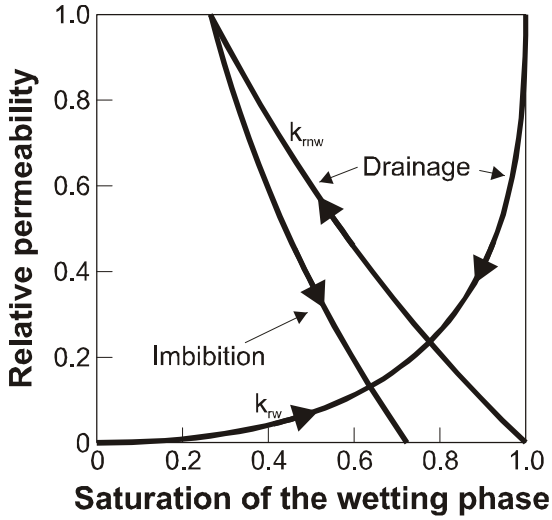

Figure 1.37: Drainage and imbibition relative permeability characteristic (after *Craig*)

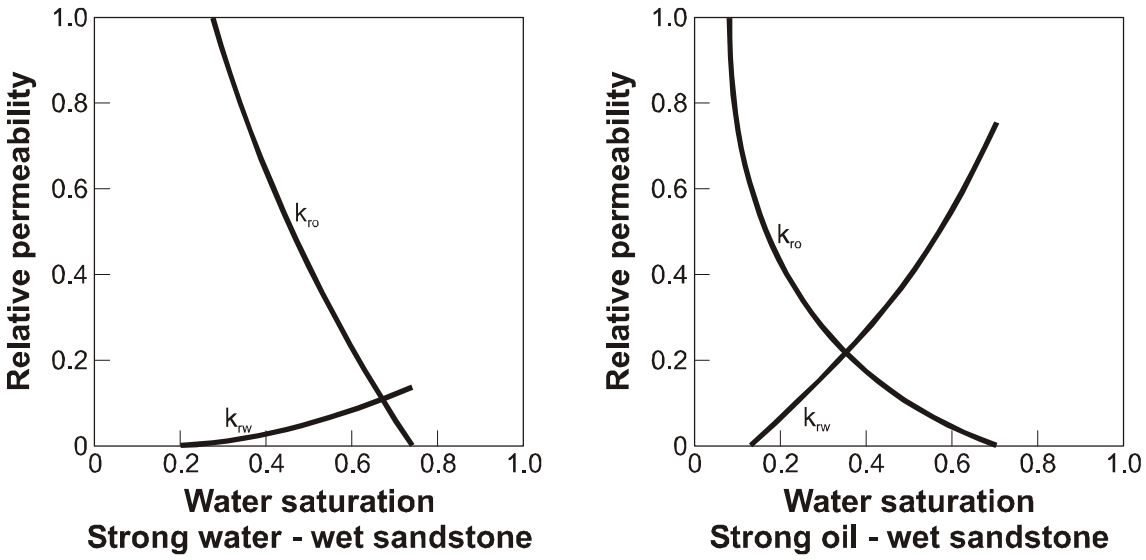

Figure 1.38: Typical water/oil relative permeability characteristic (after *Craig*)

1.5 References

1.1 Amott,E.: "Observations Relating to the Wettability of Porous Rock," *Trans.AIME* (1959) **216,** 156-62.

1.2 Anderson, W., G.: Wettability Literature Surway- Part 1: Rock/Oil/Brine Interactions and Effects of Core Handling on Wettability," *JPT* (Oct.1986) 1125-1144. (S)

1.3 Anderson, W., G.: Wettability Literature Surway- Part 2: Wettability Measurement," *JPT* (Nov.1986) 1246-1262. (S)

1.4 Craig, F.F. Jr.: "The Reservoir Engineering Aspects of Waterflooding" *Monograph Vol. 3 of the Henry L. Doherty series* (1971)

1.5 Donaldson, E.C., Thomas, R.D., and Lorenz, P.B.: "Wettability Determination and Its Effect on Recovery Efficiency," *SPEJ* (March 1969) 13-20.

1.6 Fatt, I. and Davis, D.H.: "Reduction in Permeability with overburden pressure" *Trans. AIME* **195** (1952) p.329

1.7 Hall, H.N.: *5. Petroleum Technology* (Jan. 1953)

1.8 Hassler; G.L. and Brunner, E.(1945):"Measurement of Capillary Pressure in Small Core Samples", *Trans.AIME*, **160**, p. 114-123

1.9 Krumbein, W.C. and Sloss, L.L.: "Stratigraphy and Sedimentation" *Appleton century publication*, Crofts Inc. New York.

1.10 Leach, R.O. et al.: "A Laboratory and Field Study of Wettability Adjustment in Waterflooding," *JPT* (Feb.1962) 206-12; *Trans., AIME,* **225**.

1.11 Leas, W.S., Jenks, W.J. and Russel, Ch.D.: "Relative permeability to Liquid in Liquid Gas System" *Trans. AIME **192*** (1951)

1.12 Link,P.K.: "Basic Petroleum Geology" *OGCI Publications*, Tulsa Oklahoma USA (1983)

1.13 O'Meara, D.J. and Crump, J.G.: "Measuring Capillary Pressure and Relative Permeability in a Single Centrifuge Experiment", SPE Paper 14419, presented at the 60th Annual Technical Conference and Exhibition of SPE, held in Las Vegas, NV, Sept. 22-25, 14 p

1.14 Monicard, R.P.: "Properties of Reservoir Rocks: Core Analysis" *Institut Francais du Petrole Publications Ed. Technip*, Paris (1980)

1.15 Morse, R.A., Terwilliger, P.L. Yuster; S.T.: "Relative Permeability Measurements on Small Core Samples" *Producers Monthly II* (1947)

1.16 Osoba, J.S. et al.: "Laboratory Measurements of Relative Permeability" *Trans. AIME **192*** (1951)

1.17 Rappaport, L.A. and Leas, W.J.: "Relative Permeability to Liquid in Liquid Gas System" *Trans AIME **195*** (1952)

1.18 Slobod, R.L., Chambers, A. and Prehn, W.L.: "Use of Centrifuge for Determining Connate Water, Residual Oil, and Capillary Pressure Curves in Small Core Samples, Trans.AIME, Vol.192, p.127-134

1.19 Treiber, L.E., Archer, D.L. and Owens, W.W.: " A Laboratory Evaluation of the Wettability of Fifty Oil Producing Reservoirs," SPEJ (Dec. 1972) 531-40; *Trans AIME, **253**.*

1.20 Torsaeter, A., Abtahi, M: "Experimental Reservoir Engineering. Laboratory Handbook", www.ipt.ntnk.no/~ oletor/labbook - 2003 pdf

1.21 Wunderlich, R.W.: "Imaging of Wetting and Nonwetting Phase Distributions: Application to Centrifuge Capillary Pressure Measurements", *SPE Paper 14422* presented at the 60th Annual Technical Conference and Exhibition of *SPE*, held in Las Vegas, NV, September 22-25, 11p

2 Equations of Single-Phase Filtration

A quantitative description of a physical process always requires a mathematical formulation. These mathematics aim at approximating these processes in a more or less sufficient way, but they will always refer only to the most important aspects of the process. These mathematics are summarized by the term *mathematical model.*

Any system properties not included in the mathematical model can't be taken into consideration in further calculations.

The description of motion of a continuum are based on the so called constitutive assumptions or constitutive equations. They usually take the form of relationships between fluxes and driving forces. We mention as examples of fluxes those of mass, momentum and energy of various kinds. The conceptional assumption is more comprehensive than the equation, although outwardly the assumptions take the form of equations. We do so to emphasize that these equations define the assumed behavior of ideal continua. These equations are definitions extracted from physical experiences, perhaps fortified by experimental evidence. The constitutive equations are often referred to as phenomenological equations because of their dependence on experimental evidence. There exist a large number of constitutive equations describing relationships between fluxes and driving forces. For example: *Newton*'s law relating shearing force to velocity gradient; *Fourier*'s law relating heat flow to temperature gradient; *Fick*'s law relating flow of matter of a component to its concentration gradient in a multicomponent system; *Ohm*'s law relating electrical current to electrical potential gradient etc.

In all these cases we see a simple, linear dependence of a flow on some conjugated force. Such a simple relationship does not always hold. There are more or less powerful approaches for abstracting and simplifying natural phenomena. In each case the simplification is carried to the point where the model is still amenable to mathematical treatment, yet is not so simple as to miss those features of the studied phenomena it is intended to describe. While these equations determine the features of a mathematical model we refer to this as fundamental equations.

A more general law of the continuum theory is the law of conservation of the extensive properties as mass, momentum and energy. The resulting equations of continuity are generally written in the form of partial differential equations. They are commonly referred to as field equations. However, either the fundamental nor the field equations contain information regarding the properties of the particular continua under consideration. They form an under defined mathematical model, insufficient to yield specific answers unless further equations are supplied.

Mathematical models of filtration are generally based on *Darcy*'s law. The field equation express the conservation of the fluid mass. The mechanical properties of the fluids are formulated through the equations of state. In order to solve this set of equations, further equations are required to determine the initial state and the boundary conditions.

Basically one must distinguish between mass flow and filtration. During mass flow all mass particles of the system are in motion. In case of filtration only a certain part of the particles are moving, all other mass particles form a solid matrix.

2.1 Fundamental Equation of Filtration.

2.1.1 Differential Form of the *Darcy*-Law

Consider a certain volumetric element in space with fixed boundaries. The size of the volume must be selected in a manner so that random effects may be statistically eliminated. To simplify but without losing the generality we take a cylindrical element. The surface of this element is build from stream lines and the base surfaces are perpendicular to it. Its length is δs and has a cross section δA. Equal forces are acting on the bulk of fluid within the control volume. Two types of forces should be distinguished: body forces and surface forces. Regarding *Newton*'s law of motion, the fluid body will accelerate as long as the resultant acceleration is not zero, but it will keep its velocity; we seek a value for velocity such that the resultant acceleration equals the null vector.

In filtration process the most important forces are listed in the following:

- force of compression(acting on surface)
- force of gravity(acting on body)
- forces of inertia(acting on body)
- frictional forces(acting on surfaces)
- capillary forces(acting on surfaces)

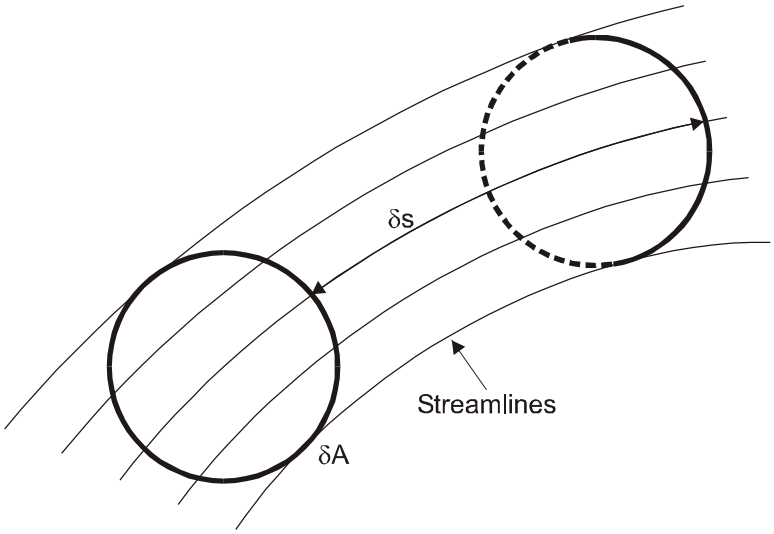

Figure 2.1: Schematic diagram of a field segment

Convective and local acceleration are mostly so small in case of filtration, forces of inertia may be neglected for steady state and non-steady state filtration as well.

Frictional forces are generally composed from two terms. The first represent the adhesive forces and is proportional to the velocity inside the pore channels. The second term refers to the turbulence and is proportional to the squared velocity. If the flow is laminar the second term disappears.

The frictional force is actually to be regarded as a surface force acting on the surfaces inside the pore channels. A very complicated labyrinthic structure of the pore channels makes accurate calculations impossible. Therefore only an average value referring to one volume unit is considered. Therefore in case of filtration frictional forces become volumetric forces, but these are only fictious - just as is the velocity of filtration - since it results only from a mathematical derivation and not from observation and measurement.

Capillary forces are surface forces between two immiscible fluids which are separated by an interface inside the pore channels. Calculation of these forces is only possible in sum, in reference to the cross-sections of the pore channels. The capillary force is therefore regarded as a fictitious surface force. In the case of a one-phase filtration, capillary forces are considered only if the water-bearing layer is partially empty.

Such cases are known to exist in hydrology and are called unsaturated filtrations or unconfined flow.

We assume that only the force of compression F_p, the force of gravity F_g, and the frictional force F_μ, which are proportional to the velocity of filtration, are important. The forces of inertia and the forces of turbulent friction can be neglected.

The following equation for the equilibrium of forces may be set up:

$$F_\mu + F_p + F_g = 0 \tag{2.1}$$

In reference to a defined elementary volumetric element in Figure 2.1 those forces may be mathematically specified as follows:

- The force of compression:

$$F_p = -\phi\delta A \nabla p \delta s\,, \tag{2.2}$$

where $\phi\delta A$ is the free surface (pore surface) of the element and $\nabla p \delta s$ the pressure difference along δs.

- The force of gravity:

$$F_g = -\rho g \phi \delta A \vec{i}_3 \, \delta\vec{s}\,, \tag{2.3}$$

where the unit vector $\vec{i}_3$ is directed upwards.

- The laminar frictional force:

$$F_\mu = -B\mu\delta A\vec{u}\delta\vec{s}, \tag{2.4}$$

where B is a coefficient fort a given porous medium.

Substituting Eq. 2.2 - Eq. 2.4 into Eq. 2.1 leads to:

$$-\left(\nabla p + \mu\frac{B}{\phi}u + \vec{i}_3\rho g\right)\cdot\phi\delta A\delta\vec{s} = 0, \tag{2.5}$$

or after reducing:

$$\nabla p + \mu\frac{B}{\phi}\vec{u} + \vec{i}_3\rho g = 0. \tag{2.6}$$

In addition, the term ϕ/B is defined as k and interpreted as the permeability. After transforming Eq. 2.6 the differential form of the law of *Darcy* is obtained:

$$\vec{u} = -\frac{k}{\mu}(\nabla p + \vec{i}_3\rho g) \tag{2.7}$$

We introduce a so called potential function instead of pressure:

$$\psi = gx_3 + \int_{p_o}^{p}\frac{dp}{\rho}; \qquad \rho = \rho(p) \tag{2.8}$$

where p_o is a reference pressure at x_3.

Then Eq. 2.7 becomes:

$$\vec{u} = -\frac{k\rho}{\mu}\nabla\psi, \tag{2.9}$$

Differentiation of Eq. 2.8, yields:

$$\rho\nabla\psi = \nabla p + \rho g\vec{i}_3 \tag{2.10}$$

If Eq. 2.10 is substituted into Eq. 2.9, then Eq. 2.7 is obtained.

2.1.2 Anisotropic Porous Media

The Eq. 2.9 is a linear vector-vector equation. In an isotropic porous medium the permeability k is a scalar, but in an anisotropic medium is a tensor.

Thus

$$\bar{u} = -\frac{\rho}{\mu}\bar{k}\nabla\psi \tag{2.11}$$

in detailed form:

$$\begin{bmatrix} u_1 \\ u_2 \\ u_3 \end{bmatrix} = -\frac{\rho}{\mu}\begin{bmatrix} k_{11} & k_{12} & k_{13} \\ k_{21} & k_{22} & k_{23} \\ k_{31} & k_{32} & k_{33} \end{bmatrix}\begin{bmatrix} \frac{\partial\psi}{\partial x_1} \\ \frac{\partial\psi}{\partial x_2} \\ \frac{\partial\psi}{\partial x_3} \end{bmatrix}. \tag{2.12}$$

If the matrix is symmetrical $(k_{ij} = k_{ji})$ it is possible to transform the coordinate system so that all values apart from the main diagonal become zero. Directions parallel to these coordinate axes are called principal directions (axis) of the porous medium. These principal directions are orthogonal to each other. Writing Eq. 2.12 for a coordinate system with axis parallel to the principal directions of the porous medium, the *Darcy*'s law becomes the following:

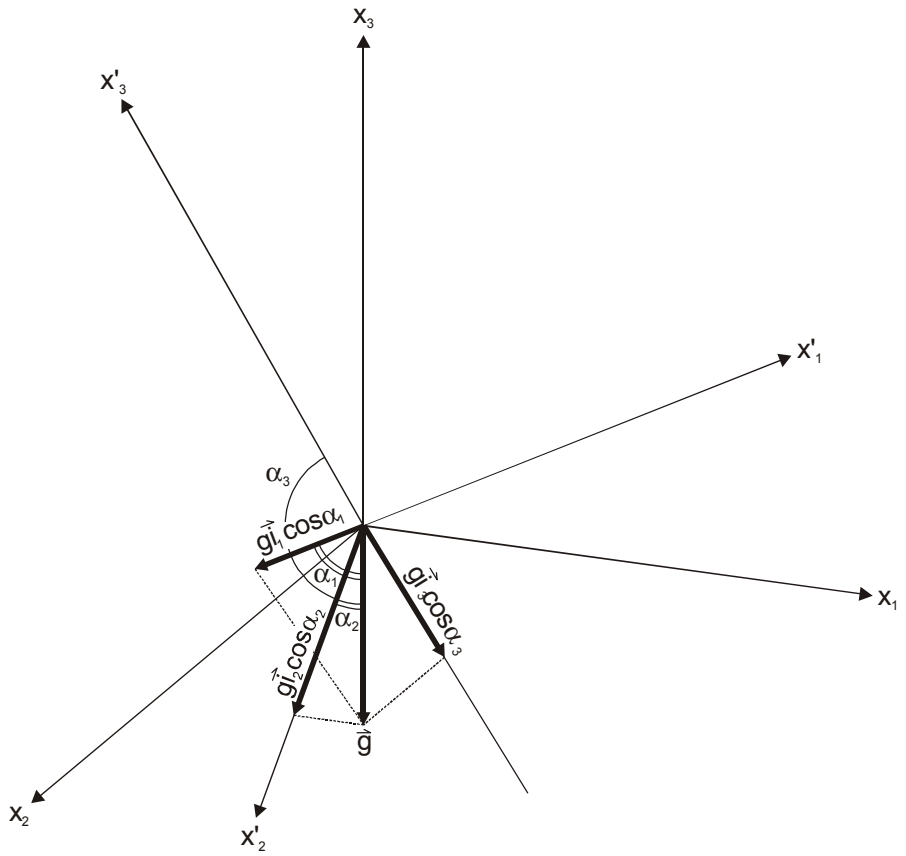

Figure 2.2: Transformation of the coordinate system

$$\begin{bmatrix} u'_1 \\ u'_2 \\ u'_3 \end{bmatrix} = -\frac{\rho}{\mu} \begin{bmatrix} k_1 & 0 & 0 \\ 0 & k_2 & 0 \\ 0 & 0 & k_3 \end{bmatrix} \begin{bmatrix} \frac{\partial \psi'}{\partial x'_1} \\ \frac{\partial \psi'}{\partial x'_2} \\ \frac{\partial \psi'}{\partial x'_3} \end{bmatrix}, \tag{2.13}$$

where:

$$\psi' = g \sum_{i=1}^{3} x'_i \cos\alpha_i + \int_{p_o}^{p} \frac{dp}{\rho(p)} \tag{2.14}$$

α_i are defined as the angles between the coordinate axes and vector of gravity. In this coordinate system Eq. 2.13 becomes a little bit more complicated:

$$\vec{u} = -\frac{\rho}{\mu}\bar{k}\nabla\psi' = -\frac{\bar{k}}{\mu}\left(\nabla p + \rho g \sum_{i=1}^{3} \vec{i}_i \cos\ \alpha_i\right) \tag{2.15}$$

Figure 2.2 Transformation of the coordinate system $(x_1 x_2 x_3)$ into (x'_1, x'_2, x'_3) . The potential function ψ in the coordinate system (x'_1, x'_2, x'_3) is different to the one in the coordinate system $(x_1 x_2 x_3)$ since gravity is not parallel to the x_3 axis.

According to Eq. 2.15 the velocity of filtration is proportional to the potential gradient. However, the proportions are not the same in different coordinate directions.

2.2 Equation of State

2.2.1 Incompressible Fluids

The potential described by Eq. 2.8 includes the density of the fluid. It is a function of pressure. If this is not the case the fluid is considered incompressible:

$$\frac{d\rho}{dp} = 0 \tag{2.16}$$

or after integration:

$$\rho = \text{constant}. \tag{2.17}$$

2.2.2 Low Compressibility Fluids

For low compressible fluids one may assume that the fractional change of volume of the fluid as pressure changes at constant temperature is constant. This constant is called the coefficient of isothermal compressibility which is defined by:

$$c = -\frac{1}{V_f}\left(\frac{dV_f}{dp}\right)_T. \tag{2.18}$$

By substituting: (2.19)

$$V_f = m/\rho, \tag{2.20}$$

where m is the mass of fluid, a constant, into Eq. 2.18 we obtain:

$$c = -\frac{1}{\frac{m}{\rho}}\frac{d\left(\frac{m}{\rho}\right)}{dp} = \frac{1}{\rho}\frac{d\rho}{dp}, \tag{2.21}$$

After integration of Eq. 2.21, yields:

$$\rho = \rho_o e^{c(p-p_o)}, \tag{2.22}$$

where: ρ_o is the density of fluid at any reference pressure (p_0).

Applying TAYLOR's rule and neglecting the terms of higher order we get the following approximation:

$$\rho \approx \rho_0 \cdot [1 + c(p - p_o)] \tag{2.23}$$

2.2.3 Formation Volume Factor

The volume of produced fluid at surface conditions is usually different than the volume of fluid entering the wellbore at reservoir conditions. This change of volume is mainly due to changes in pressure and temperature. Since these fluids are compressible a change of phase also can take place (gas evolving from oil), but in this text only one phase is considered. This change of volume should be accounted for by using a conversion factor (B) which is called Formation Volume Factor. This conversion factor can be defined as:

$$B = \frac{\text{volume of fluid under reservoir conditions}}{\text{volume of fluid at standard conditions}}$$

Formation Volume Factor for oil is the volume of 1 standard m^3 oil (1 m^3 tank oil) under reservoir conditions p,T and solution gas-oil ratio R_s.

Tthe rate of fluid under reservoir conditions can be calculated by:

$$q_o(p, T, R_s) = B_o(p, T, R_s) q_{os} \tag{2.24}$$

2.2.4 Ideal and Real Gases

For ideal gases according to the law of *Boyle-Mariott*:

$$pV = \frac{m}{M}RT, \tag{2.25}$$

where m is the mass of gas, M the molecular weight and V the volume. Since the density of a gas is defined as:

$$\rho = \frac{m}{V}. \tag{2.26}$$

Substituting Eq. 2.25 into Eq. 2.26, yields:

$$\rho = \frac{M}{RT}p \tag{2.27}$$

Taking the derivative of Eq. 2.27 yields:

$$\frac{d\rho}{dp} = \frac{M}{RT} \tag{2.28}$$

Dividing Eq. 2.28 by Eq. 2.27 we obtain:

$$c_g = \frac{1}{\rho}\frac{d\rho}{dp} = \frac{1}{p} \tag{2.29}$$

For real gases Eq. 2.27 becomes:

$$\rho = \frac{M}{RTZ(p)}\frac{p}{}, \tag{2.30}$$

where $Z(p)$ is the real gas compressibility factor. Thus the compressibility of a real gas is defined as:

$$c_g = \frac{1}{\rho}\frac{d\rho}{dp} = \frac{1}{p} - \frac{1}{Z(p)}\frac{\partial Z}{\partial p} \tag{2.31}$$

The formation volume factor for gas is defined by:

$$B_g = \frac{\rho_s}{\rho_g} \tag{2.32}$$

Substituting Eq. 2.30 into Eq. 2.32 , yields:

$$B_g = \frac{Mp_s/RT_s}{Mp/RTZ(p)} \tag{2.33}$$

After simplification Eq. 2.33 becomes:

$$B_g = \frac{p_s TZ(p)}{pT_s} = C \cdot \frac{TZ}{p} \tag{2.34}$$

Where T_S,p_S are the standard temperature and pressure.

The volume of gas under any pressure and temperature can also be calculated by:

$$V(p, T) = V_s B_g \tag{2.35}$$

where: V_S is the volume of gas at standard conditions.

2.2.5 Equation of continuity

The equation of continuity describes the law of mass conservation. We use a rectangular coordinate system and consider a parallelepiped as a control volume (see Figure 2.3) with a porosity ϕ.

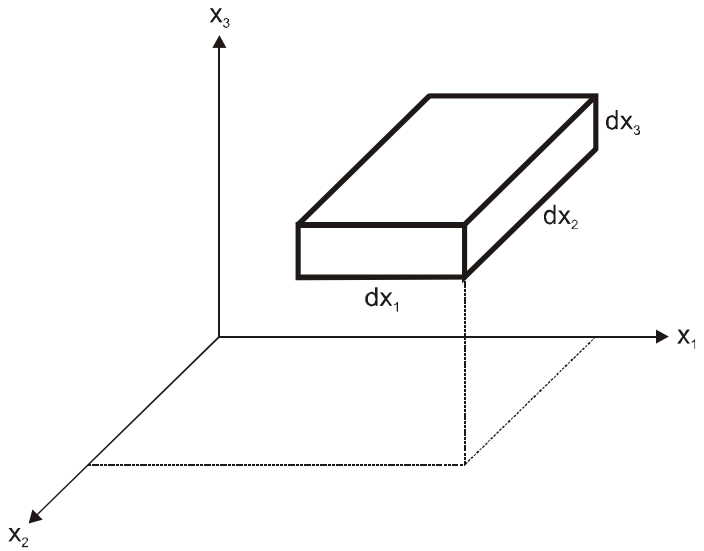

Figure 2.3: Volume element in a cartesian coordinate system

The pore volume is then:

$$\phi dx_1 dx_2 dx_3 . \tag{2.36}$$

The fluid mass content in the control volume is:

$$\rho\phi dx_1 dx_2 dx_3 . \tag{2.37}$$

The change of quantity during a time interval *dt* is:

$$\frac{\partial(\rho\phi)}{\partial t} dx_1\ dx_2\ dx_3\ dt. \tag{2.38}$$

On the other side, the quantity of fluid flowing through the surface at x_1 and $x_1 + dx_1$ is:

$$(\rho u_1)_{x_1}\ dx_2\ dx_3\ dt \tag{2.39}$$

and

$$(\rho u_1)_{x_1 + dx_1}\ dx_2\ dx_3 dt\,. \tag{2.40}$$

The change of flowing quantity results in:

$$-\frac{\partial}{\partial x_1}(\rho u_1) dx_1 dx_2 dx_3 dt\,. \tag{2.41}$$

Also considering the filtration in the direction of other coordinates. Eq. 2.38 and Eq. 2.41 result in:

$$-\frac{\partial}{\partial t}(\phi\rho) \;=\; \sum_{i=1}^{3} \frac{\partial}{\partial x_i}(\rho u_i). \tag{2.42}$$

where the term $dx_1 dx_2 dx_3$ were already cancelled. After writing it in vector form Eq. 2.42 becomes:

$$-\frac{\partial}{\partial t}(\phi\rho) \;=\; \nabla(\rho \vec{u}) \tag{2.43}$$

Substituting Eq. 2.15 into Eq. 2.43 yields :

$$\nabla\left(\frac{\bar{k}}{\mu}\rho^2 \nabla\psi\right) \;=\; \frac{\partial}{\partial t}(\phi\rho) \tag{2.44}$$

Or in detailed form:

$$\frac{\partial}{\partial x_1}\left(\frac{k_1}{\mu}\rho^2\frac{\partial\psi}{\partial x_1}\right) + \frac{\partial}{\partial x_2}\left(\frac{k_2}{\mu}\rho^2\frac{\partial\psi}{\partial x_2}\right) + \frac{\partial}{\partial x_3}\left(\frac{k_3}{\mu}\rho^2\frac{\partial\psi}{\partial x_3}\right) \;=\; \frac{\partial}{\partial t}(\phi\rho) \tag{2.45}$$

Differentiation of Eq. 2.14 yields:

$$\rho^2 \nabla \psi = \rho \nabla p + \rho^2 g \sum_{i=1}^{3} \vec{i}_i \cos \alpha_i . \tag{2.46}$$

If the 3rd coordinate direction is vertical then Eq. 2.46 become more simple:

$$\rho^2 \nabla \psi = \rho \nabla p + \rho^2 g \vec{i}_3$$

Substituting Eq. 2.46 into Eq. 2.44 yields:

$$\nabla \left[\frac{\bar{k}}{\mu} \rho \nabla p \right] + \nabla \left[\rho^2 \frac{\bar{k}}{\mu} g \vec{i}_3 \right] = \frac{\partial}{\partial t} (\phi \rho) . \tag{2.47}$$

If the 3rd coordinate direction is vertical then Eq. 2.47The second term on the left hand side is often very small compared to the first. For these cases the following equation is sufficient:

$$\nabla \left[\frac{\bar{k}}{\mu} \rho \nabla p \right] = \frac{\partial}{\partial t} (\phi \rho) . \tag{2.48}$$

2.3 Special Forms of the Equation of Filtration

2.3.1 Incompressible Fluids

Assuming an incompressible fluid and porous media, then ρ, ϕ and μ are constant and Eq. 2.48 becomes:

$$\nabla[\bar{k}\nabla p] = 0. \tag{2.49}$$

In the case of a homogenous porous media and $\bar{k} = const$ then Eq. 2.49 becomes:

$$\nabla[\bar{k}\nabla p] = k_1\frac{\partial^2 p}{\partial x_1^2} + k_2\frac{\partial^2 p}{\partial x^2{}_2} + k_3\frac{\partial^2 p}{\partial x_3^2} = 0. \tag{2.50}$$

Eq. 2.50 can be simplified by introducing a new independent variable:

$$\eta_i = x_i\sqrt{\frac{k_1}{k_i}},\ i = 1, 2, 3 \tag{2.51}$$

Then Eq. 2.50 becomes the Laplace equation:

$$\frac{\partial^2 p}{\partial \eta_1^2} + \frac{\partial^2 p}{\partial \eta_2^2} + \frac{\partial^2 p}{\partial \eta_3^2} = 0 \tag{2.52}$$

For isotropic porous media Eq. 2.49 becomes:

$$\nabla[\bar{k}\nabla p] = \nabla^2 p = \frac{\partial^2 p}{\partial x_1^2} + \frac{\partial^2 p}{\partial x_2^2} + \frac{\partial^2 p}{\partial x_3^2} = 0 \tag{2.53}$$

2.3.2 Low Compressibility Fluids

Based on Eq. 2.22 the following transformation can be made:

$$\rho\nabla p = \rho_0 e^{c(p-p_0)}\nabla p = \frac{1}{c}\nabla\left(\rho_0 e^{c(p-p_0)}\right) = \frac{1}{c}\nabla\rho \tag{2.54}$$

Substituting Eq. 2.54 into Eq. 2.48 becomes:

$$\nabla\left[\frac{\bar{k}}{c\mu}\nabla\rho\right] = \frac{\partial}{\partial t}(\phi\rho) \tag{2.55}$$

Differentiation of Eq. 2.23 gives:

$$\nabla\rho = \rho_o c \nabla p . \tag{2.56}$$

Substituting Eq. 2.23 and Eq. 2.56 into Eq. 2.55 results in:

$$\nabla\left[\frac{\bar{k}}{\mu}\rho_o \nabla p\right] = \frac{\partial}{\partial t}\{\phi\rho_o[1 + c(p - p_o)]\} \tag{2.57}$$

In Eq. 2.57 ρ_0, c and p_0 are constant. The viscosity μ can be regarded as constant as well hence the fluid compressibility is small.

For a homogeneous isotropic and incompressible porous media and constant fluid viscosity, Eq. 2.55 becomes:

$$\nabla^2 p = \frac{1}{K}\frac{\partial p}{\partial t}, \tag{2.58}$$

where:

$$K = \frac{k}{\mu c \phi} \tag{2.59}$$

$K[m^2 s^{-1}]$ is defined as the piezometric conductivity. Eq. 2.58 is identical to the *Fourier*-equation of heat conductivity.

2.3.2.1 Elastic Porous Media

The porosity and the permeability of an elastic porous medium are both functions of pressure:

$$k = k(p), \qquad \phi = \phi(p) \tag{2.60}$$

The actual functions have to be determined by measurements.

Without serious restictions one may assume that the interdependencies are small and the alteration of porosity and permeability are proportional to pressure changes. Then these functions in Eq. 2.60 are similar to Eq. 2.22 and may be written as follows:

$$\begin{aligned} k &= k_o e^{c_k(p - p_o)} \\ \phi &= \phi_o e^{c_\phi(p - p_o)} \end{aligned} \tag{2.61}$$

Substituting Eq. 2.61 together with Eq. 2.22 into Eq. 2.48 leads to:

$$\nabla\left[\frac{k_o\rho_o}{\mu}e^{(c+c_k)(p-p_o)}\nabla p\right] = \frac{\partial}{\partial t}[\phi_o\rho_o e^{(c+c_\phi)(p-p_o)}] \tag{2.62}$$

Eq. 2.62 can be written as:

$$\frac{k_o\rho_o}{\mu(c+c_k)}\nabla[\nabla(e^{(c+c_k)(p-p_o)})]= \\ \frac{\phi_o\rho_o(c+c_\phi)}{c+c_k}e^{(c_\phi-c_k)(p-p_o)}\frac{\partial}{\partial t}[e^{(c+c_\phi)(p-p_o)}] \tag{2.63}$$

After differentiation it is quite evident that Eq. 2.63 and Eq. 2.64 are identical. After simplification:

$$\nabla^2[e^{(c+c_k)(p-p_o)}] = \frac{\phi_o\mu(c+c_\phi)}{k_o}e^{(c_\phi-c_k)(p-p_o)}\frac{\partial}{\partial t}[e^{(c+c_k)(p-p_o)}] \tag{2.64}$$

Since c_ϕ *and* c_k are very small it can be assumed:

$$e^{(c_\phi-c_k)(p-p_o)} = 1 \tag{2.65}$$

and $c+c_k = c+c_\phi$

In addition:

$$e^{(c+c_k)(p-p_o)} \cong 1+(c+c_k)(p-p_o) \tag{2.66}$$

Substituting Eq. 2.65 and Eq. 2.66 into Eq. 2.64 leads to:

$$\nabla^2 p = \frac{\phi_o\mu(c+c_\phi)}{k_o}\frac{\partial p}{\partial t} = \frac{\phi_o\mu c_t}{k_o}\frac{\partial p}{\partial t}. \tag{2.67}$$

Eq. 2.67 shows that the compressibilities of the fluid and the porous medium are added in the piezometric conductivity term:

$$c_t = c+c_\phi \tag{2.68}$$

where c_t is the total or ultimate compressibility of the system.

2.4 Real and Ideal Gases

From Eq. 2.30 the real gas density is:

$$\rho = \frac{Mp}{RT\,Z}, \tag{2.69}$$

and the compressibilty is

$$c_g = \frac{1}{\rho} \cdot \frac{d\rho}{dp} \tag{2.70}$$

Substituting Eq. 2.69 into Eq. 2.48 and taking the porosity as constant since the rock compressibility is several orders of magnitude less than the gas compressibility, the right side of the Eq. 2.48 can be developed in the following way:

$$\begin{aligned} &\frac{\partial}{\partial t}(\phi\rho) = \phi\frac{\partial\rho}{\partial t} = \phi\frac{1}{\rho}\frac{\partial\rho}{\partial p}\left(\rho\frac{\partial p}{\partial t}\right) = \\ &= \phi\, c_g\frac{Mp}{RT\,Z}\frac{\partial p}{\partial t} = \frac{M}{2RT}\phi c_g\mu\frac{2p}{\mu Z}\frac{\partial p}{\partial t}, \end{aligned} \tag{2.71}$$

Thus, Eq. 2.48 becomes:

$$\nabla\left[\frac{\bar{k}}{\mu}\frac{Mp}{RT\,Z}\nabla p\right] = \frac{M}{2RT}\phi c_g\mu\frac{2p}{\mu Z}\frac{\partial p}{\partial t}, \tag{2.72}$$

After simplification of Eq. 2.72, yields:

$$\nabla\left[\bar{k}\frac{2p}{\mu Z}\nabla p\right] = \phi c_g\mu\frac{2p}{\mu Z}\frac{\partial p}{\partial t}, \tag{2.73}$$

Al-Hussainy, *Ramey*, *Crawford* then introduced the following function:

$$m(p) = 2\int_{p_b}^{p}\frac{p\,dp}{\mu Z}, \tag{2.74}$$

which is called the *real gas pseudo pressure.* This function enabled the following derivations:

$$\nabla m(p) = \frac{dm(p)}{dp}\nabla p = \frac{2p}{\mu Z}\nabla p, \tag{2.75}$$

and

$$\frac{\partial m(p)}{\partial t} = \frac{dm(p)}{dp}\frac{\partial p}{\partial t} = \frac{2p}{\mu Z}\frac{\partial p}{\partial t} \tag{2.76}$$

Substitution of Eq. 2.75 and Eq. 2.76 into Eq. 2.73 results in:

$$\nabla[\bar{k}\nabla m(p)] = \phi c_g \mu \frac{\partial m(p)}{\partial t}, \tag{2.77}$$

Assuming that the porous medium is isotropic and homogeneous, Eq. 2.77 becomes:

$$\nabla^2 m(p) = \frac{\phi c_g \mu}{k} \frac{\partial m(p)}{\partial t}. \tag{2.78}$$

This equation is identical to Eq. 2.58 for low compressibility fluids. The differences that c_g and μ are both functions of pressure and hence Eq. 2.78 will not be linear.

Ideal gases are characterized by the following terms:

$$Z = 1, \quad c_g = \frac{1}{\bar{p}} \quad \text{and} \quad \mu = \text{constant},$$

where $\bar{p}$ is defined as the average pressure of the considered volume and time interval.

For ideal gas Eq. 2.74 becomes:

$$m(p) = \frac{p^2}{\mu}. \tag{2.79}$$

Substitution of this equation into Eq. 2.78 leads to:

$$\nabla^2 p^2 = \frac{\phi \mu}{k \bar{p}} \frac{\partial p^2}{\partial t} \tag{2.80}$$

2.5 Boundary and Initial Conditions

2.5.1 Boundary Conditions

The space where filtration takes place may be limited or infinite. Infinity is more a mathematical fiction than a fact but it is very useful for the solution of the equations.

A boundary is considered open if the fluid is able to pass through and closed if it is not. In the case of a closed boundary the following mathematical formulations may be made:

$$\begin{aligned} \vec{u}.\vec{n} &= -\frac{k\rho}{\mu}\nabla\psi\vec{n} = \left[-\frac{k\rho}{\mu}\frac{\partial\psi}{\partial n}\right]_\Gamma = 0, \\ \frac{\partial\psi}{\partial n} &= 0, \quad \vec{x} \in \Gamma, \end{aligned} \tag{2.81}$$

Where $\vec{n}$ is a unit vector normal to the boundary Γ.

In case of an open boundary it is either the potential or the gradient of the potential given at the boundary as a function of time:

$$\psi_\Gamma = \psi(\vec{x}, t), \quad \vec{x} \in \Gamma \tag{2.82}$$

or

$$\psi'_\Gamma = \frac{\partial\psi(\vec{x}, t)}{\partial n}, \quad \vec{x} \in \Gamma, \tag{2.83}$$

In both cases the velocity across the boundary is calculated by:

$$u_n = \frac{k\rho}{\mu}\frac{\partial\psi}{\partial n} \tag{2.84}$$

It is possible to combine the boundary conditions Eq. 2.82 and Eq. 2.83. This leads to a general equation for the boundary conditions:

$$a\frac{\partial\psi}{\partial n} + b\psi = c, \quad \vec{x} \in \Gamma, \tag{2.85}$$

a, b and *c* are functions of time.

The condition in Eq. 2.81 is valid at the top or bottom boundaries of an oil-, gas- or water-bearing layer. In addition it is also valid at faults and pinch outs. The condition in Eq. 2.82 is valid in the case of water intruding from the surface into the reservoir.

Eq. 2.83 must be applied at the surface of a well (inner boundary) producing (or injecting) at a given rate.

2.5.2 Initial Conditions

In order to solve filtration problems which have time dependent solutions it is necessary to know the state of the system at a certain date. This is usually the temporal starting point $t = 0$. The expression initial conditions refers to this practice. The state of the system at $t = 0$ is called initial condition:

$$\psi(\vec{x}, t_0) = \psi^0(\vec{x}), \tag{2.86}$$

and

$$p(\vec{x}, t_0) = p^0(\vec{x}) \tag{2.87}$$

By solving problems such as filtration of incompressible fluids or a steady state filtration $(t \to \infty)$ no initial conditions are required.

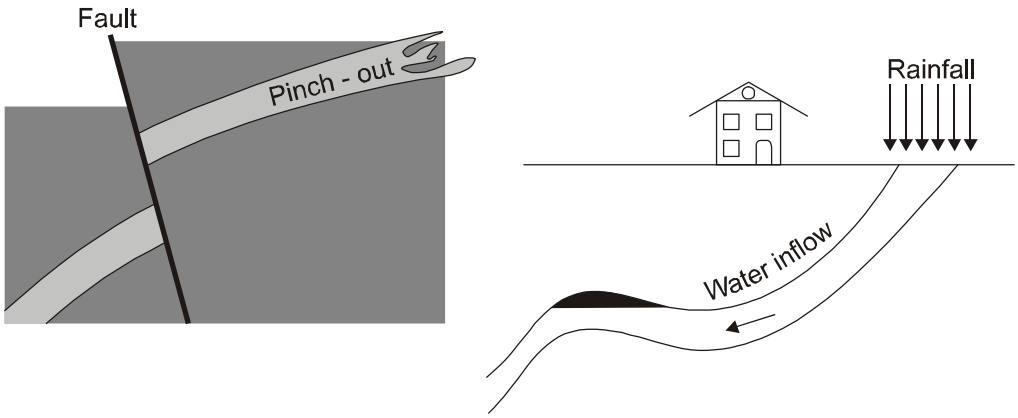

Figure 2.4: Illustration of the boundary conditions

2.5.3 Discontinuities in Porous Media

Permeability may change by leaps and bounds at the contact surface of two regions of the porous medium. In such a case the potential and the normal component of the velocity at the boundary must be continuous:

$$\psi_1 = \psi_2 \tag{2.88}$$

and

$$\rho \frac{k_1}{\mu} \frac{\partial \psi_1}{\partial n} = \rho \frac{k_2}{\mu} \frac{\partial \psi_2}{\partial n}. \tag{2.89}$$

Both ψ_1 and ψ_2 are potential functions of the two regions separated by the discontinuity surface.

2.6 Schematic of the Filtration Equations

Equation of State

$$\rho = \rho(p)$$
$$\phi = \phi(p)$$

Equation of Mass Conservation

$$\nabla(\rho\bar{u}) = -\frac{\partial}{\partial t}(\phi\rho)$$

Equation of Flow Darcy-Law

$$\bar{u} = -\frac{\rho}{\mu}\bar{k}\nabla\psi$$
$$\rho\nabla\psi = \nabla p + \rho g\bar{i}_3$$

$$\nabla\left[\frac{\rho}{\mu}\bar{k}\nabla p\right] = \frac{\partial}{\partial t}(\phi\rho)$$

Incompressible Fluid and Porous Medium: $\rho, \mu, \phi = const$

$$\nabla(\bar{k}\nabla p) = 0$$

Homogenous and isotropic Porous Medium

$$\nabla(\nabla p) = \nabla^2 p = 0$$

Low compressible Fluid and elastic Porous Medium

$$\rho = \rho_0(1 + c_f(p - p_0))$$
$$\phi = \phi_0(1 + c_\phi(p - p_0))$$
$$c_t = c_f + c_\phi$$

$$\nabla(\bar{k}\nabla p) = \phi_0 c_t \mu\frac{\partial p}{\partial t}$$

Homogenous and isotropic Porous Medium

$$\nabla^2 p = \frac{1}{K}\frac{\partial}{\partial t}(p) \qquad K = \frac{k}{\phi c_t \mu}$$

Real Gas: $\rho = \frac{Mp}{RTZ}$ $\qquad m(p) = 2\int_{p_0}^{p}\frac{p}{Z\mu}dp$

$$\nabla(\bar{k}\nabla m(p)) = \phi c_g \mu\frac{\partial m(p)}{\partial t}$$

Homogenous and isotropic Porous Medium

$$\nabla^2 m(p) = \frac{\phi c_g \mu}{k}\frac{\partial m(p)}{\partial t}$$

Ideal Gas: $Z = 1;\ c_g = \frac{1}{\bar{p}};\ \mu_g = const;\ m(p) = \frac{p^2}{\mu}$

$$\nabla^2 p^2 = \frac{\phi\mu}{k\bar{p}}\frac{\partial p^2}{\partial t}$$

Appendix A

Derivation of Laplace Equation in Radial Coordinates

The Laplace equation in the Cartesian coordinate system is:

$$\frac{\partial^2 p}{\partial x^2} + \frac{\partial^2 p}{\partial y^2} = 0 \tag{A.1}$$

To convert Eq. A.1 to a radial coordinate system the independent variables r and θ have to be considered. The Cartesian coordinates can be expressed:

$$\begin{aligned} x &= r\cos\theta \\ y &= r\sin\theta \end{aligned}$$

$$\frac{\partial p(x,y)}{\partial r} = \frac{\partial p}{\partial x}\frac{\partial x}{\partial r} + \frac{\partial p}{\partial y}\frac{\partial y}{\partial r} \tag{A.2}$$

$$\frac{\partial p(x,y)}{\partial \theta} = \frac{\partial p}{\partial x}\frac{\partial x}{\partial \theta} + \frac{\partial p}{\partial y}\frac{\partial y}{\partial \theta} \tag{A.3}$$

Since:

$$\begin{aligned} \frac{\partial x}{\partial r} &= \cos\theta;\ \frac{\partial y}{\partial r} = \sin\theta \\ \frac{\partial y}{\partial \theta} &= -r\sin\theta;\ \frac{\partial y}{\partial \theta} = r\cos\theta \end{aligned} \tag{A.4}$$

and

$$\begin{aligned} \frac{\partial p}{\partial r} &= \frac{\partial p}{\partial x}\cos\theta + \frac{\partial p}{\partial y}\sin\theta \\ \frac{\partial p}{\partial \theta} &= -\frac{\partial p}{\partial x}r\sin\theta + \frac{\partial p}{\partial y}\cos\theta \end{aligned} \tag{A.5}$$

Inserting Eq. A.4 and Eq. A.5 in Eq. A.2 and Eq. A.3 yields following results:

$$\frac{\partial p}{\partial r} = \frac{\partial p}{\partial x}\frac{\partial x}{\partial r} + \frac{\partial p}{\partial y}\frac{\partial y}{\partial r} = \frac{\partial p}{\partial x}\cos\theta + \frac{\partial p}{\partial y}\sin\theta \tag{A.6}$$

$$\frac{\partial p}{\partial \theta} = \frac{\partial p}{\partial x}\frac{\partial x}{\partial \theta} + \frac{\partial p}{\partial y}\frac{\partial y}{\partial \theta} = \frac{\partial p}{\partial x}(-r\sin\theta) + \frac{\partial p}{\partial y}r\cos\theta \tag{A.7}$$

Multiplying Eq. A.6 with $\cos\theta$ leads to:

$$\frac{\partial p}{\partial r}\cdot\cos\theta = \frac{\partial p}{\partial x}\cos^2\theta + \frac{\partial p}{\partial y}\cos\theta\sin\theta \tag{A.8}$$

Multiplying Eq. A.7 with $\sin\theta$ and some rearrangements lead to:

$$\frac{1}{r}\cdot\frac{\partial p}{\partial\theta}\cdot(-\sin\theta) = \frac{\partial p}{\partial x}\sin^2\theta - \frac{\partial p}{\partial y}\cos\theta\sin\theta \tag{A.9}$$

Adding Eq. A.8 and Eq. A.9 yield:

$$\frac{\partial p}{\partial r}\cdot\cos\theta + \frac{1}{r}\cdot\frac{\partial p}{\partial\theta}\cdot(-\sin\theta) = \frac{\partial p}{\partial x}\cdot(\cos^2\theta + \sin^2\theta) = \frac{\partial p}{\partial x} \tag{A.10}$$

If Eq. A.6 is multiplyed with $\sin\theta$ and Eq. A.7 with $\cos\theta$ the same calculation leads to:

$$\frac{\partial p}{\partial r}\cdot\sin\theta + \frac{1}{r}\cdot\frac{\partial p}{\partial\theta}\cdot\cos\theta = \frac{\partial p}{\partial y} \tag{A.11}$$

Since

$$\frac{\partial}{\partial x}\left[\frac{\partial p(r,\theta)}{\partial x}\right] = \frac{\partial r}{\partial x}\frac{\partial}{\partial r}\left(\frac{\partial p}{\partial x}\right) + \frac{\partial\theta}{\partial x}\frac{\partial}{\partial\theta}\left(\frac{\partial p}{\partial x}\right) \tag{A.12}$$

and

$$\frac{\partial}{\partial y}\left[\frac{\partial p(r,\theta)}{\partial y}\right] = \frac{\partial r}{\partial y}\frac{\partial}{\partial r}\left(\frac{\partial p}{\partial y}\right) + \frac{\partial\theta}{\partial x}\frac{\partial}{\partial\theta}\left(\frac{\partial p}{\partial y}\right) \tag{A.13}$$

and

$$\begin{aligned}\frac{\partial r}{\partial x} &= \frac{x}{r} = \cos\theta, \quad \frac{\partial\theta}{\partial x} = \frac{-\sin\theta}{r}\\ \frac{\partial r}{\partial y} &= \frac{y}{r} = \sin\theta, \quad \frac{\partial\theta}{\partial y} = \frac{\cos\theta}{r}\end{aligned} \tag{A.14}$$

Then Eq. A.12 becomes:

$$\begin{aligned}\frac{\partial^2 p}{\partial x^2} = {} & \cos\theta\frac{\partial}{\partial r}\left[\cos\theta\frac{\partial p}{\partial r} - \frac{1}{r}\sin\theta\frac{\partial p}{\partial\theta}\right]\\ & -\frac{\sin\theta}{r}\frac{\partial}{\partial\theta}\left[\cos\theta\frac{\partial p}{\partial r} - \frac{1}{r}\sin\theta\frac{\partial p}{\partial\theta}\right]\end{aligned} \tag{A.15}$$

Also Eq. A.13 becomes:

$$\begin{aligned}\frac{\partial^2 p}{\partial y^2} = {} & \sin\theta\frac{\partial}{\partial r}\left[\sin\theta\frac{\partial p}{\partial\theta} + \frac{1}{r}\cos\theta\frac{\partial p}{\partial r}\right]\\ & +\frac{\cos\theta}{r}\frac{\partial}{\partial\theta}\left[\sin\theta\frac{\partial p}{\partial\theta} + \frac{1}{r}\cos\theta\frac{\partial p}{\partial r}\right]\end{aligned} \tag{A.16}$$

Substitute Eq. A.15 and Eq. A.16 into Eq. A.1, with simplifications, yields :

$$\frac{\partial^2 p}{\partial r^2} + \frac{1}{r}\frac{\partial p}{\partial r} + \frac{1}{r^2}\frac{\partial^2 p}{\partial \theta^2} = 0 \tag{A.17}$$

Eq. A.17 can be written as:

$$\frac{1}{r}\frac{\partial}{\partial r}\left(r\frac{\partial p}{\partial r}\right) + \frac{1}{r^2}\frac{\partial^2 p}{\partial \theta^2} = 0 \tag{A.18}$$

3 Solutions of the Single-Phase Equation of Filtration

In order to find a suitable solution to the filtration equation, one should know what type of condition can be used to describe a flow regime. Generally there are two conditions: Non-Steady State and Steady State.

The **Non-Steady State** may be subdivided into the following conditions:

A - Transient condition:

This condition is valid at an early, relatively short time, where the pressure response in the reservoir is not affected by the presence of an outer boundary, thus the reservoir appears infinite acting. In well testing this condition is applicable when the production rate is deliberately changed for a short time, the pressure response is measured for a few hours and the boundary effects will not be felt and therefore the reservoir is mathematically infinite.

B - Late Transient condition:

This condition exists in the period when the boundary effects start to show up in the pressure response. This will occur when the well test period takes a longer time, or the reservoir is smaller than expected.

C - Pseudo-Steady State condition:

The Pseudo (or Semi) Steady Sate condition occurs after the late transient condition and is valid for a reservoir which has been producing for a sufficient period of time so that the boundary effect has been felt by the pressure response. The outer boundary could be impermeable to fluids (no flow boundary) or a constant pressure boundary.

Steady State condition:

The Steady State condition occurs also after the late transient period. This condition is applicable when the production rate is constant and fluid withdrawal will be exactly balanced by fluid entry across the open boundary, so that there is no change in pressure with time in the whole reservoir.

3.1 Steady State Filtration

3.1.1 Steady State Filtration of Low Compressibility Fluid

Filtration is steady state if the potential (and so the flow) at any point of the system is independent of time ($\partial p/\partial t = 0$). For constant fluid viscosity, Eq. 2.57 will be reduced to:

$$\nabla(\bar{k}\nabla p) = 0 \tag{3.1}$$

Eq. 3.1 is similar to Eq. 2.49 for incompressible fluids.

For homogeneous and isotropic porous media ($\bar{k} = k$ = constant) follows:

$$\nabla^2 p = 0 \tag{3.2}$$

A linear one dimensional model is used for the sake of simplicity. Mathematically it can be described by:

$$\frac{\partial^2 p}{\partial x^2} = 0 \tag{3.3}$$

and its solution after integrating Eq. 3.3 twice is given by:

$$p = ax + b \tag{3.4}$$

where: a and b are constants of integration. The actual value of the pressure is then determined by boundary conditions.

A production rate *(q)* is assumed negative when flowing out of the porous medium and positive when flowing into it. Thus q becomes negative when produced and positive when injected.

The boundary conditions are used to determine a and b as follows:

At $x = 0$ *is* $p = p_i$.

Then b is determined from Eq. 3.4 as:

$$b = p_i \tag{3.5}$$

At $x = L$ is $\frac{kA}{\mu}\frac{dp}{dx} = qB$

where B is the formation volume factor and q is negative. Taking the derivative of Eq. 3.4 then

$$\frac{dp}{dx} = a, \tag{3.6}$$

and by substituting into the second boundary condition (B.C.), a is determined as:

$$a = \frac{\mu q B}{kA} \tag{3.7}$$

Substituting Eq. 3.5 and Eq. 3.7 into Eq. 3.4 yields:

$$p - p_i = \frac{\mu q B}{kA} x \tag{3.8}$$

The value of p - p_i becomes negative in case of flow taking place in direction of the x-axis (q is negative) and positive in the inverse case.

3.1.2 Steady State Filtration in a Radial System

The Cartesian coordinates can be transformed into radial coordinates, as shown in Appendix A, Chapter 2, which will leave Eq. 3.2 in the following form:

$$\frac{1}{r}\frac{\partial}{\partial r}\left(r\frac{\partial p}{\partial r}\right) + \frac{1}{r^2}\frac{\partial^2 p}{\partial \theta^2} = 0 \tag{3.9}$$

If the pressure (or potential) distribution is independent of θ, then the filtration is radially symmetrical, and

$$\frac{\partial^2 p}{\partial \theta^2} = 0$$

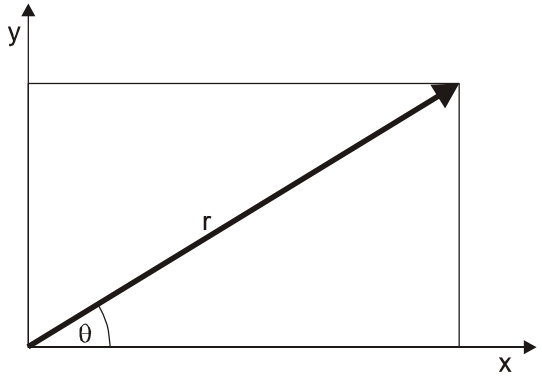

Figure 3.1: The Radial Coordinate System

This simplifies Eq. 3.9 to:

$$\frac{1}{r}\frac{\partial}{\partial r}\left(r\frac{\partial p}{\partial r}\right) = 0 \tag{3.10}$$

Eq. 3.10 can be expressed in the following form also:

$$\boxed{\frac{\partial^2 p}{\partial r^2} + \frac{1}{r}\frac{\partial p}{\partial r} = 0} \tag{3.11}$$

Integrating Eq. 3.10 twice leads to:

$$p = a \cdot \ln r + b \tag{3.12}$$

We set a constant pressure at the inner radius r_w:

$$p = p_{wf} \text{ at } r = r_w \tag{3.13}$$

and a constant rate q. From Darcy equation:

$$\frac{kA}{\mu}\frac{dp}{dr} = -qB \text{ at } r = r_w, \tag{3.14}$$

where $A = 2\pi r_w h$ is the inner surface and h the thickness of the layer. Note: outfow rate is negative while inflow rate is positive. Taking the derivative of Eq. 3.12 with respect to r ($dp/dr = a/r$) and substituting it into Eq. 3.14 yields: (3.15)

$$a = -\frac{\mu qB}{2\pi hk}. \tag{3.16}$$

b can be calculated from Eq. 3.12 as:

$$b = p_{wf} - a \ln r_w \tag{3.17}$$

and

$$b = p_{wf} + \frac{\mu q B}{2\pi h k} \ln r_w \tag{3.18}$$

Substituting the values of a and b into Eq. 3.12 leads to:

$$p_{wf} - p = \frac{\mu q B}{2\pi h k} \ln \frac{r}{r_w} \tag{3.19}$$

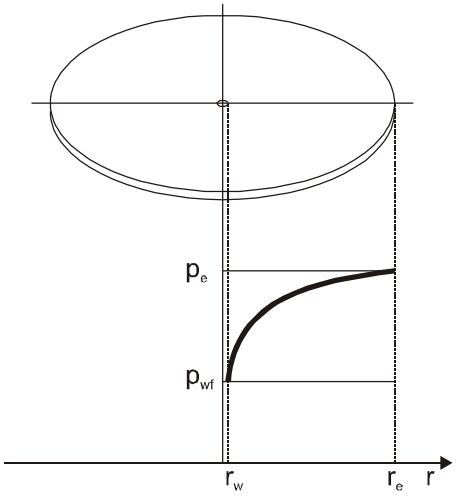

Figure 3.2: Illustration of steady-state filtration in a radial system

Considering an outer boundary ($r = r_e$) with constant pressure p_e Eq. 3.19 leads to:

$$q = -\frac{2\pi h k}{\mu B} \frac{p_e - p_{wf}}{\ln(r_e / r_w)}. \tag{3.20}$$

This equation is known as ***Dupuit*** equation.

If the inner radius r_w represent a well then p_{wf} is called as *bottom hole flowing pressure*.

3.1.3 Steady State Gas Filtration

From Eq. 1.47 and substituting of ρ by Eq. 2.30 one can set up the following equation:

$$\frac{Mp}{RTZ(p)}dp = \frac{\mu Q_m}{Ak}\left(1+\frac{\beta Q_m}{\mu A}\right)dx \tag{3.21}$$

Then Eq. 3.21 is integrated along a linear segment:

$$2\int_{p_i}^{p}\frac{p}{Z(p)\mu}dp = -\frac{2Q_mRT}{MAk}\left(1+\frac{\beta Q_m}{\mu A}\right)x \tag{3.22}$$

Substituting Eq. 2.74 into Eq. 3.22 we obtain:

$$m(p)-m(p_i) = -\frac{2Q_mRT}{MAk}\left(1+\frac{\beta Q_m}{\mu A}\right)x \tag{3.23}$$

In the case of a radial symmetric filtration (see Figure 3.2) the surface area is $A = 2r\pi h$ and Eq. 3.21 becomes:

$$2\int_{p_i}^{p}\frac{p}{Z(p)\mu}dp = -\frac{2Q_mRT}{MAk}\int_{r_w}^{r}\left(\frac{1}{r}+\frac{\beta Q_m}{2\pi r^2 h\mu}\right)dr \tag{3.24}$$

or

$$m(p)-m(p_{wf}) = -\frac{Q_mRT}{\pi hMk}\left[\ln\frac{r}{r_w}+\frac{\beta Q_m}{2\pi h\mu}\left(\frac{1}{r_w}-\frac{1}{r}\right)\right] \tag{3.25}$$

Assuming that the pressure difference between the two ends of a linear porous body is not very large, then *Z(p)* is substituted by $\bar{Z}$, for $p = p_i$ and Eq. 3.25 becomes:

$$p_i^2-p_{wf}^2 = -\frac{\mu Q_mRT\bar{Z}}{\pi hMk}\left[\ln\frac{r_e}{r_w}+\frac{\beta Q_m}{2\pi h\mu r_w}\left(1-\frac{r_w}{r_e}\right)\right] \tag{3.26}$$

The fraction r_w/r_e is generally considered small and so the last term $(1-r_w/r_e) \sim 1$.

At a given exterior radius r_e the pressure is p_i. Then Eq. 3.26 may be set up as follows:

$$p_i^2-p_{wf}^2 = -AQ_m-BQ_m^2 \tag{3.27}$$

where:

$$A = \frac{\mu RT\bar{Z}}{\pi hMk}\ln\frac{r_e}{r_w} \qquad B = \frac{\beta RT\bar{Z}}{2\pi^2 h^2 kMr_w}$$

Q_m is negative for producing wells and positive for injection wells. Eq. 3.27 can be transformed into the following form:

$$\frac{p_i^2 - p_{wf}^2}{|Q_m|} = A + B|Q_m| \tag{3.28}$$

This equation is useful to calculate gas well production rates as a function of p_{wf}. In practice the following equation is also used:

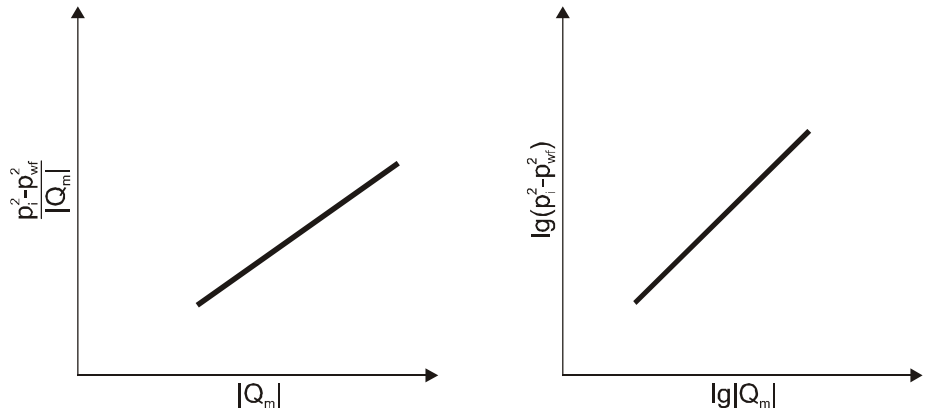

Figure 3.3: Plots of production equation for gas wells

$$\boxed{Q_m = C(p_i^2 - p_{wf}^2)^n} \tag{3.29}$$

The constants C and n have to be determined by fitting of Eq. 3.29 to the measured Q_m and p_{wf} values. In the same way we can evaluate the constants in Eq. 3.27 instead calculating them with Eq. 3.28. The graphical illustrations are shown in Figure 3.3.. Eq. 3.28 indicates that the slope of the line in Figure 3.3a is equal to B and the intercept is A.

3.2 Non-Steady State Filtration in Infinite Acting Systems

3.2.1 Radial Systems with Constant Production Rate

Eq. 2.58 transformed into the radial yields:

$$\frac{\partial^2 p}{\partial r^2} + \frac{1}{r}\frac{\partial p}{\partial r} = \frac{1}{K}\frac{\partial p}{\partial t} \qquad K = \frac{k}{\mu \phi c} \tag{3.30}$$

This equation is of essential importance when solving technical problems. It is a base for calculations of production rates of hydrocarbon wells and deep water wells. Further it is also applied for the evaluation of pressure build-up curves and for the water inflow into hydrocarbon reservoirs.

It is assumed that the fluid bearing layer has a thickness h, a porosity ϕ, a permeability k and is horizontal, homogeneous, isotropic and infinite. The fluid has a viscosity μ and a compressibility c.

The radius of the well is r_w. At $t = 0$ the pressure is the same everywhere:

$$p = p_i \quad r > r_w \quad t = 0 \tag{3.31}$$

The well should produce continuously at a rate q. According to *Darcy*'s law we obtaine the following equation:

$$\frac{2\pi r_w h k}{\mu}\left(\frac{\partial p}{\partial r}\right)_{r = r_w} = -qB \tag{3.32}$$

The boundary condition in infinity is:

$$p = p_i \qquad r = \infty \qquad t > 0 \tag{3.33}$$

We seek for a solution in the form:

$$p = p(r,t) \text{ for } r_w < r < \infty \quad t > 0 \tag{3.34}$$

To explain the solution method used below we take Pythagoras theorem as an example. To calculate the hypotenuse of a right triangle we are looking for a solution of:

$$z = z(x, y) \tag{3.35}$$

where x and y are the side lengths and z is a function of two variables, x and y. It is possible to reduce the number of independent variables by introducing a new one in the form of:

$$w = x^2 + y^2 \tag{3.36}$$

So the variables x and y in Eq. 3.35 can be replaced by

$$z = z(w) \tag{3.37}$$

In a similar manner we assume that p is a function of only one variable z and we introduce the following relationship:

$$z = \frac{r^2}{K \cdot t} \tag{3.38}$$

Based on this assumption we get:

$$\frac{1}{K}\frac{\partial p}{\partial t} = \frac{1}{K}\frac{\partial p}{\partial z}\frac{\partial z}{\partial t} = \frac{r^2}{K^2 t^2}\frac{dp}{dz} = -\frac{z}{Kt}\frac{dp}{dz} \tag{3.39}$$

$$\frac{\partial p}{\partial r} = \frac{dp}{dz}\frac{\partial z}{\partial r} = \frac{2r}{Kt}\frac{dp}{dz} = \frac{2r^2}{Kt}\frac{1}{r}\frac{dp}{dz} = \frac{2z}{r}\frac{dp}{dz} \tag{3.40}$$

$$\frac{\partial^2 p}{\partial r^2} = \frac{2}{Kt}\frac{dp}{dz} + \frac{4r^2}{K^2 t^2}\frac{d^2 p}{dz^2} = \frac{2}{Kt}\frac{dp}{dz} + \frac{4z}{Kt}\frac{d^2 p}{dz^2} \tag{3.41}$$

Substituting Eq. 3.39 - Eq. 3.41 into Eq. 3.30 yields:

$$4z\frac{d^2 p}{dz^2} + (4 + z)\frac{dp}{dz} = 0 \tag{3.42}$$

To solve Eq. 3.42 the boundary conditions must also be transformed. Using Eq. 3.38 the B.C. in Eq. 3.33 can be transferred into:

$$p = p_i \quad z = \infty \quad t > 0 \tag{3.43}$$

Using Eq. 3.38 and Eq. 3.40, the first B.C. in Eq. 3.32 can be transformed as well to:

$$z\frac{dp}{dz} = -\frac{\mu q B}{4\pi h k} \tag{3.44}$$

Eq. 3.42 can be written as:

$$z\frac{d^2p}{dz^2}+\frac{dp}{dz} = -\frac{z}{4}\frac{dp}{dz} \tag{3.45}$$

or:

$$\frac{d}{dz}\left(z\frac{dp}{dz}\right) = -\frac{1}{4}z\frac{dp}{dz} \tag{3.46}$$

Let $y = z\frac{dp}{dz}$

then Eq. 3.46 becomes:

$$\frac{d}{dz}y = -y/4 \tag{3.47}$$

By separation of variables:

$$\frac{d}{dz}y = -\frac{y}{4} \tag{3.48}$$

By integrating Eq. 3.48 yields:

$$\ln y - \ln A_1 = -\frac{z}{4} \tag{3.49}$$

where A_1 is a constant of integration, taking the exponential of Eq. 3.49

$$y = A_1 e^{-z/4} \tag{3.50}$$

or

$$z\frac{dp}{dz} = A_1 e^{-z/4} \tag{3.51}$$

and the second substitution with the notation $\xi = z/4$ and by separation of variables, Eq. 3.51 becomes:

$$dp = A_1\frac{e^{-\xi}}{\xi}d\xi \tag{3.52}$$

Integrating Eq. 3.52 yields:

$$p_i - p = A_1 \int_{z/4}^{\infty} \frac{e^{-\xi}}{\xi} d\xi \tag{3.53}$$

Using Eq. 3.51 and the boundary condition in Eq. 3.44 and assuming that r_w is very small so that the condition $\frac{r_w^2}{4Kt} \approx 0$ is valid, A_1 can be determined as:

$$A_1 = -\frac{\mu q B}{4\pi h k} \tag{3.54}$$

The integral in Eq. 3.53 cannot be solved in a closed form. This integral is defined as the so called *exponential integral* and its numerical solution can be found in any mathematical handbook:

$$Ei(-x) = -\int_{x}^{\infty} \frac{e^{-\xi}}{\xi} d\xi \tag{3.55}$$

Finally Eq. 3.53 becomes:

$$p_i - p(r, t) = \frac{\mu q B}{4\pi h k} Ei\left(-\frac{r^2}{4Kt}\right) \tag{3.56}$$

The calculation of the pressure drop at the well bottom is made by substituting $r = r_w$ and $p(r,t) = p_{wf}(t)$ into Eq. 3.56:

$$p_i - p_{wf} = \frac{\mu q B}{4\pi h k} Ei\left(-\frac{r_w^2}{4Kt}\right) \tag{3.57}$$

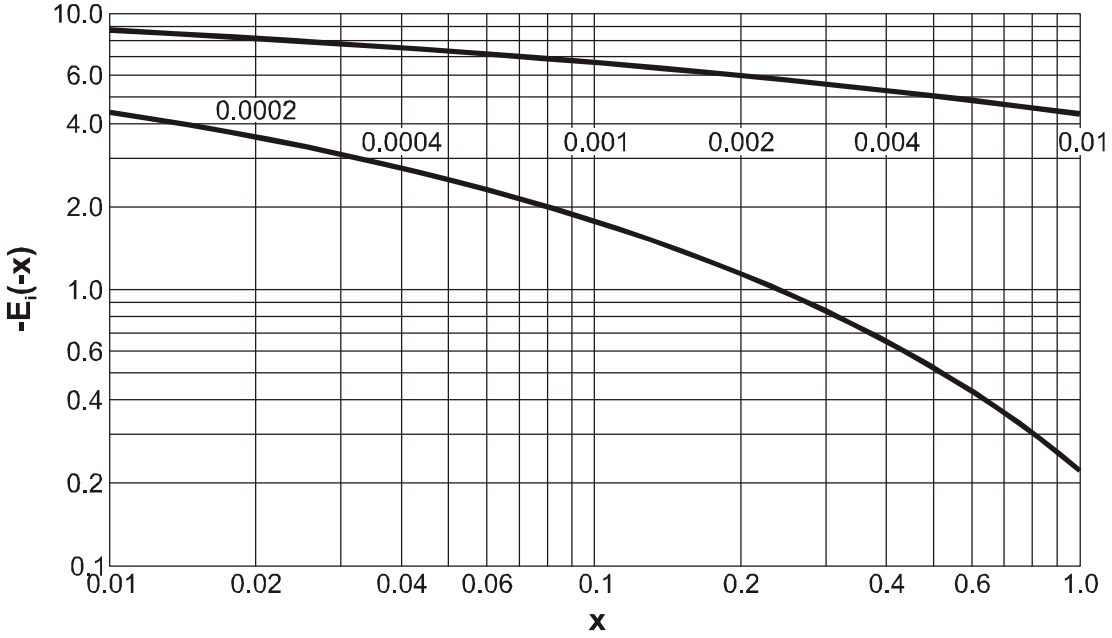

Figure 3.4: Plots of the *Ei(-z)*- function (after *Chaumet*)

3.2.2 Properties of the *Ei*-Function

The function $-Ei(-z)$ is illustrated in Figure 3.4. In the vicinity of $z = 0$ the TAYLOR-Series of $-Ei(-z)$ is defined as:

$$-Ei(-z) = -\gamma - \ln z + z - \frac{z^2}{4} + ... \tag{3.58}$$

where $\gamma = 0,57722$ is the EULER-Constant.

If $z \ll 1$ the series in Eq. 3.58 will have very small values in terms higher than the third term, which makes the following approximation valid:

$$-Ei(-z) = -0,57722 - \ln z \tag{3.59}$$

then:

$$-Ei\left(-\frac{r^2}{4Kt}\right) = -0,57722 - \ln \frac{4Kt}{r^2} = 0,80907 + \ln \frac{Kt}{r^2} \tag{3.60}$$

3.2.3 Pressure Drop in Space and Time

Substitution of Eq. 3.60 into Eq. 3.56 leads to:

$$p_i - p(r,t) = -\frac{\mu q B}{4\pi h k}\left(0,80907 + \ln\frac{Kt}{r^2}\right) \tag{3.61}$$

The error of this approximation becomes less than 1 % if the following condition is satisfied:

$$\frac{Kt}{r^2} > 10 \tag{3.62}$$

Eq. 3.61 enables the calculation of the pressure drop between two selected radii. The pressure is evaluated at the the two radii seperately using Eq. 3.61 and the difference gives the pressure drop between the two points. A graphical illustration of these values indicates a parallelism of the pressure drop curves. This means that the pressure difference between two radii becomes a constant for a given production time interval.

This fact can be verified mathematically with Eq. 3.61 where r_w and r_e are the two considered radii:

$$p_i - p_{wf} = -\frac{\mu q B}{4\pi h k}\left(0,80907 + \ln\frac{Kt}{r_w^2}\right) \tag{3.63}$$

$$p_i - p_e = -\frac{\mu q B}{4\pi h k}\left(0,80907 + \ln\frac{Kt}{r_e^2}\right) \tag{3.64}$$

By substracting Eq. 3.64 from Eq. 3.63 we get:

$$p_e - p_{wf} = -\frac{\mu q B}{4\pi h k}\ln\frac{r_e^2}{r_w^2} = -\frac{\mu q B}{2\pi h k}\ln\frac{r_e}{r_w} \tag{3.65}$$

The pressure difference is therefore independent of time but Eq. 3.65 is only valid if

$\frac{Kt}{r^2} > 10$.

Further it is possible to illustrate the spatial distribution of pressure according to Eq. 3.61 as shown in Figure 3.5.

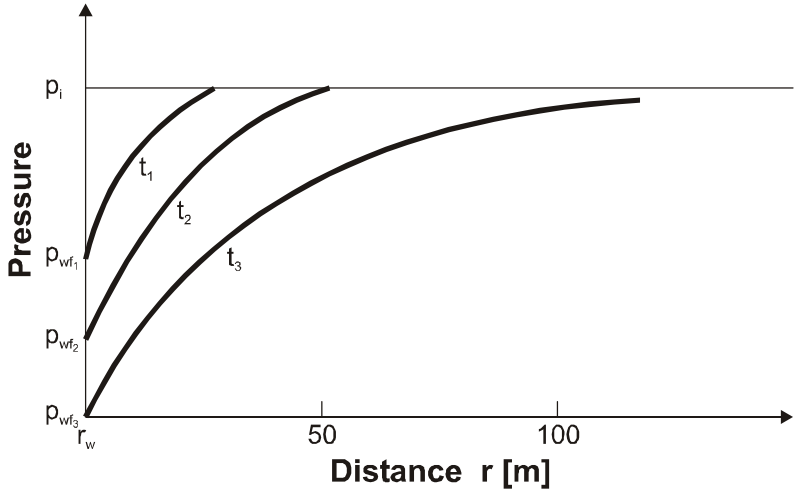

Figure 3.5: Plots of pressure drop in the vicinity of a well (infinite reservoir, compressible fluid)

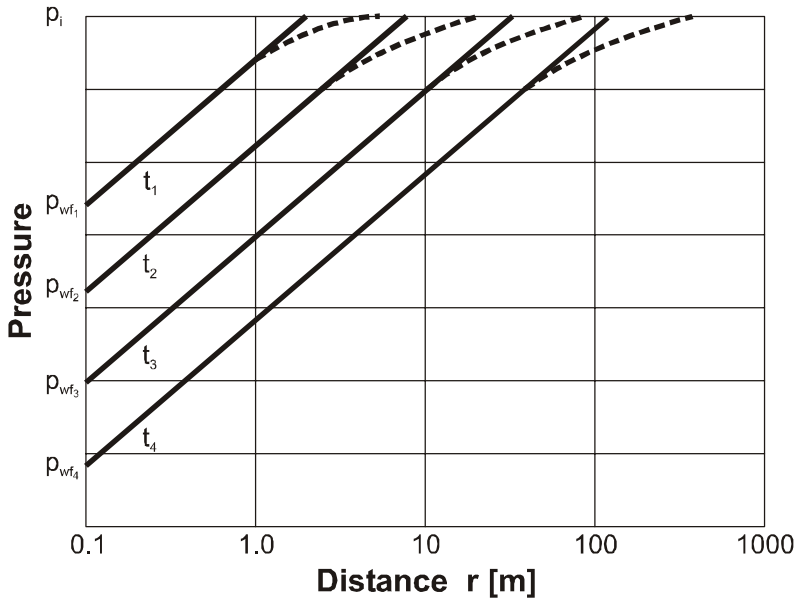

Figure 3.6: Plots of pressure drop in the vicinity of a well (infinite reservoir, compressible fluid)

Figure 3.6 shows the pressure distribution as a function of log *r* for various *t.* The continuous line represents calculations by Eq. 3.61, the staggered line calculations by Eq. 3.56. The linear section of the plot is shifted parallel in time.

Example 3.1:

The following data of an oil bearing layer are known:

Permeability: $k = 10$ *[mD]* $= 20.10^{-15}$ *[m²]*

Porosity: $\phi = 0.2$[-]

Thickness: $h = 5$ *[m]*

Well Radius: $r_w = 0.1$ *[m]*

Oil Viscosity: $\mu = 10^{-3}$ *[Pa.s]*

Oil Compressibility: $c = 10^{-9}$ *[Pa^{-1} (10^{-4} bar^{-1})]*

Production rate: $q = -10$ *[m³/day] (Bo=1)*

For how long should the well be produced to allow the use the Eq. 3.61 in the following cases:

a) For calculation of the bottom hole flowing pressure

b) For calculation of the pressure at 100 [m] distance from the well

Solution:

At the well radius 3.61 is valid if :

$$t_1 > \frac{10 r_w^2}{K} = \frac{10 \cdot 10^{-2}}{0,1} = 1 \text{ [sec]}$$

At a 100 m distance from the well the time limit for application of Eq. 3.61 instead of Eq. 3.57 will be much higher:

$$t_2 > \frac{10 r_w^2}{K} = \frac{10 \cdot 10^{4}}{0,1} = 10^6 \text{ [sec]} = 11,6 \text{ [days]}$$

Example 3.2:

The task is to determine the pressure at the well radius and at r = 100 [m] after 30 days of production. The reservoir data are to be taken from Example 3.1.

Solution:

Since:

$$\frac{\mu qB}{4\pi hk} = \frac{10^{-3}\,\frac{-10}{86400}}{4 \cdot \pi \cdot 5 \cdot 0,02 \cdot 10^{-12}} = -0,92 \cdot 10^{5}\ [\text{Pa}]$$

$$K = \frac{k}{\mu c \phi} = \frac{0,02 \cdot 10^{-12}}{10^{-3} \cdot 10^{-9} \cdot 0,2} = 0,1\ [\text{m}^2\text{sec}^{-1}]$$

Time is large enough to apply Eq. 3.61. The bottom hole flowing pressure is calculated as follows:

$$p_{wf} = p_i + \frac{\mu qB}{4\pi hk}\left(0,80907 + \ln\frac{Kt}{r_w^2}\right)$$

$$= 10 \cdot 10^{6} - 0,92 \cdot 10^{5}\left(0,80907 + \ln\frac{0,1 \cdot 30 \cdot 86400}{0,1^2}\right) = 8,35\ [\text{MPa}]$$

$$p_{(r=100)} = p_i + \frac{\mu qB}{4\pi hk}\left(0,80907 + \ln\frac{Kt}{r_w^2}\right)$$

$$= 10 \cdot 10^{6} - 0,92 \cdot 10^{5}\left(0,80907 + \ln\frac{0,1 \cdot 30 \cdot 86400}{100^2}\right) = 9,36\ [\text{MPa}]$$

3.2.4 The Spatial Distribution of Flow

We assume a cylinder with radius r, centered by the well inside an infinite, homogenous and isotropic layer. The quantity of fluid flowing through the cylindrical surface is a function of time and may be calculated from *Darcy*'s law:

$$q(r,t) = -\frac{2\pi rhk}{B\mu}\frac{\partial p}{\partial r} \tag{3.66}$$

Eq. 3.40, Eq. 3.38 and Eq. 3.51 yield:

$$\frac{\partial p}{\partial r} = \frac{2r}{Kt}\frac{dp}{dz} = \frac{2r}{Kt}A_1\frac{e^{-\frac{z}{4}}}{z} \tag{3.67}$$

respectively from Eq. 3.67 and Eq. 3.38

$$\frac{\partial p}{\partial r} = \frac{2r}{Kt}\left(\frac{\mu qB}{4\pi hk}\right)\frac{Kt}{r^2}e^{-\frac{r^2}{4Kt}} = \frac{\mu qB}{2\pi rhk}e^{-\frac{r^2}{4Kt}} \tag{3.68}$$

Substituting Eq. 3.68 into Eq. 3.66 gives:

$$q(r,t) = -qe^{-\frac{r^2}{4Kt}} \tag{3.69}$$

In Figure 3.7 the relation $q(r,t)/q$ is illustrated as a function of Kt/r^2.

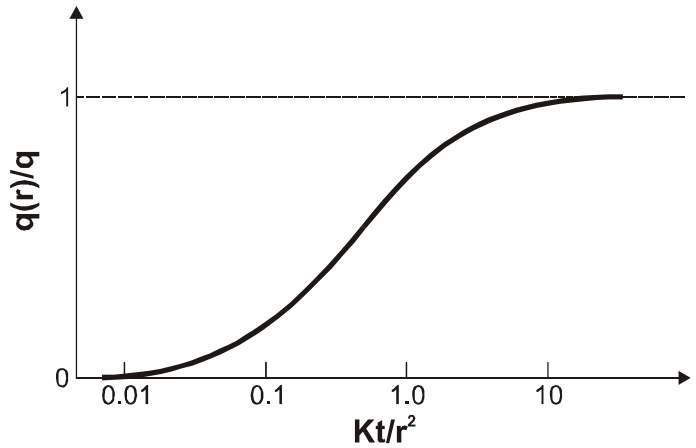

Figure 3.7: The flow rate in function of the dimensionless variable Kt/r^2 (after *Chaumet*)

3.3 Dimensionless Variables

Simplifications of the calculation may be achieved by introducing the so called dimensionless variables.

radius: $r \rightarrow r_D = \frac{r}{r_w}$

time: $t \rightarrow t_D = \frac{Kt}{r_w^2} = \frac{kt}{\phi\mu c r_w^2}$

pressure: $p \rightarrow P_D = (p - p_i)\frac{2\pi hk}{qB\mu}$

Thus

$$r = r_D r_w \tag{3.70}$$

$$t = t_D \frac{r_w^2}{K} \tag{3.71}$$

$$p = P_D\left(\frac{qb\mu}{2\pi hk}\right) + p_i = P_D C + p_i \tag{3.72}$$

Substitution of the variables given in Eq. 3.70 - Eq. 3.72 into Eq. 3.30 and Eq. 3.31- Eq. 3.33 leads to the following formulas:

$$\frac{\partial^2}{\partial(r_D r_w)^2}[P_D C + p_i] + \frac{1}{r_D r_w}\frac{\partial}{\partial(r_D r_w)}[P_D C + p_i] = \frac{1}{K}\frac{\partial}{\partial\left(\frac{t_D r_w^2}{K}\right)}[P_D C + p_i] \tag{3.73}$$

$$P_D C + p_i = p_i \qquad r_D r_w > r_w \qquad \frac{t_D r_w^2}{K} = 0 \tag{3.74}$$

$$\frac{2\pi r_w hk}{B\mu}\frac{\partial}{\partial(r_D r_w)}[P_D C + p_i] = -q \tag{3.75}$$

$$P_D C + p_i = p_i \qquad r_D r_w = \infty \qquad \frac{t_D r_w^2}{K} \geq 0 \tag{3.76}$$

A similar transformation of the variables in Eq. 3.30 can be done and as r_w, c, p_i, K are constants and therefore can be cancelled. Thus Eq. 3.73 - Eq. 3.76 become:

$$\frac{\partial^2 P_D}{\partial r_D^2} + \frac{1}{r_D}\frac{\partial P_D}{\partial r_D} = \frac{\partial P_D}{\partial t_D} \tag{3.77}$$

$$P_D = 0 \qquad r_D > 1 \qquad t_D = 0 \tag{3.78}$$

$$\left(\frac{\partial P_D}{\partial r_D}\right)_{r_D = 1} = -1 \qquad t_D > 0 \tag{3.79}$$

$$P_D = 0 \qquad r_D = \infty \qquad t_D > 0 \tag{3.80}$$

Solutions of this boundary value problem are obtained by using Eq. 3.56. Rearranging of this equation leads to:

$$\frac{2\pi hk}{Bq\mu}(p_i - p) = \frac{1}{2} Ei\left(-\frac{r^2/r_w^2}{4Kt/r_w^2}\right) \tag{3.81}$$

Substituting the dimensionless variables into Eq. 3.81 yields:

$$P_D = -\frac{1}{2} Ei\left(-\frac{r_D^2}{4t_D}\right) \tag{3.82}$$

Thus P_D may be regarded as a function of t_D/r_D^2:

$$P_D(t_D/r_D^2) = -\frac{1}{2} Ei\left(-\frac{1}{4}\frac{1}{(t_D/r_D^2)}\right) \tag{3.83}$$

Figure 3.8 shows the function P_D according to Eq. 3.82 with $r_e/r_w = \infty$.

The logaritmic approximation (for $t_D/r_D^2 > 10$) of Eq. 3.82 becomes:

$$P_D = \frac{1}{2}[0.80907 + \ln(t_D/r_D{}^2)] \tag{3.84}$$

At the wellbore $r_D = 1$, so Eq. 3.84 becomes more simple:

$$P_{Dw} = \frac{1}{2}[0,\, 80907 + \ln t_D] \tag{3.85}$$

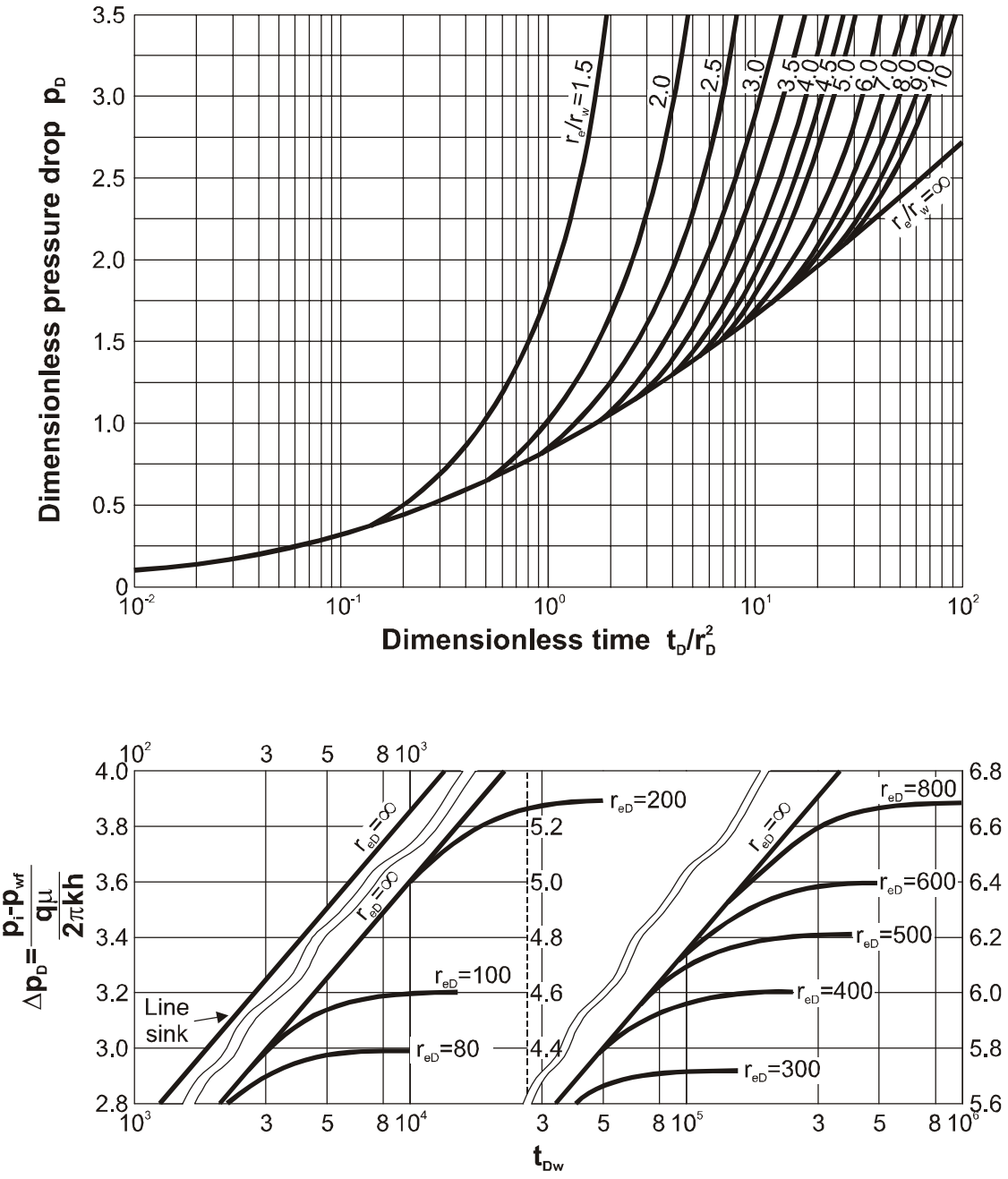

Figure 3.8: Solution for the infinitive and finite radial filtration problem with closed boundary and constant pressure drop (after *Van Everdingen* and *Hurst*)

Example 3.3:

Convert the following variables to dimensionless variables using the data in Example 3.1.

r = 100[m], t = 30[days] p = 9.63[MPa]

Solution:

$$r_D = \frac{r}{r_w} = 1000$$

$$t_D = \frac{Kt}{r_w^2} = \frac{0,1 \cdot 30 \cdot 86400}{0,1^2} = 2,59 \cdot 10^7$$

$$P_D = (p - p_i)\frac{2\pi hk}{q\mu} = (9,63 \cdot 10^6 - 10 \cdot 10^6)\frac{2 \cdot \pi \cdot 5 \cdot 0,02 \cdot 10^{-12}}{10^{-3}\frac{-10}{86400}} =$$

$$0,37 \cdot 10^6 \cdot 0,54286 \cdot 10^{-5} = -2,01$$

Example 3.4:

Calculate the pressure at a distance of 100 [m] from the well after 5 days of production. Use the data given in Example 3.1 - Example 3.3.

Solution:

At this time the approximations used in Eq. 3.61 and Eq. 3.84 are not applicable, so one must use Eq. 3.83 or the graphical illustration of the Ei function in Figure 3.8.

The first task is to calculate the dimensionless variables:

$$(t_D/r_D^2) = \left(\frac{Kt}{r_w^2}\right)\left(\frac{r^2}{r_w^2}\right) = \frac{Kt}{r^2} = \frac{0,1 \cdot 5 \cdot 86400}{100^2} = 4,32$$

$$K = 0,1\ [\mathrm{m^2 sec^{-1}}] \quad \frac{Bq\mu}{2\pi hk} = -1,84 \cdot 10^5\ [\mathrm{Pa}]$$

From the $(r_e/r_w = \infty)$ *curve in Figure 3.8,* P_D *=1.15.*

Since:

$$P_D = -\frac{1}{2}Ei\left(-\frac{r_D^2}{4t_D}\right) = 1,15$$

From Eq. 3.72 follows:

$$p = p_i + p_D\frac{qB\mu}{2\pi hk} = 10\cdot 10^6 - 1,84\cdot 10^5\cdot 1,15 = 9,79\ [\text{MPa}] \tag{3.86}$$

3.4 The Infinite Radial System with Constant Pressure at the Interior Boundary

Sometimes the well is produced under a constant bottom hole flowing pressure (p_{wf}), rather than under a constant production rate, for example to control water conning problems.

The function *p(r;t)* is no longer of interest for us in this case. Because the bottom hole pressure p_{wf} and the pressure in infinity are both given and thus pressure at r will range between these two values. The main interest though appears to lie in the determination of the flow rate q or the cumulative production Q at the well radius r_w. These two variables are both regarded as functions of time.

Eq. 3.30 and the conditions in Eq. 3.31 and Eq. 3.33 are still valid. The boundary condition in Eq. 3.32 though is substituted by:

$$p = p_{wf} \qquad r = r_w \qquad t > 0 \tag{3.87}$$

The flow rate is calculated by Darcy-low (see Eq. 3.32):

$$q(t) = -\frac{2\pi r_w hk}{B\mu}\left(\frac{\partial p}{\partial r}\right)_{r = r_w} \tag{3.88}$$

and the cumulative outflow by integrating Eq. 3.88:

$$Q(t) = \int_0^t q(t)dt = -\frac{2\pi r_w hk}{B\mu}\int_0^t \left(\frac{\partial p}{\partial r}\right)_{r = r_w} dt\,. \tag{3.89}$$

Again dimensionless variables are applied:

$$r_D = \frac{r}{r_w} \tag{3.90}$$

$$t_D = \frac{Kt}{r_w^2} = \frac{k}{\mu\phi c r_w^2}t \tag{3.91}$$

$$P_D = \frac{p_i - p}{p_i - p_{wf}} = \frac{p_i - p}{\Delta p_{wf}} \tag{3.92}$$

r_D and t_D are similar to those used in Eq. 3.70 and Eq. 3.71, only P_D is different. Also note that Eq. 3.56 is not applicable in this case since the production q is not constant.

Eq. 3.90 - Eq. 3.92 are then substituted into Eq. 3.30, Eq. 3.31 and Eq. 3.33. The B.C. in Eq. 3.87 can be converted to dimensionless B.C. using Eq. 3.92. The following equations are obtained:

$$\frac{\partial^2 P_D}{\partial r_D^2} + \frac{1}{r_D}\frac{\partial P_D}{\partial r_D} = \frac{\partial P_D}{\partial t_D} \tag{3.93}$$

$$P_D = 0 \qquad r_D > 1 \qquad t_D = 0 \tag{3.94}$$

$$P_D = 1 \qquad r_D = 1 \qquad t_D > 0 \tag{3.95}$$

$$P_D = 0 \qquad r_D = \infty \qquad t_D > 0 \tag{3.96}$$

The above boundary value problem (B.V.P.) described by Eq. 3.93 - Eq. 3.96 is similar to the B.V.P. described by Eq. 3.77 - Eq. 3.80, except that the B.C. in Eq. 3.79 is replaced by the B.C. in Eq. 3.95. Substituting the dimensionless variables in Eq. 3.89, leads to:

$$Q(t) = \left(-\frac{2\pi r_w hk}{B\mu}\right)\int_0^{t_D}\left(\frac{\partial}{\partial(r_D r_w)}[p_i - \Delta p_{wf} P_D]\right)_{r_D=1}\frac{\mu\phi c r_w^2}{k}dt_D = \tag{3.97}$$

$$2\pi h\phi r_w^2 c\Delta p_{wf}/B\int_0^{t_D}\left(\frac{\partial P_D}{\partial r_D}\right)_{r_D=1}dt_D$$

Let:

$$Q_D(t_D) = \int_0^{t_D}\left(\frac{\partial P_D}{\partial r_D}\right)_{r_D=1}dt_D \tag{3.98}$$

Figure 3.9 to Figure 3.12 show the graphical solution of Eq. 3.98.

Since $Q_D(t_D)$ can be obtained from Table 3.3 at the end of Chapter 3 or from Figure 3.9 - Figure 3.12 (for $r_e/r_w = \infty$) as a function of t_D then:

$$\boxed{Q(t) = \frac{2\pi h\phi r_w^2 c}{B}\Delta p_{wf} Q_D(t_D)} \tag{3.99}$$

Where $\Delta p_{wf} = p_i - p_{wf}$

Example 3.5:

Consider the well data from Example 3.1. The bottom hole flowing pressure is fixed at:

$p_{wf} = 8$ [MPa]

Calculate the cumulative production after 100 days.

Solution:

The dimensionless time results in:

$$t_D = \frac{Kt}{r_w^2} = \frac{0,1}{0,1^2} 100 \cdot 86400 = 8,64 \cdot 10^7$$

From the Van Everdinger and Hurst solution (Table 3.3).

$$Q_D(t_D) = 8,895 \cdot 10^6$$

The cumulative oil production after 100 days will be (B = 1.0):

$$Q = 2\pi h \phi r_w^2 c \Delta p_{wf} Q_D(t_D) =$$
$$2 \cdot \pi \cdot 5 \cdot 0,2 \cdot 0,1^2 \cdot 10^{-9} \cdot 2 \cdot 10^6 \cdot 8,895 \cdot 10^6 = 1117,2 \text{ [m}^3\text{]}$$

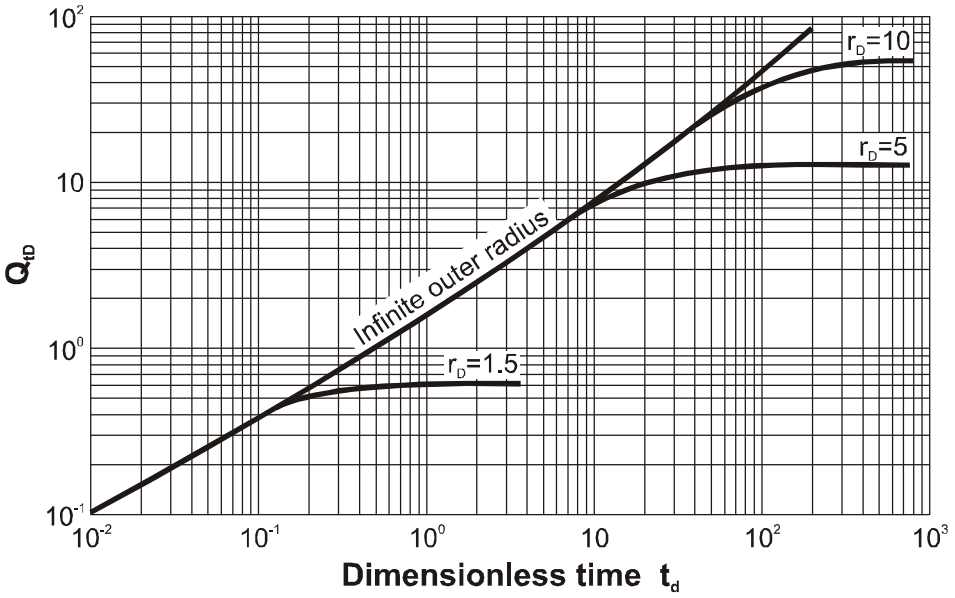

Figure 3.9: Solution for the infinitive and finite radial filtration problem with closed boundary and constant bottom hole pressure (after *Silder*)

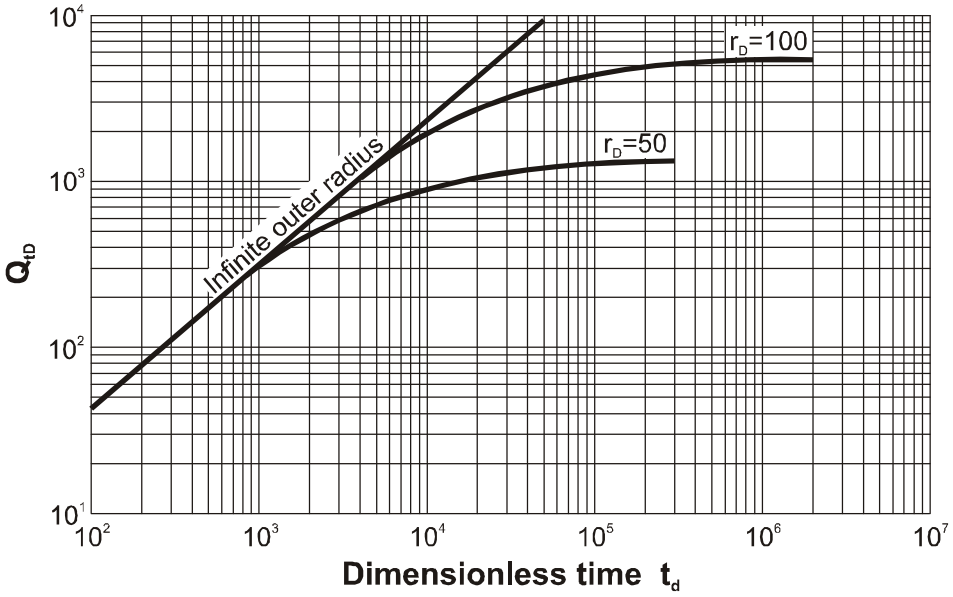

Figure 3.10: Solution for the infinitive and finite radial filtration problem with closed boundary and constant bottom hole pressure (after *Silder*)

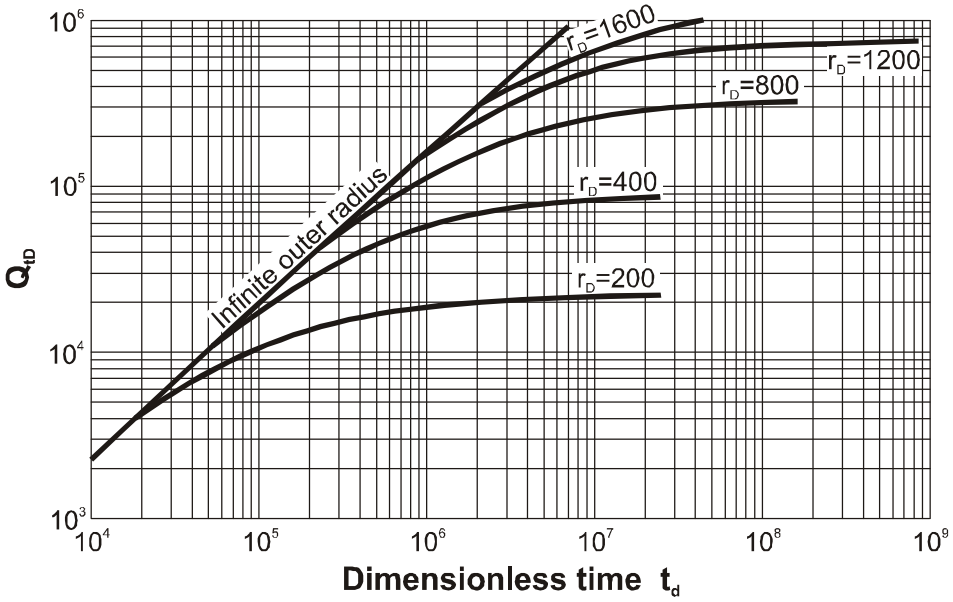

Figure 3.11: Solution for the infinitive and finite radial filtration problem with closed boundary and constant bottom hole pressure (after *Silder*).

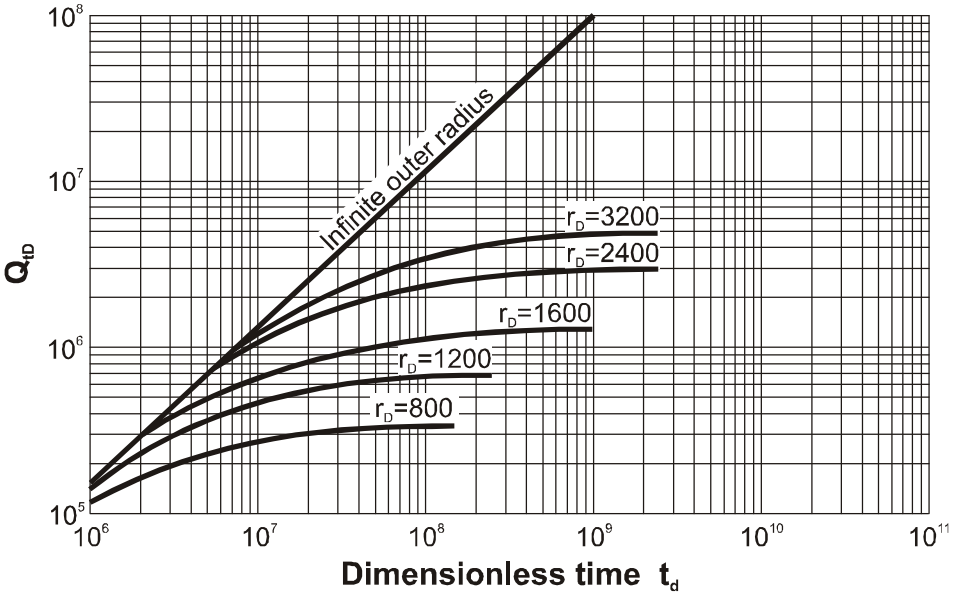

Figure 3.12: Solution for the infinitive and finite radial filtration problem with closed boundary and constant bottom hole pressure (after *Silder*).

3.5 Non-Steady State Filtration in a Finite System

3.5.1 Constant Production Rate

3.5.1.1 Closed Exterior Boundary

The dimensionless variables of Eq. 3.70 - Eq. 3.72 are again applied. The differential equation given by Eq. 3.77, the initial condition in Eq. 3.78 and the boundary condition in Eq. 3.79 are further valid.

The only difference can be found at the exterior boundary. In this case the boundary is not considered to be located in infinity but at a finite distance with radius r_{eD}:

$$\frac{\partial^2 P_D}{\partial r_D^2} + \frac{1}{r_D}\frac{\partial P_D}{\partial r_D} = \frac{\partial P_D}{\partial t_D} \tag{3.100}$$

$$P_D = 0 \qquad r_D > 1 \qquad t_D = 0 \tag{3.101}$$

$$\left(\frac{\partial P_D}{\partial r_D}\right)_{r_D = 1} = -1 \qquad t_D > 0 \tag{3.102}$$

$$\frac{\partial P_D}{\partial r_D} = 0 \qquad r_D = r_{eD} \qquad t_D > 0 \tag{3.103}$$

We now seek a solution for the boundary value problem described by Eq. 3.100 - Eq. 3.103 in the form of:

$$P_D = P_D(r_D, t_D) \tag{3.104}$$

This solution can be achieved by transforming Eq. 3.100 - Eq. 3.103 into the complex plane, followed by integration and retransformation.

This operation is called LAPLACE transformation and is a little bit complicated. Only the results are given here:

$$P_D = \frac{2}{r_{eD}^2 - 1}\left(\frac{r_D^2}{4} + t_D\right) \tag{3.105}$$

$$- \frac{r_{eD}^2 \ln r_D}{r_{eD}^2 - 1} - \frac{3r_{eD}^2 - 4r_{eD}^2 \ln r_{eD} - 2r_{eD}^2 - 1}{4(r_{eD}^2 - 1)^2}$$

$$+ \pi \sum_{n=1}^{\infty} \frac{e^{-\alpha_n^2 t_D} J_1^2(\alpha_n r_{eD})[J_1(\alpha_n) Y_0(\alpha_n r_D) - Y_1(\alpha_n) J_0(\alpha_n r_D)]}{\alpha_n [J_1^2(\alpha_n r_{eD}) - J_1^2(\alpha_n)]}$$

α_n are the roots of the equation:

$$J_1(\alpha_n r_{eD}) Y_1(\alpha_n) - J_1(\alpha_n) Y_1(\alpha_n r_{eD}) = 0 \tag{3.106}$$

where J_i and Y_i are the Bessel functions.

Eq. 3.105 is expressed graphically in Figure 3.8 for different values of r_{eD}. If $r_w \ll r_e$ it is possible to write the well flowing pressure formula in a more simple form:

$$P_{Dw} = \frac{2t_D}{r_{eD}^2} + \ln r_{eD} - \frac{3}{4} + 2 \sum_{n=1}^{\infty} \frac{e^{-\alpha_n^2 t_D} J_1^2(\alpha_n r_{eD})}{\alpha_n^2 [J_1^2(\alpha_n r_{eD}) - J_1^2(\alpha_n)]} \tag{3.107}$$

The roots increase monotonous, if n increases. This means:

$$e^{-\alpha_1^2 t_D} > e^{-\alpha_2^2 t_D} > e^{-\alpha_3^2 t_D}$$

This is the cause for a monotonous decrease of the exponential factor. From this one may conclude that if t_D is large enough this sum will become very small and thus can be neglected.

The approximation for large t_D is:

$$\boxed{P_{Dw} = \frac{2t_D}{r_{eD}^2} + \ln r_{eD} - \frac{3}{4}} \tag{3.108}$$

If the pressure disturbance has not yet reached the exterior boundary, Eq. 3.77 - Eq. 3.80 and Eq. 3.100 - Eq. 3.103 will have an identical solution which is:

$$P_{Dw} = \frac{1}{2}[\ln t_D + 0,80907 + Y_D(t_D)] \tag{3.109}$$

where:

$$Y_D(t_D) = -(\ln t_D + 0,80907) + \frac{4t_D}{r_{eD}^2} + 2\left(\ln r_{eD} - \frac{3}{4}\right) + 4\sum_{n=1}^{\infty} \frac{e^{-\alpha_n^2 t_D} J_1^2(\alpha_n r_{eD})}{\alpha_n^2 [J_1^2(\alpha_n r_{eD}) - J_1^2(\alpha_n)]} \tag{3.110}$$

Eq. 3.110 is the combination of the equations Eq. 3.85 and Eq. 3.107. It is evident that the function $Y_D(t_D)$ will become zero, if the exterior boundary is not yet reached. The solutions of the finite and the infinite systems are therefore identical for a given time t .

With dimensioned variables Eq. 3.109 becomes:

$$p_{wf} = p_i + \frac{\mu q B}{4\pi h k}\left(0,80907 + \ln \frac{Kt}{r_w^2} + Y(t)\right) \tag{3.111}$$

3.5.1.2 Boundary with Constant Pressure

If the system has an open boundary, but a constant pressure at the exterior boundary.

Eq. 3.100 - Eq. 3.102 remain the same, but the boundary condition in Eq. 3.103 is substituted by:

$$P_D = 0 \qquad t_D > 0 \qquad r_D = r_{eD} \tag{3.112}$$

The solution of the boundary value problem is described by Eq. 3.100 - Eq. 3.102 and Eq. 3.112 considering again that $r_w \ll r_e$ is given by:

$$P_D = \ln r_{eD} - 2\sum_{n=1}^{\infty} \frac{e^{-\beta_n^2 t_D} J_0^2(\beta_n r_{eD})}{\beta_n^2 [J_1^2(\beta_n) - J_0^2(\beta_n r_{eD})]} \tag{3.113}$$

β_n are defined as the roots of this equation:

$$J_1(\beta_n) Y_0(\beta_n r_{eD}) - Y_1(\beta_n) J_1(\beta_n r_{eD}) = 0$$

It t_D is large enough it is possible to neglect the summation term in Eq. 3.113, then Eq. 3.113 becomes:

$$\boxed{P_D = \ln \frac{r_e}{r_w}} \tag{3.114}$$

which is identical with Eq. 3.20.

3.5.2 Constant Pressure at the Interior Boundary and Closed Exterior Boundary

Just as in Section 3.4: The rate at the interior boundary (e.g. at the well radius) is not fixed, but the pressure p_{wf} is set at a certain value. Again the dimensionless pressure form is used. The differential equation and the boundary conditions may then be written as follows:

$$\frac{\partial^2 P_D}{\partial r_D^2} + \frac{1}{r_D}\frac{\partial P_D}{\partial r_D} = \frac{\partial P_D}{\partial t_D} \tag{3.115}$$

$$P_D = 0 \qquad 1 \le r_D \le r_{eD} \qquad t_D = 0 \tag{3.116}$$

$$P_D = 1 \qquad r_D = 1 \qquad t_D > 0 \tag{3.117}$$

$$\frac{\partial P_D}{\partial r_D} = 0 \qquad r_D = r_{eD} \qquad t_D > 0 \tag{3.118}$$

The solution of the above B.V.P. is given by Eq. 3.99, but the dimensionless cumulative inflow $Q_D(t_D)$. is determined from Figure 3.9 - Figure 3.12 for different ratios of $r_{eD} = r_e / r_w$.

Example 3.6:

Consider the data given in example 3.5 and the exterior radius (r_e) of the reservoir was estimated as 320 [m]. Calculate the cumulative production after 100 days.

Solution:

From the solution of example 3.5, t_D is 8.64 10^7

From Figure 3.9a: $Q_D = 3.5\ 10^6$

The cumulative production will be:

$$Q = \frac{2\pi h r_w^2 c}{B} \Delta p_{wf} Q_D(t_D) = 440 \text{ [m}^3\text{]}$$

3.6 Non-Steady State Filtration in Linear System

Linear flow systems are applicable in the case of a massive fracture or a horizontal well, where the fluids flow linearly to the fracture or the wellbore of the horizontal well.

3.6.1 Linear Flow with Constant Production Rate

For a vertically fractured wells, the fracture intersects the wellbore perpendicularly, or horizontal wells in an infinite acting reservoir, the fluids will flow linearly to the vertical fracture or the horizontal well especially at the beginning of the flow and after a relatively short time period.

Consider a one dimensional flow problem described by:

$$\frac{\partial^2 p}{\partial x^2} = \frac{1}{K}\frac{\partial p}{\partial t} \tag{3.119}$$

$$\frac{\partial p}{\partial x} = -q\frac{B\mu}{Ak} \qquad x = 0 \qquad t > 0 \tag{3.120}$$

$$p(\infty, t) = p_i \qquad x = \infty \qquad t > 0 \tag{3.121}$$

$$p(x, 0) = p_i \qquad x > 0 \qquad t = 0 \tag{3.122}$$

Gringarten, Ramey and Raghavan used a flow model "Uniform Flux Fracture" which is the first approximation to the behavior of a vertically fractured well. Fluid enter the fracture at a uniform rate per unit surface area of the fracture, so that there is a pressure drop created by the fracture. This pressure difference can be calculated from the following equation:

$$p - p_i = \frac{qB\mu}{Ak}\left\{\frac{\sqrt{2\pi Kt}}{x_f} erf\left(\frac{x_f}{2\sqrt{Kt}}\right) - Ei\left(\frac{-x_f^2}{4Kt}\right)\right\}, \tag{3.123}$$

where:

x_f is half length of the vertical fracture and

A is the surface area of the flow

In order to convert Eq. 3.123 to a dimensionless equation the following dimensionless variable is introduced:

$$t_{Dx_f} = t_D\left(\frac{r_w}{x_f}\right)^2 \tag{3.124}$$

using the definition of p_D and t_D the dimensionless pressure is obtained by:

$$p_D = \sqrt{\pi t_{Dx_f}}\, erf\left(\frac{1}{2\sqrt{t_{Dx_f}}}\right) - \frac{1}{2}Ei\left(\frac{-1}{4t_{Dx_f}}\right) \tag{3.125}$$

For $t_{Dxf} > 10$ Eq. 3.125 can be approximated by

$$p_D = \frac{1}{2}[\ln t_{Dx_f} + 2.80907] \tag{3.126}$$

For $t_{Dxf} > 0.1$ Eq. 3.125 becomes:

$$p_D = \sqrt{\pi t_{Dx_f}} \tag{3.127}$$

which indicates that during a short time the flow into the fracture is linear.

Figure 3.13 shows the relation between p_D and t_{Dxf}. For $t_{Dxf} > 0.1$ a half slope straight line is obtained which indicates linear flow behaviour.

Example 3.7:

A) Calculate the pressure drop created by a vertical fracture having a length of 5 [m] after 5.2 and 15.6 min. Use the data in example 3.1.

B) Compare the pressure drop in part A with the pressure drop, created by the unfractured well in example 3.1 after 15.6 min.

***Solution**:*

$$K = \frac{k}{\phi\mu c} = \frac{0,02 \cdot 10^{-12}}{0,2 \cdot 10^{-3} \cdot 10^{-9}} = 0,1\ [\mathrm{m^2 sec^{-1}}]$$

A) After 5.2 min.

$$t_{D1} = K\frac{t_1}{r_w^2} = 0,1 \cdot \frac{5,2 \cdot 60}{0,1^2} = 3,12 \cdot 10^3$$

$$t_{Dx_{f1}} = t_{D1}\left(\frac{r_w}{x_f}\right)^2 = 3,12 \cdot 10^3 \cdot \left(\frac{0,1}{2,5}\right)^2 = 5,0$$

From Figure 3.13, $P_{D1} = 2.25$

The pressure drop after 5.2 min. is:

$$\Delta p_1 = \frac{\mu Bq}{2\pi hk} p_{D1} = \frac{(-10/184300)10^{-3}}{2 \cdot 3,14 \cdot 5 \cdot 0,02 \cdot 10^{-12}}(2,25) = 415 \text{ [kPa]}$$

After 15.6 min.:

$$t_{D2} = K\frac{t_2}{r_w^2} = 0,1 \cdot \frac{15,6 \cdot 60}{0,1^2} = 9,36 \cdot 10^3$$

$$t_{Dx_{f2}} = t_{D2}\left(\frac{r_w}{x_f}\right)^2 = 15$$

Since $t_{Dxf} > 10$ *, then* p_{D2} *can be calculated from:*

$$p_{D2} = \frac{1}{2}[\ln t_{Dx_f} + 0,80907] = 2,76$$

Then the pressure drop after 15.6 min. is:

$$\Delta p = \frac{\mu Bq}{2\pi hk} p_{D2} = 509 \text{ [kPa]}$$

B) For the unfractured well in example 3.1 and after 15.6 min.:

$\frac{t_D}{r_w^2} > 10$ *, then* p_D *can be calculated from:*

$$p_{Dw} = \frac{1}{2}[\ln t_D + 0,80907] = 4,43$$

$$\frac{\Delta p_{unf}}{\Delta p_f} = \frac{p_{unf}}{p_{Df}} = \frac{4,43}{2,76} = 1,61$$

The pressure drop created by the unfractured well, after 15.6 min., is 1.6 times higher than the one created by the same well with a single vertical fracture.

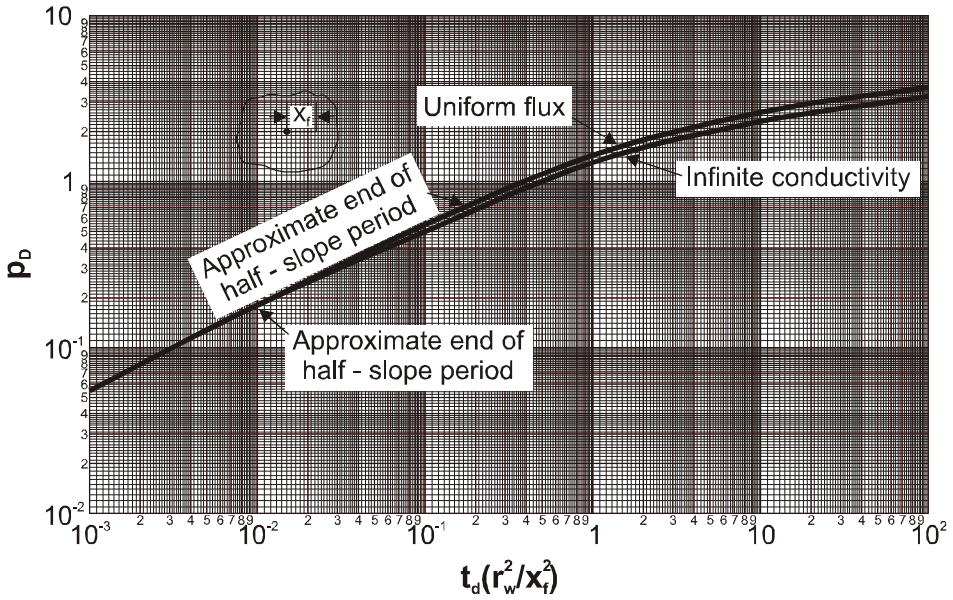

Figure 3.13: Dimensionless pressure for single fractured well in an infinite acting system (after *Gringarten, Ramey, and Ragavan*)

Table 3.1: Solution of Transient Filtration in the Case of Infinite Radial System

Mathematical Formulation	**Dimensioned**	**Dimensionless**
Distance	r	$r_D = \frac{r}{r_w}$
Time	t	$t_D = \frac{Kt}{r_w^2}$
Pressure	p	$P_D = (p - p_i)\frac{2\pi hk}{qB\mu}$
Differential Equation	$\frac{\partial^2 p}{\partial r^2} + \frac{1}{r}\frac{\partial p}{\partial r} = \frac{1}{K}\frac{\partial p}{\partial t}$	$\frac{\partial^2 P_D}{\partial r_D^2} + \frac{1}{r_D}\frac{\partial P_D}{\partial r_D} = \frac{\partial P_D}{\partial t_D}$
Initial Condition	$p = p_i;\ \ r \geq r_w;\ \ t = 0$	$P_D = 0;\ r_D \geq 1;\ t_D = 0$
Boundary Conditions 1.) Well Radius	$\frac{2\pi r_w hk}{\mu}\left(\frac{\partial p}{\partial r}\right)_{r = r_w} = -qB$	$\left(\frac{\partial P_D}{\partial r_D}\right)_{r_D = 1} = -1$
2.) Outer Boundary	$p = p_i;\ \ r = \infty$	$P_D = 0;\ \ r_D = \infty$
Solution	$p_i - p(r, t) = \frac{\mu qB}{4\pi hk} Ei\left(-\frac{r^2}{4Kt}\right)$	$P_D\left(\frac{t_D}{r_D^2}\right) = -\frac{1}{2} Ei\left(-\frac{r_D^2}{4t_D}\right)$
Solution in Case of $\frac{Kt}{r^2} \geq 10$	$p_i - p(r, t) = -\frac{\mu qB}{4\pi hk}\left(0,80907 + \ln\frac{Kt}{r^2}\right)$	$P_D = \frac{1}{2}\left[0,80907 + \ln\frac{t_D}{r_D^2}\right]$

Table 3.2: Solution of Transient Filtration in the Case of Infinite Radial System

Conditions	Constant Production	Constant Borehole Pressure
Dimensionless Variables:		
Distance	$r_D = \frac{r}{r_w}$	$r_D = \frac{r}{r_w}$
Time	$t_D = \frac{Kt}{r_w^2}$	$t_D = \frac{Kt}{r_w^2}$
Pressure	$P_D = (p - p_i)\frac{2\pi hk}{qB\mu}$	$P_D = \frac{p_i - p}{p_i - p_{wf}}$
Differential Equation	$\frac{\partial^2 P_D}{\partial r_D^2} + \frac{1}{r_D}\frac{\partial P_D}{\partial r_D} = \frac{\partial P_D}{\partial t_D}$	$\frac{\partial^2 P_D}{\partial r_D^2} + \frac{1}{r_D}\frac{\partial P_D}{\partial r_D} = \frac{\partial P_D}{\partial t_D}$
Initial Condition	$P_D = 0;\ r_D \geq 1;\ t_D = 0$	$P_D = 0;\ r_D \geq 1;\ t_D = 0$
Boundary Conditions		
1.) Well Radius	$\left(\frac{\partial P_D}{\partial r_D}\right)_{r_D = 1} = -1;\ t_D > 0$	$P_D = 1;\ r_D = 1;\ t_D > 0;$
2.) Outer Boundary	$P_D = 0;\ r_D = \infty;\ t_D > 0$	$P_D = 0;\ r_D = \infty;\ t_D > 0;$
Borehole Pressure	$r_D = 1;\ t_D > 0$	Trivial $[P_D = 1;\ r_D = 1]$
Cumulative Influx	$P_D = \frac{1}{2}[0,80907 + \ln t_D]$	$Q_D(t_D) = \int_0^{t_D}\left(\frac{\partial P_D}{\partial r_D}\right)_{r_D = 1} dt_D$
	Trivial $[Q(t) = qt]$	$Q(t) = 2\pi h\phi r_w^2 c\Delta p_{wf} Q_D(t_D)$

3.7 The Principle of Superposition

In mathematics the superposition theorem states that any sum of individual solutions of a linear differential equation is also a solution of this differential equation, but for different boundary conditions. In practice, the superposition theorem is considered to be one of the most powerful tools to get the solutions of complex flow problems without solving the differential equation for different boundary conditions over and over again.

3.7.1 The First Law of Superposition

Consider a well producing with a continuously changing bottom hole pressure as it is shown in Figure 3.14. The pressure can then be approximated by a step function. For all single pressure changes the cumulative production (influx) can be calculated by Eq. 3.99. According to the theorem of superposition the overall influx caused by the n subsequent finite pressure drops is the sum of the elementary solutions:

$$W_e(t) = C \sum_{j=0}^{n} \Delta p_{wf} Q_D(t_D - t_{Dj}) \tag{3.128}$$

where C is a constant. Eq. 3.128 is the original form of the van Everdingen-Hurst solution.

Vogt and Wang improved this model assuming piecewise linear pressure change instead of a stepping one.

Eq. 3.128 can be written in the following form too:

$$W_e(t) = C \sum_{j=0}^{n} \frac{\Delta p_{wf}}{\Delta t_D} Q_D(t_D - t_{Dj}) \Delta t_D \tag{3.129}$$

or after replacing the summation by integral:

$$W_e(t) = C \int_0^{t_D} \frac{dp_{wf}}{d\tau} Q_D(t_D - \tau) d\tau \tag{3.130}$$

τ is the integration variable. The pressure derivative can be approximated piecewise by finite differences:

$$\frac{dp_{wf}}{d\tau} = \frac{p_j - p_{j-1}}{t_{Dj} - t_{Dj-1}} \quad t_{Dj-1} \le \tau \le t_{Dj} \tag{3.131}$$

and then the integral in Eq. 3.131 can be splitted into n terms:

$$W_e(t_n) = -C\left\{\frac{p_0-p_1}{t_{D1}}\int_0^{t_{D1}} Q_D(t_{Dn}-\tau)d\tau + \frac{p_1-p_2}{t_{D2}-t_{D1}}\int_{t_{D1}}^{t_{D2}} Q_D(t_{Dn}-\tau)d\tau + \right. \tag{3.132}$$

$$\left. .....+\frac{p_{n-1}-p_n}{t_{Dn}-t_{Dn-1}}\int_{t_{Dn-1}}^{t_{Dn}} Q_D(t_{Dn}-\tau)d\tau\right\}$$

Let $u = t_{Dn}-\tau$, then $du = -d\tau$, and the integrals in Eq. 3.132 can be rewritten as follows:

$$\int_{t_{Dj-1}}^{t_{Dj}} Q_D(t_{Dn}-\tau)d\tau = \int_{t_{Dn}-t_{Dj}}^{t_{Dn}-t_{Dj-1}} Q_D(u)du = \tag{3.133}$$

$$-\int_0^{t_{Dn}-t_{Dj}} Q_D(u)du + \int_0^{t_{Dn}-t_{Dj-1}} Q_D(u)du$$

Introducing the integral of the $Q_D(t_D)$ function

$$Q_D{}^*(t_D) = \int_0^{t_D} Q_D(u)du \tag{3.134}$$

Eq. 3.132 yields:

$$W_e(t_n) = -C\left\{\frac{p_0-p_1}{t_{D1}}Q_D{}^*(t_{Dn}) + \left(\frac{p_1-p_2}{t_{D2}-t_{D1}} - \frac{p_0-p_1}{t_{D1}}\right)Q_D{}^*(t_{Dn}-t_{D1}) + \right. \tag{3.135}$$

$$\left. ..... + \left(\frac{p_{n-1}-p_n}{t_{Dn-1}-t_{Dn}} - \frac{p_{n-2}-p_{n-1}}{t_{Dn-1}-t_{Dn-2}}\right)Q_D{}^*(t_{Dn}-t_{Dn-1})\right\}$$

Let be $\Delta p_{j+1} = p_j - p_{j+1}$ and $\Delta t_{j+1} = t_j - t_{j+1}$ then Eq. 3.135 becomes:

$$W_e(t_n) = -C\left\{\frac{\Delta p_1}{t_{D1}} Q_D^*(t_{Dn}) + \left(\frac{\Delta p_2}{\Delta t_{D2}} - \frac{\Delta p_1}{t_{D1}}\right) Q_D^*(t_{Dn} - t_{D1}) + \right. \tag{3.136}$$

$$\left. ..... + \left(\frac{\Delta p_n}{\Delta t_{Dn}} - \frac{\Delta p_{n-1}}{\Delta t_{Dn-1}}\right) Q_D^*(t_{Dn} - t_{Dn-1})\right\}$$

$$= -C \sum_{j=0}^{n-1} \Delta\left(\frac{\Delta p_j}{\Delta t_{Dj}}\right) Q_D^*(t_{Dn} - t_{Dj})$$

where

$$\Delta\left(\frac{\Delta p_j}{\Delta t_{Dj}}\right) = \frac{\Delta p_j}{\Delta t_{Dj}} - \frac{\Delta p_{j-1}}{\Delta t_{Dj-1}} \tag{3.137}$$

Comparing Eq. 3.136 with Eq. 3.128 it is evident that:

$$\sum_{j=0}^{n} \Delta p_j Q_D(t_{Dn} - t_{Dj}) = \sum_{j=0}^{n-1} \Delta\left(\frac{\Delta p_j}{\Delta t_{Dj}}\right) Q_D^*(t_{Dn} - t_{Dj}) \text{ if } n \to \infty \tag{3.138}$$

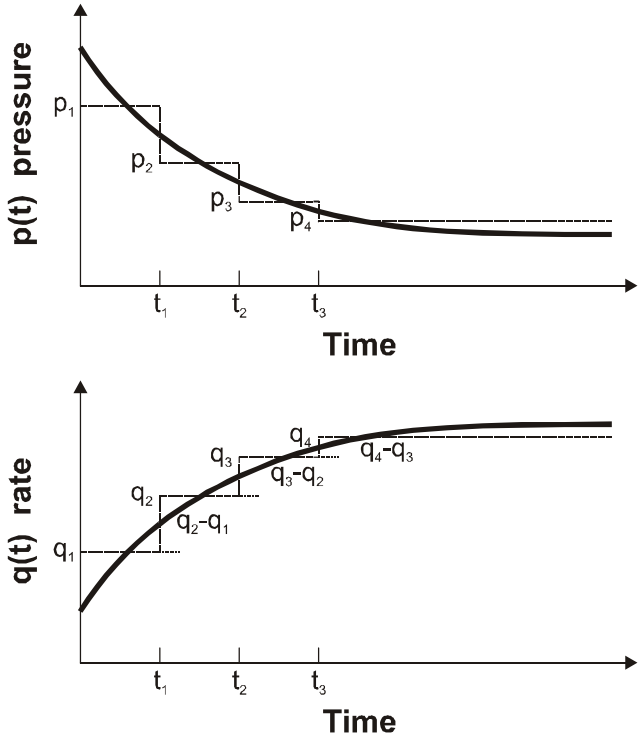

Figure 3.14: Variable production rate in case of a ideal reservoir (after *Hurst*)

3.7.2 The Second Law of Superposition

Figure 3.15 illustrates the pressure change of two wells inside an infinite reservoir. At first well 1 is put on production, with rate q_1, at a time t_1. The pressure change at any time $t > t_1$ at point R can be calculated using Eq. 3.56:

$$\Delta p_1 = \frac{q_1 \mu B}{4\pi hk} Ei\left(-\frac{r_1^2}{4K(t-t_1)}\right) \tag{3.139}$$

If the rate of well 1 is set to $q_1 = 1$ then the pressure drop is defined as Δp_1^*. Eq. 3.56 yields again:

$$\Delta p_1^* = \frac{\mu B}{4\pi hk} Ei\left(-\frac{r_1^2}{4K(t-t_1)}\right) \tag{3.140}$$

or dimensionless:

$$P_{D1}^* = \frac{2\pi hk}{\mu B}\Delta p_1^* = \frac{1}{2} Ei\left(-\frac{r_{D1}^2}{4(t_D - t_{D1})}\right) \tag{3.141}$$

Using Eq. 3.139 and Eq. 3.140 it is trivial to state that if well 1 producec at a constant rate $q_1 \neq 1$ the pressue change at point R will be proportinal to q_1:

$$\Delta p_1 = q_1 \Delta p_1^* \tag{3.142}$$

and

$$P_{D1} = \hat{q}_1 P_{D1}^* \tag{3.143}$$

where $\hat{q}_1$ is equal to q_1 but it is dimensionless. Analogous the formulas for well 2 producing with a rate $q_2 = 1$ and starting at a time t_2 may be set up:

$$\Delta p_2^* = \frac{\mu B}{4\pi hk} Ei\left(-\frac{r_2^2}{4K(t-t_2)}\right) \tag{3.144}$$

$$P_{D2}^* = \frac{2\pi hk}{\mu B}\Delta p_2^* = \frac{1}{2} Ei\left(-\frac{r_{D2}^2}{4(t_D - t_{D2})}\right) \tag{3.145}$$

$$\Delta p_2 = q_2 \Delta p_2^* \tag{3.146}$$

and

$$P_{D2} = \hat{q}_2 P_{D2}^* \tag{3.147}$$

If both wells are under production the pressure changes at point R may be added:

$$P_D = P_{D1} + P_{D2} = \hat{q}_1 P_{D1}^* + \hat{q}_2 P_{D2}^* \tag{3.148}$$

$$\Delta p = p_i - p_r(t) = q_1 \Delta p_1^* + q_2 \Delta p_2^* = \tag{3.149}$$

$$\frac{\mu B}{4\pi hk}\left\{ q_1 Ei\left(-\frac{r_1^2}{4K(t-t_1)}\right) + q_2 Ei\left(-\frac{r_2^2}{4K(t-t_2)}\right)\right\}$$

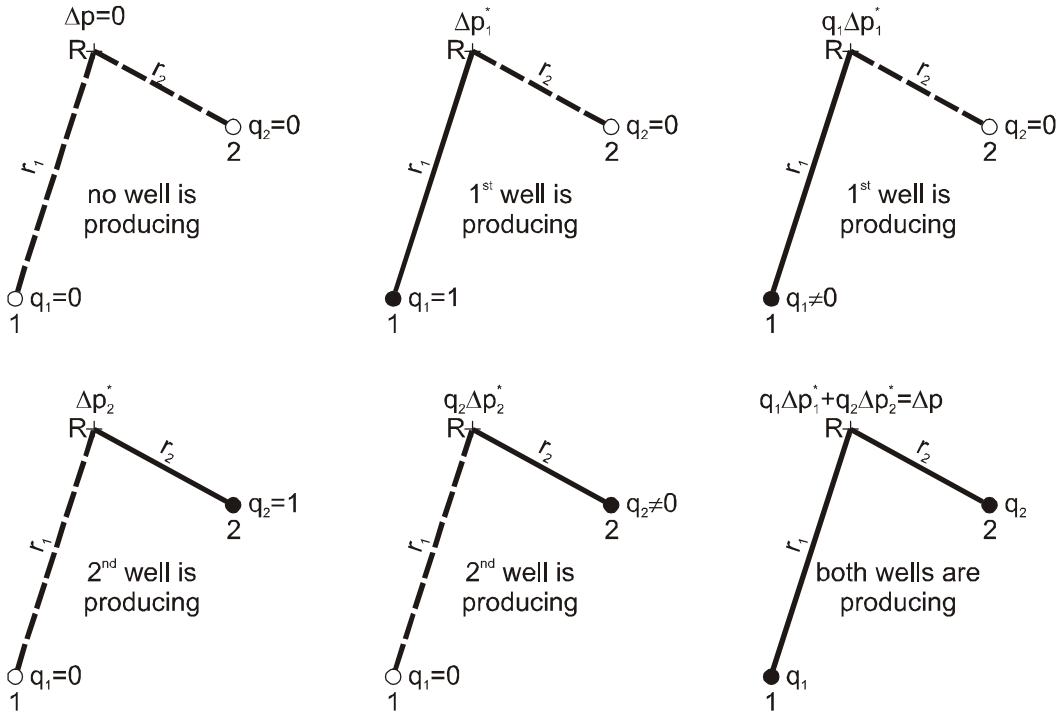

Figure 3.15: Pressure change at point R in infinite reservoir, with two production wells

3.7.3 Calculation of Multi-Well Problems

Fig. 3.16 shows various wells put on production with constant rates inside an *infinite acting* reservoir. Wells started with production successively at the times t_1, t_2, t_3.

The diagram includes the overall production rate. Bottom hole flowing pressure of well 1 is determined by the second law of superposition as follows:

$$P_{D1} = \sum_{j=1}^{n} \hat{q}_j \; P_{Dj}{}^{*}_{1} \tag{3.150}$$

or from Eq. 3.148 - Eq. 3.149:

$$p_i - p_{wf1}(t) = \frac{\mu B}{4\pi hk} \sum_{j=1}^{n} q_j Ei\left(-\frac{r_j^{\,2}}{4K(t-t_j)}\right) \tag{3.151}$$

r_1 is the radius of well 1. Summation is only made for $t > t_j$.

3.7.4 Single Well with Variable Production Rates

When applying the second law of superposition the distances of the wells $2 \rightarrow n$ from well 1 are not considered. As shown in Figure 3.17 the wells $2 \rightarrow n$ are projected imaginatively into well 1. Then every r_j is substituted by r_w:

$$p_i - p_{wf1}(t) = \frac{\mu B}{4\pi hk} \sum_{j=1}^{n} q_j Ei\left(-\frac{r_w^{\,2}}{4K(t-t_j)}\right) \tag{3.152}$$

The value of the bottom hole pressure is the result of this equation where the q_j represent the rate changes at the times t_j.

For the calculation of the flowing pressure it is permitted to use the logarithmic approximation formula Eq. 3.61. Thus Eq. 3.152 becomes:

$$p_i - p_{wf1}(t) = -\frac{\mu B}{4\pi hk}\sum_{j=1}^{n} q_j\left(0,80907 + \ln\frac{K(t-t_j)}{r_w^2}\right) = \tag{3.153}$$

$$-\frac{\mu B}{4\pi hk}\left\{\sum_{j=1}^{n} q_j \ln(t-t_j) + \left(0,80907 + \ln\frac{K}{r_w^2}\right)\sum_{j=1}^{n} q_j\right\}$$

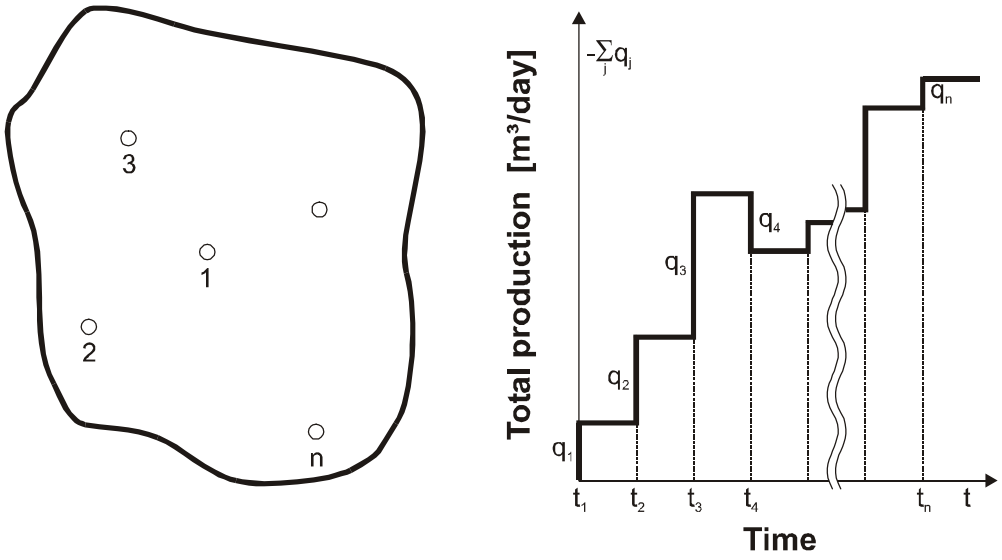

Figure 3.16: Superposition of several wells in a infinite reservoir

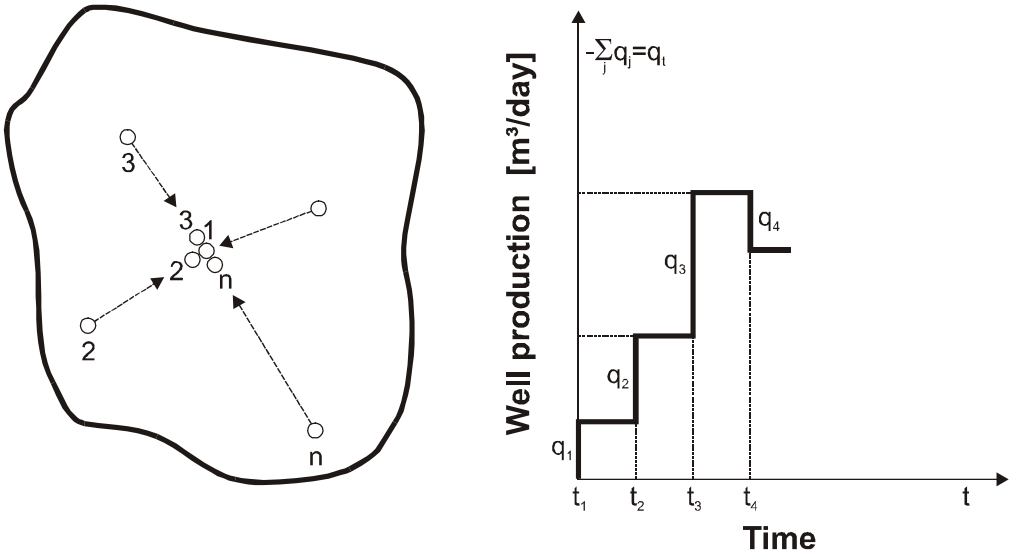

Figure 3.17: Application of the second law of superposition on a well with a variable production

3.7.5 Pressure Build-up of Shut-In Well

At first the well is put on production during time t_1 with a constant rate q_1. Then at the end of t_1 the well is shut in ($q_2 = 0$) for the time Δt. The pressure drop after the time $t = t_1 + \Delta t$ may then be calculated by Eq. 3.153 as follows:

$$p_i - p_{wf1}(t_1 + \Delta t) = -\frac{\mu B}{4\pi hk} \tag{3.154}$$

$$\left\{ q_1 \ln (t_1 + \Delta t) + q_2 \ln (\Delta t) + \left(0,80907 + \ln \frac{K}{r_w^2} \right)(q_1 + q_2) \right\}$$

Eq. 3.154 considers the well is on production during the time $t = t_1 + \Delta t$, but the well was shut in during the time Δt. To make up for this discrepancy, we assume that the well is producing with a rate $q_2 = -q_1$ (as injector) during the shut-in time Δt. Then:

$$q_1 + q_2 = 0$$

So Eq. 3.154 is simplified to:

$$p_{ws}(t_1 + \Delta t) = p_i + \frac{Bq_1\mu}{4\pi hk} \ln \frac{(t_1 + \Delta t)}{\Delta t} \tag{3.155}$$

Instead of p_{wf} (flowing pressure) p_{ws} (shut in pressure) was used which states that the well is shut in. Usage of the common logarithm changes Eq. 3.155 to:

$$\boxed{p_{ws} = p_i + \frac{0,1832Bq_1\mu}{hk} \log \frac{(t_1 + \Delta t)}{\Delta t}} \tag{3.156}$$

This equation calculates the pressure build-up at the well bottom at time t_1 until the end of the build-up test. This curve is of great importance since the determination of permeability and static reservoir pressure is made possible. Figure 3.18 illustrates a pressure build-up curve. When the shut-in pressure (p_{ws}) is plotted versus Horner time in a Semi-log plot, Eq. 3.156 should give a straight line portion and the slope of this portion is -m and according to Eq. 3.156:

$$hk = \frac{01832\mu q_1 B}{-m} \tag{3.157}$$

3.7.6 Method of Image

The second law of superposition may also be useful in the case boundaries exist inside or at the edges of the reservoir. This boundary may be a fault as well as a pinch out. Such a case is illustrated in Figure 3.19.

If an image of well 1, mirrored to the other side of the fault, will be produced with the same rate, the problem is reduced to a dual-well problem in an infinite reservoir as discussed before.

It can easily be taken for granted that for symmetry reasons no flow will occur through the axis of symmetry (fault). Therefore the potential distribution inside the *real region* will be identical in both cases. In the cartesian coordinate system the distance between point $B(x_1,x_2)$ and the well $(x_{10},0)$ is:

$$r_1^{\,2} = (x_1 - x_{10})^2 + x_2^{\,2} \tag{3.158}$$

and from the image well $(-x_{10},0)$:

$$r_2^{\,2} = (x_1 + x_{10})^2 + x_2^{\,2} \tag{3.159}$$

According to Eq. 3.149 the pressure drop is given by:

$$p(\vec{x}, t) - p_i = \frac{B\mu q}{4\pi hk}\left[Ei\left(-\frac{r_1^{\,2}}{4Kt}\right) + Ei\left(-\frac{r_2^{\,2}}{4Kt}\right)\right] \tag{3.160}$$

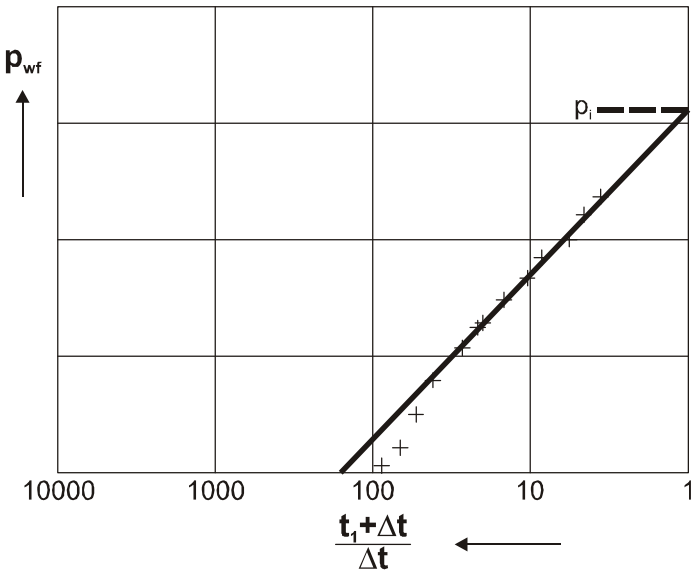

Figure 3.18: Pressure build-up analysis plot (after *Horner*)

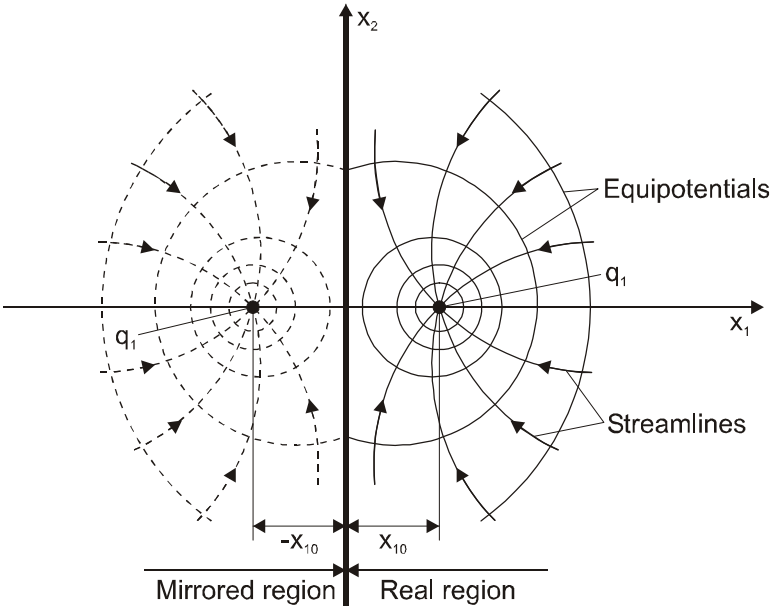

Figure 3.19: Production from a well near impermeable boundary (after *Bear*)

By applying the approximation Eq. 3.61:

$$p(\vec{x}, t) - p_i = \frac{\mu q B}{2\pi h k}\left\{0,80907 + \ln\frac{Kt}{r_1^2} + \ln\frac{r_1}{r_2}\right\} \tag{3.161}$$

or with cartesian coordinates

$$p(\vec{x}, t) - p_i = \frac{\mu q B}{2\pi h k}\left\{0,80907 + \ln\frac{Kt}{(x_1 - x_{10})^2 + x_2^2} + \frac{1}{2}\ln\frac{(x_1 - x_{10})^2 + x_2^2}{(x_1 + x_{10})^2 + x_2^2}\right\} \tag{3.162}$$

The pressure drop is calculated by setting $r_1 = r_w$ and $r_2 = 2x_{10}$. Eq. 3.160 yields:

$$p(\vec{x}, t) - p_i = \frac{\mu q B}{4\pi h k}\left\{Ei\left(-\frac{r_w^2}{4Kt}\right) + Ei\left(-\frac{x_{10}^2}{Kt}\right)\right\} \tag{3.163}$$

3.7.6.1 Pressure Buildup Test Near No Flow Boundary

The well is put on production with a constant rate q, until the time t_1 and then it is shut in. The pressure build-up curve can be calculated in the same manner as demonstrated before (by using the second law of superposition).

$$p_{ws} - p_i = \frac{\mu q B}{4\pi hk}\left\{ Ei\left(-\frac{r_w^2}{4Kt}\right) - Ei\left(-\frac{r_w^2}{4K(t-t_1)}\right) + Ei\left(-\frac{x_{10}^2}{Kt}\right) - Ei\left(-\frac{x_{10}^2}{K(t-t_1)}\right)\right\} \tag{3.164}$$

where the shut-in time is $\Delta t = t - t_1$.

For the first two *Ei*-functions it is possible to use the logarithmic approximation formula without any restriction. Thus Eq. 3.164 according to Eq. 3.154 may be written as follows:

$$p_{ws} - p_i = \frac{\mu q B}{4\pi hk}\left\{ \ln\frac{(t_1+\Delta t)}{\Delta t} + Ei\left(-\frac{x_{10}^2}{K(t_1+\Delta t)}\right) - Ei\left(-\frac{x_{10}^2}{K\Delta t}\right)\right\} \tag{3.165}$$

since:

$$\Delta t = t - t_1,$$

If Δt is small the last *Ei*-term becomes zero and the preceding one is practically constant, then:

$$Ei\left(-\frac{x_{10}^2}{K(t_1+\Delta t)}\right) \approx Ei\left(-\frac{x_{10}^2}{Kt_1}\right) = b \tag{3.166}$$

Then 3.165 becomes:

$$p_{ws} = p_i + \frac{Bq\mu}{4\pi hk}\left\{ \ln\frac{(t_1+\Delta t)}{\Delta t} - b\right\} \tag{3.167}$$

If Δt is large it is possible to apply the logarithmic approximation to 3.165 for all terms and thus:

$$p_{ws} - p_i = \frac{\mu q B}{4\pi hk}\left\{ \ln\frac{(t_1+\Delta t)}{\Delta t} + \ln\frac{K(t_1+\Delta t)}{x_{10}^2} - \ln\frac{K\Delta t}{x_{10}^2}\right\}, \tag{3.168}$$

and

$$p_{ws} = p_i + \frac{Bq\mu}{2\pi hk} \ln \frac{(t_1 + \Delta t)}{\Delta t} \tag{3.169}$$

Figure 3.20 shows the pressure build-up curve. The first section of the curve is described by Eq. 3.167 (after a short time no boundary effects) and the second by Eq. 3.169 (after the pressure disturbance reached the boundary).

The slope of the second straight line (displayed in the semilogarithmic coordinate sheet) is exactly the double of the slope of the first. ($m_2=2m_1$).

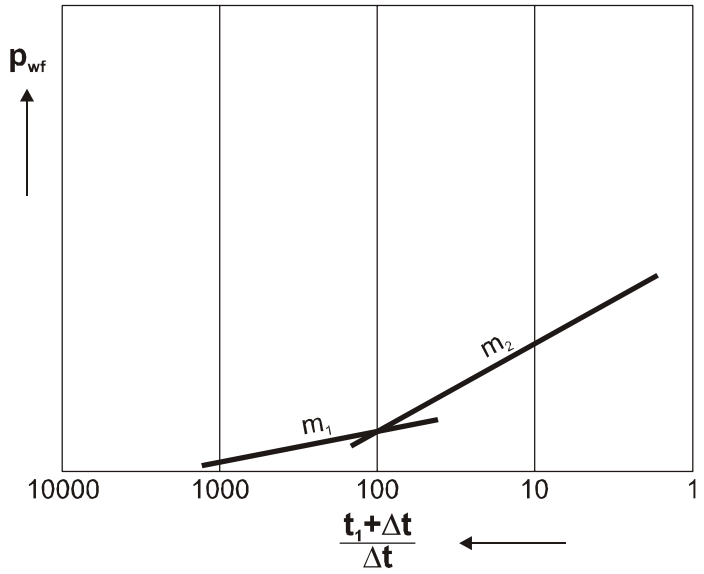

Figure 3.20: Pressure build-up curve near a discontinuity

3.7.6.2 Constant Pressure Boundary

Now let us consider the case of a constant potential at the outer boundary as shown in Figure 3.21. The specific boundary condition given by Eq. 2.81 is used. If the real region is again mirrored, the image well will now be regarded as an injection well, It is evident that the distribution of the potential in the real region will again be the same for both cases. We ignore the boundary, but we consider the image injection well. The corresponding equation is given by Eq. 3.151. The rate for an injection well is $q_2 = -q_1$:

$$p_i - p(\vec{x}, t) = \frac{\mu q B}{4\pi hk}\left\{ Ei\left(-\frac{r_1^2}{4Kt}\right) - Ei\left(-\frac{r_2^2}{4Kt}\right)\right\} \tag{3.170}$$

Using the logarithmic approximation and cartesian coordinates yields:

$$p_i - p(\vec{x}, t) = -\frac{\mu q B}{4\pi hk}\ln\frac{r_2^2}{r_1^2} = -\frac{\mu q B}{4\pi hk}\ln\frac{(x_1 + x_{10})^2 + x_2^2}{(x_1 - x_{10})^2 + x_2^2} \tag{3.171}$$

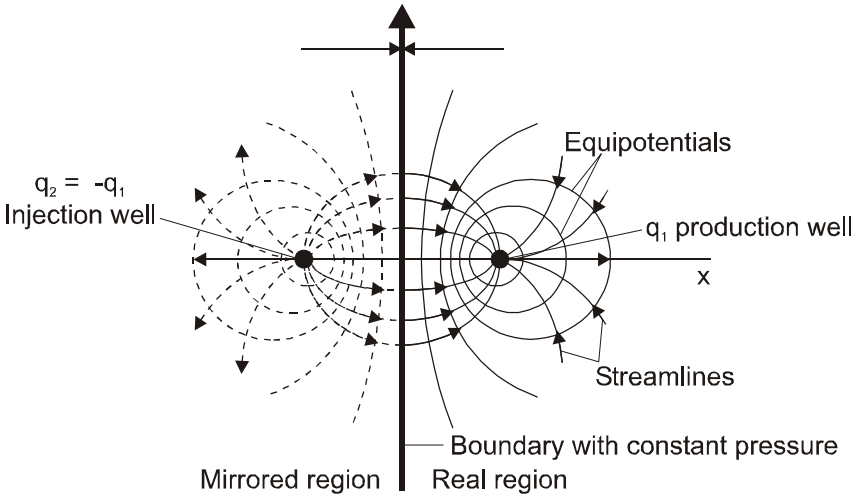

Figure 3.21: Production in the vicinity of a boundary with a constant potential (after *Bear*)

The pressure change at well bottom can be calculated by a more simple equation. For this case:

$$x - x_{10} = r_w \qquad \text{and} \qquad x + x_{10} \cong 2x_{10}$$

therefore:

$$p_i - p_{wf} = -\frac{\mu q B}{2\pi hk}\ln\frac{2x_{10}}{r_w} \tag{3.172}$$

3.8 References

3.1 Bear, J.: "Dynamics of fluids in Porous Media" *Elsevier* New York (1972)

3.2 Chaumet, P.: "Cours de production" *Thome III Econlement monophasique de Fluides dans les millieux poreux*. I.F.P. Publications, Editions Technip, Paris (1964).

3.3 Van Everdingen, A.F. and Hurst, W.: "The application of the Laplace transformations to flow problems in Reservoir" *Trans. AIME* (1949)

3.4 Gringarten, A.C., Ramey, H. Jr., and Raghavan, R. "Applied pressure analysis for fractured wells" *J. Pet. Tech*. (July 1975) 887-892; *Trans. AIME* 259.

3.5 Slider, H.C.: "Practical Pertroleum Reservoir Engineering Methods". *Petroleum Publishing Company* Tulsa O.K., U.S.A.(1976)

Table 3.3: *Hurst - Van Everdingen*: Constant Pressure Q_{tD} Functions for Infinite Acting Radial Reservoirs

t_D	Q_{tD}	t_D	Q_{tD}	t_D	Q_{tD}	t_D	Q_{tD}
0.00	0.000	41	21.298	96	41.735	355	121.966
0.01	0.112	42	21.701	97	42.084	360	123.403
0.05	0.278	43	22.101	98	42.433	365	124.838
0.10	0.404	44	22.500	99	42.781	370	126.270
0.15	0.520	45	22.897	100	43.129	375	127.699
0.20	0.606	46	23.291	105	44.858	380	129.126
0.25	0.689	47	23.684	110	46.574	385	130.550
0.30	0.758	48	24.076	115	48.277	390	131.972
0.40	0.898	49	24.466	120	49.968	395	133.391
0.50	1.020	50	24.855	125	51.648	400	134.808
0.60	1.140	51	25.244	130	53.317	405	136.223
0.70	1.251	52	25.633	135	54.976	410	137.635
0.80	1.359	53	26.020	140	56.625	415	139.045
0.90	1.469	54	26.406	145	58.265	420	140.453
		55	26.791	150	59.895	425	141.859
1.0	1.569	56	27.174	155	61.517	430	143.262
2.0	2.447	57	27.555	160	63.131	435	144.664
3.0	3.202	58	27.935	165	64.737	440	146.064
5.0	4.539	60	28.691	175	67.928	450	148.856
6.0	5.153	61	29.068	180	69.512	455	150.249
7.0	5.743	62	29.443	185	71.090	460	151.640
8.0	6.314	63	29.818	190	72.661	465	153.029
9.0	6.869	64	30.192	195	74.226	470	154.416
10	7.411	65	30.565	200	75.785	475	155.801
11	7.940	66	30.937	205	77.338	480	157.184
12	8.457	67	31.308	210	78.886	485	158.565
13	8.964	68	31.679	215	80.428	490	159.945
14	9.461	69	32.048	220	81.965	495	161.322
15	9.949	70	32.417	225	83.497	500	162.698
16	10.434	71	32.785	230	85.023	510	165.444
17	10.913	72	33.151	235	86.545	520	168.183
18	11.386	73	33.517	240	88.062	525	169.549
19	11.855	74	33.883	245	89.575	530	170.914
20	12.319	75	34.247	250	91.084	540	173.639
21	12.778	76	34.611	255	92.589	550	176.357
22	13.233	77	34.974	260	94.090	560	179.069
23	13.684	78	35.336	265	95.588	570	181.774
24	14.131	79	35.697	270	97.081	575	183.124
25	14.573	80	36.058	275	98.571	580	184.473
26	15.013	81	36.418	280	100.057	590	187.166
27	15.450	82	36.777	285	101.540	600	189.852
28	15.883	83	37.136	290	103.019	610	192.533
29	16.313	84	37.494	295	104.495	620	195.208
30	16.742	85	37.851	300	105.968	625	196.544
31	17.167	86	38.207	305	107.437	630	197.878
32	17.590	87	38.563	310	108.904	640	200.542
33	18.011	88	38.919	315	110.367	650	203.201
34	18.429	89	39.272	320	111.827	660	205.854
35	18.845	90	39.626	325	113.284	670	208.502
36	19.259	91	39.979	330	114.738	675	209.825
37	19.671	92	40.331	335	116.189	680	211.145
38	20.080	93	40.684	340	117.638	690	213.784
39	20.488	94	41.034	345	119.083	700	216.417
40	20.894	95	41.385	350	120.526	710	219.046

Table 3.4: Continuation

720	221.670	1,175	337.142	1,900	510.861	4,050	990.108
725	222.980	1,180	338.376	1,925	516.695	4,100	1,000.858
730	224.289	1,190	340.843	1,950	522.520	4,150	1,011.595
740	226.904	1,200	343.308	1,975	825.337	4,200	1,022.318
750	229.514	1,210	345.770	2,000	534.145	4,250	1,033.028
760	232.120	1,220	348.230	2,025	539.945	4,300	1,043.724
770	234.721	1,225	349.460	2,050	545.737	4,350	1,054.409
775	236.020	1,230	350.688	2,075	551.522	4,400	1,065.082
780	237.318	1,240	353.144	2,100	557.299	4,450	1,075.743
790	239.912	1,250	355.597	2,125	563.068	4,500	1,086.390
800	242.501	1,260	358.048	2,150	568.830	4,550	1,097.024
810	245.086	1,270	360.496	2,175	574.585	4,600	1,107.646
820	247.668	1,275	361.720	2,200	580.332	4,650	1,118.257
825	248.957	1,280	362.942	2,225	586.072	4,700	1,128.854
830	250.245	1,290	365.386	2,250	591.806	4,750	1,139.439
840	252.819	1,300	367.828	2,275	597.532	4,800	1,150.012
850	255.388	1,310	370.267	2,300	603.252	4,850	1,160.574
860	257.953	1,320	372.704	2,325	608.965	4,900	1,171.125
870	260.515	1,325	373.922	2,350	614.672	4,950	1,181.666
875	261.795	1,330	375.139	2,375	620.372	5,000	1,192.198
880	263.073	1,340	377.572	2,400	626.066	5,100	1,213.222
890	265.629	1,350	380.003	2,425	631.755	5,200	1,234.203
900	268.181	1,360	382.432	2,450	637.437	5,300	1,255.141
910	270.729	1,370	384.859	2,475	643.113	5,400	1,276.037
920	273.274	1,375	386.070	2,500	648.781	5,500	1,296.893
925	274.545	1,380	387.283	2,550	660.093	5,600	1,317.709
930	275.815	1,390	389.705	2,600	671.379	5,700	1,338.486
940	278.353	1,400	392.125	2,650	682.640	5,800	1,359.225
950	280.888	1,410	394.543	2,700	693.877	5,900	1,379.927
960	283.420	1,420	396.959	2,750	705.090	6,000	1,400.593
970	285.948	1,425	398.167	2,800	716.280	6,100	1,421.224
975	287.211	1,430	399.373	2,850	727.449	6,200	1,441.820
980	288.473	1,440	401.786	2,900	738.598	6,300	1,462.383
990	290.995	1,450	404.197	2,950	749.725	6,400	1,482.912
1,000	293.514	1,460	406.608	3,000	760.833	6,500	1,503.408
1,010	296.030	1,470	409.013	3,050	771.922	6,600	1,523.872
1,020	298.543	1,475	410.214	3,100	782.992	6,700	1,544.305
1,025	299.799	1,480	411.418	3,150	794.042	6,800	1,564.706
1,030	301.053	1,490	413.820	3,200	805.075	6,900	1,585.077
1,040	303.560	1,500	416.220	3,250	816.090	7,000	1,605.418
1,050	306.065	1,525	422.214	3,300	827.088	7,100	1,625.729
1,060	308.567	1,550	428.196	3,350	838.067	7,200	1,646.011
1,070	311.066	1,575	434.168	3,400	849.028	7,300	1,666.265
1,075	312.314	1,600	440.128	3,450	859.974	7,400	1,686.490
1,080	313.562	1,625	446.077	3,500	870.903	7,500	1,706.688
1,090	316.055	1,650	452.016	3,550	881.816	7,600	1,726.859
1,100	318.545	1,675	457.945	3,600	892.712	7,700	1,747.002
1,110	321.032	1,700	463.863	3,650	903.594	7,800	1,767.120
1,120	323.517	1,725	469.771	3,700	914.459	7,900	1,787.212
1,125	324.760	1,750	475.669	3,750	925.309	8,000	1,807.278
1,130	326.000	1,775	481.558	3,800	936.144	8,100	1,827.319
1,140	328.480	1,800	487.437	3,850	946.966	8,200	1,847.336
1,150	330.958	1,825	493.307	3,900	957.773	8,300	1,867.329
1,160	333.433	1,850	499.167	3,950	968.566	8,400	1,887.298
1,170	335.906	1,875	505.019	4,000	979.344	8,500	1,907.243

Table 3.5: Continuation

8,600	1,927.166	2.510^{7}	2.96110^{6}
8,700	1,947.065	3.010^{7}	3.51710^{6}
8,800	1,966.942	4.010^{7}	4.61010^{6}
8,900	1,986.796	5.010^{7}	5.68910^{6}
9,000	2,006.628	6.010^{7}	6.75810^{6}
9,100	2,026.438	7.010^{7}	7.81610^{6}
9,200	2,046.227	8.010^{7}	8.86610^{6}
9,300	2,065.996	9.010^{7}	9.91110^{6}
9,400	2,085.744	1.010^{8}	1.09510^{7}
9,500	2,105.473	1.510^{8}	1.60410^{7}
9,600	2,125.184	2.010^{8}	2.10810^{7}
9,700	2,144.878	2.510^{8}	2.60710^{7}
9,800	2,164.555	3.010^{8}	3.10010^{7}
9,900	2,184.216	4.010^{8}	4.07110^{7}
10,000	2,203.861	5.010^{8}	5.03210^{7}
12,500	2,688.967	6.010^{8}	5.98410^{7}
15,000	3,164.780	7.010^{8}	6.92810^{7}
17,500	3,633.368	8.010^{8}	7.86510^{7}
20,000	4,095.800	9.010^{8}	8.79710^{7}
25,000	5,005.726	1.010^{9}	9.72510^{7}
30,000	5,899.508	1.510^{9}	1.42910^{8}
35,000	6,780.247	2.010^{9}	1.88010^{8}
40,000	7,650.096	2.510^{9}	2.32810^{8}
50,000	9,363.099	3.010^{9}	2.77110^{8}
60,000	11,047.299	4.010^{9}	3.64510^{8}
70,000	12,708.358	5.010^{9}	4.51010^{8}
75,000	13,531.457	6.010^{9}	5.36810^{8}
80,000	14,350.121	7.010^{9}	6.22010^{8}
90,000	15,975.389	8.010^{9}	7.06610^{8}
100,000	17,586.284	9.010^{9}	7.90910^{8}
125,000	21,560.732	1.010^{10}	8.74710^{8}
1.510^{5}	2.53810^{4}	1.510^{10}	1.28810^{9}
2.010^{5}	3.30810^{4}	2.010^{10}	1.69710^{9}
2.510^{5}	4.06610^{4}	2.510^{10}	2.10310^{9}
3.010^{5}	4.81710^{4}	3.010^{10}	2.50510^{9}
4.010^{5}	6.26710^{4}	4.010^{10}	3.29910^{9}
5.010^{5}	7.69910^{4}	5.010^{10}	4.08710^{9}
6.010^{5}	9.11310^{4}	6.010^{10}	4.86810^{9}
7.010^{5}	1.05110^{5}	7.010^{10}	5.64310^{9}
8.010^{5}	1.18910^{5}	8.010^{10}	6.41410^{9}
9.010^{5}	1.32610^{5}	9.010^{10}	7.18310^{9}
1.010^{6}	1.46210^{5}	1.010^{11}	7.94810^{9}
1.510^{6}	2.12610^{5}	1.510^{11}	1.1710^{10}
2.010^{6}	2.78110^{5}	2.010^{11}	1.5510^{10}
2.510^{6}	3.42710^{5}	2.510^{11}	1.9210^{10}
3.010^{6}	4.06410^{5}	3.010^{11}	2.2910^{10}
4.010^{6}	5.31310^{5}	4.010^{11}	3.0210^{10}
5.010^{6}	6.54410^{5}	5.010^{11}	3.7510^{10}
6.010^{6}	7.76110^{5}	6.010^{11}	4.4710^{10}
7.010^{6}	8.96510^{5}	7.010^{11}	5.1910^{10}
8.010^{6}	1.01610^{6}	8.010^{11}	5.8910^{10}
9.010^{6}	1.13410^{6}	9.010^{11}	6.5810^{10}
1.010^{7}	1.25210^{6}	1.010^{12}	7.2810^{10}
1.510^{7}	1.82810^{6}	1.510^{12}	1.0810^{11}
2.010^{7}	2.39810^{6}	2.010^{12}	1.4210^{11}

4 Two-Phase Filtration

4.1 The Equation of Two-Phase Filtration

This chapter deals with the physical phenomenon of two immiscible fluids flowing simultaneously through porous media. Assuming that there is no mass transfer between these two phases at the interface separating them and that phase equilibrium has been achieved between the two phases. The concept of relative permeability as described in Chapter 1 actually based on the mathematical description of this phenomenon. In this chapter a general mathematical approach was developed to describe the movement of these two fluids. Using the same assumption which has been previously discussed, the fundamental equations of a two-phase filtration may be set up in the same form as in Eq. 2.7.

$$\vec{u}_1 = -\frac{kk_{r1}}{\mu_1}(\nabla p_1 + \rho_1 g\vec{i}_3) \tag{4.1}$$

$$\vec{u}_2 = -\frac{kk_{r2}}{\mu_2}(\nabla p_2 + \rho_2 g\vec{i}_3) \tag{4.2}$$

Index 1 refers to the displacing phase index 2 to the displaced phase.

The displacing phase can either be the wetting phase or the non-wetting phase. As in a one-phase filtration it is assumed that the process is isothermal and thus density and viscosity will be functions of pressure only:

$$\rho_1 = \rho_1(p_1) \qquad \rho_2 = \rho_2(p_2) \tag{4.3}$$

$$\mu_1 = \mu_1(p_1) \qquad \mu_2 = \mu_2(p_2) \tag{4.4}$$

The relation between density and pressure is given by Eq. 2.22 and Eq. 2.23. The difference between the two phase pressures is specified as the capillary pressure which is a function of saturation:

$$p_2 - p_1 = P_c(S_1) \tag{4.5}$$

The equation of continuity only differs from Eq. 2.43 in the fact that fluid 1 only takes the portion S_1 of the pore space ϕ and fluid 2 the portion S_2. S_1 and S_2 are defined as the saturations of the two phases.

It is evident that

$$S_1 + S_2 = 1 \tag{4.6}$$

and so

$$\nabla(\rho_1 \vec{u}_1) = -\frac{\partial(\phi S_1 \rho_1)}{\partial t} \tag{4.7}$$

$$\nabla(\rho_2 \vec{u}_2) = -\frac{\partial(\phi S_2 \rho_2)}{\partial t} \tag{4.8}$$

4.2 Vertical Two-Phase Filtration of Incompressible Fluids

For this case we assume a vertical one dimensional filtration of incompressible fluids in a porous medium. Therefore Eq. 4.1 - Eq. 4.8 may be written as follows:

$$u_1 = -\frac{kk_{r1}}{\mu_1}\left(\frac{\partial p_1}{\partial x} + \rho_1 g\right) \tag{4.9}$$

$$u_2 = -\frac{kk_{r2}}{\mu_2}\left(\frac{\partial p_2}{\partial x} + \rho_2 g\right) \tag{4.10}$$

$$p_2 - p_1 = P_c(S_1) \tag{4.11}$$

$$S_1 + S_2 = 1 \tag{4.12}$$

$$\frac{\partial u_1}{\partial x} + \phi\frac{\partial S_1}{\partial t} = 0 \tag{4.13}$$

$$\frac{\partial u_2}{\partial x} + \phi\frac{\partial S_2}{\partial t} = 0 \tag{4.14}$$

Instead of coordinate x_3 simple x was written. Now it is useful to introduce the total velocity of filtration as a new variable:

$$u = u_1 + u_2 \tag{4.15}$$

When adding Eq. 4.13 and Eq. 4.14:

$$\frac{\partial(u_1 + u_2)}{\partial x} + \phi\frac{(S_1 + S_2)}{\partial t} = 0 \tag{4.16}$$

it is evident that u is independent of x and therefore:

$$\frac{\partial u}{\partial x} = 0 \tag{4.17}$$

Then a new function is introduced:

$$F_1 = \frac{u_1}{u} \tag{4.18}$$

and

$$F_2 = \frac{u_2}{u} = \frac{u - u_1}{u} = 1 - F_1 \tag{4.19}$$

where F_1 is the portion of fluid 1 in reference to the total flow. F_1 and F_2 are called fractional flow functions. The usual symbol of fractional flow value or function is f_1. We use both F_1 and f_1 to distinguish between two cases. We use f_1 if the capillary pressure is neglegted and F_1 if not.

Substitute Eq. 4.18 and Eq. 4.19 into Eq. 4.9 and Eq. 4.10 leads to:

$$\frac{\partial p_1}{\partial x} = -\rho_1 g - \frac{\mu_1 F_1 u}{k k_{r1}} \tag{4.20}$$

$$\frac{\partial p_2}{\partial x} = -\rho_2 g - \frac{\mu_2 (1 - F_1) u}{k k_{r2}} \tag{4.21}$$

Taking the derivative of Eq. 4.11 yields:

$$\frac{\partial p_2}{\partial x} - \frac{\partial p_1}{\partial x} = \frac{\partial P_c(S_1)}{\partial x} = \frac{dP_c}{dS_1} \cdot \frac{\partial S_1}{\partial x} \tag{4.22}$$

Then Eq. 4.21 is subtracted from Eq. 4.20 and equating the result with Eq. 4.22 we obtain:

$$\frac{dP_c}{dS_1} \cdot \frac{\partial S_1}{\partial x} = (\rho_1 - \rho_2) g + \frac{\mu_1 F_1 u}{k k_{r1}} - \frac{\mu_2 (1 - F_1) u}{k k_{r2}} \tag{4.23}$$

F_1 is then obtained in the following form:

$$F_1 = \frac{\dfrac{\mu_2}{k_{r2}} - \dfrac{k(\rho_1 - \rho_2) g}{u}}{\dfrac{\mu_1}{k_{r1}} + \dfrac{\mu_2}{k_{r2}}} + \frac{\dfrac{k}{u}}{\dfrac{\mu_1}{k_{r1}} + \dfrac{\mu_2}{k_{r2}}} \cdot \frac{dP_c}{dS_1} \cdot \frac{\partial S_1}{\partial x} \tag{4.24}$$

Also F_1 can be expressed as:

$$F_1 = \frac{1 + \dfrac{k k_{r2}}{u \mu_2} \left(\dfrac{dP_c}{dS_1} \cdot \dfrac{\partial S_1}{\partial x} - \Delta\rho g \right)}{1 + \dfrac{\mu_1 k_{r2}}{\mu_2 k_{r1}}} \tag{4.25}$$

If

$$f_1 = \frac{\frac{\mu_2}{k_{r2}} - \frac{k(\rho_1 - \rho_2)g}{u}}{\frac{\mu_1}{k_{r1}} + \frac{\mu_2}{k_{r2}}} \tag{4.26}$$

and

$$\psi_1 = \frac{\frac{k}{u}}{\frac{\mu_1}{k_{r1}} + \frac{\mu_2}{k_{r2}}} \cdot \frac{dP_c}{dS_1} \tag{4.27}$$

then

$$F_1 = f_1 + \psi_1 \cdot \frac{\partial S_1}{\partial x} \tag{4.28}$$

where f_1 and ψ_1 are functions of S_1 and u.

Substituting $u_1 = u \cdot F_1$ into Eq. 4.13 and Eq. 4.16 leads to:

$$\frac{u}{\phi} \cdot \frac{\partial F_1}{\partial x} + \frac{\partial S_1}{\partial t} = 0 \tag{4.29}$$

or after using Eq. 4.28:

$$\frac{u}{\phi}\left[\frac{df_1}{dS_1} \cdot \frac{\partial S_1}{\partial x} + \frac{\partial}{\partial x}\left(\psi_1 \cdot \frac{\partial S_1}{\partial x}\right)\right] + \frac{\partial S_1}{\partial t} = 0 \tag{4.30}$$

4.3 The BUCKLEY-LEVERETT Solution

Eq. 4.30 is not linear, thus a solution can only be achieved numerically.

In this chapter though the problem is discussed in a simplified manner.

In the year 1942 *Buckley* and *Leverett* published their theory which enabled great progress on behalf of multiphase filtration.

This theory neglects the capillary force also considers the following assumptions:

- Incompressible fluids and porous media,
- Immiscible fluids,
- *Darcy*'s law of two phase filtration is valid and
- Linear displacement.

Eq. 4.11 and Eq. 4.27 are no longer required. According to Eq. 4.28:

$$F_1 = \frac{u_1}{u} = f_1 \,. \tag{4.31}$$

Eq. 4.30 becomes:

$$\frac{u}{\phi} \cdot \frac{df_1}{dS_1} \cdot \frac{\partial S_1}{\partial x} + \frac{\partial S_1}{\partial t} = 0 \tag{4.32}$$

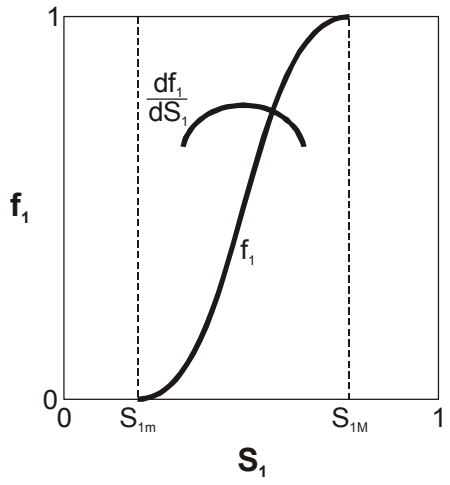

Figure 4.1: Calculation of fractional curve (after *Marle*)

The task is to compute the velocity *w* of a given saturation at any given point i.e. to "track"

the displacing front. Any given value of the saturation S_1 is valid for a specified point x and time t. Mathematically, this means that for every constant S_1 value there is a function:

$$S_1(x, t) = \text{constant} \tag{4.33}$$

which gives the location x as a function of time.

Taking the derivative of Eq. 4.33:

$$\frac{\partial S_1}{\partial x}dx + \frac{\partial S_1}{\partial t}dt = 0 \tag{4.34}$$

and since:

$$dx = wdt \tag{4.35}$$

this leads to:

$$w\frac{\partial S_1}{\partial x} + \frac{\partial S_1}{\partial t} = 0 \tag{4.36}$$

Comparing Eq. 4.36 with Eq. 4.32 leads to:

$$w = \frac{u}{\phi} \cdot \frac{df_1}{dS_1} = \frac{q_1}{A\phi} \cdot \frac{df_1}{dS_1} \tag{4.37}$$

where

q_1 is the injection rate of phase 1 and

A is the cross section area of the porous media.

This term (w) is only a function of S_1 and u. Therefore it is sufficient to know the distribution of initial saturation and the velocity of displacement in order to calculate the saturation distribution.

It is assumed that the initial distribution of saturation in a vertical porous medium at $t = 0$ corresponds to the curve shown in Figure 4.2. On one side at $x = 0$ the velocity $u_1 = u$ is constant. This means that the displacing phase is injected at a constant rate. S_{1m} and S_{1M} are the possible minimum and maximum values of S_1.

If f_1 is plotted versus S_1 as shown in Figure 4.1 which illustrates the so called S-shaped curve which is characteristical for most porous media. This curve has an inflection point at which the differential of f_1 is a maximum.

If porosity ϕ is also regarded as a constant then the speed of propagation for every value of saturation will, as a result of Eq. 4.37, be proportional to:

$$\frac{df_1}{dS_1} \tag{4.38}$$

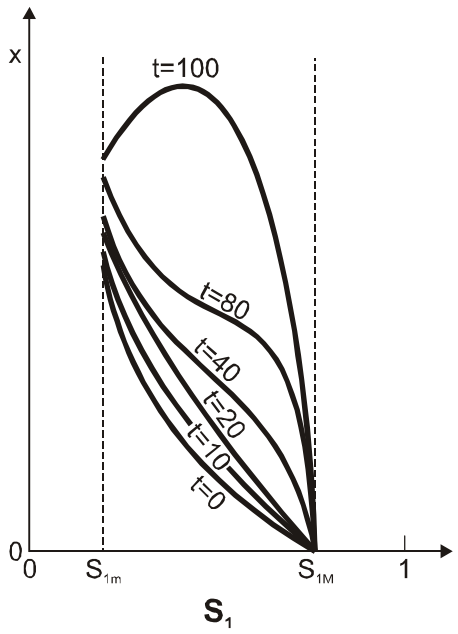

Figure 4.2: Propagation of saturation profile (after *Marle*)

As time elapses the distance travelled for all saturations is plotted. As expected the points with small or large saturation values progress at a lower speed than areas with a middle saturation value as shown in Figure 4.2.

It means that after a certain time period we will have a saturation profile without physical sense since several x-values correspond to two different saturation values. This difficulty only appears after the displacement has travelled a certain distance since the initial saturation distribution was assumed to be continuously decreasing. If at t = 0 the saturation S_1 equals S_{1m} everywhere then these problems will arise for every time t > 0. These difficulties are found also in other fields of physics for example in case of supersonic streaming of gas.

The solution achieved for the saturation distribution may only be interpreted if the profile is not continuous. (Figure 4.3 displays this discontinuity) As a consequence of the conservation of mass the location of the discontinuity must be fixed in a way so that the areas on both sides of the discontinuity are equal in size. (In Figure 4.3 the cross-hatched area).

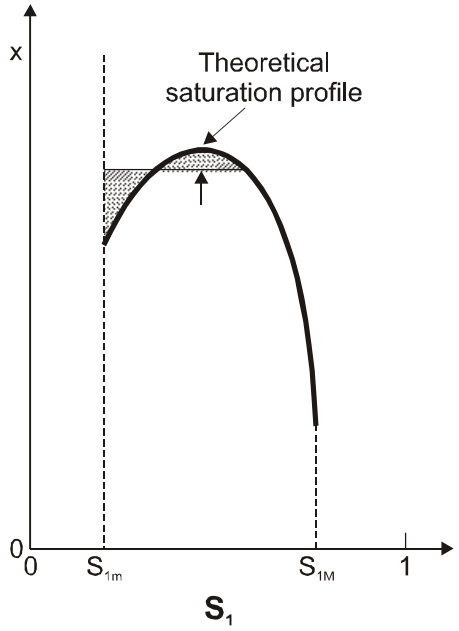

Figure 4.3: The displacement front as discontinuity of saturation (after *Marle*)

4.3.1 The Welge-Method

Let the initial saturation in a porous medium be S_{1a} which can either be smaller or larger than S_{1m}. Then the profile of saturation is plotted at sequential dates $t_1<t_2<t_3$...

The discontinuity in saturation and the front saturation S_{1f} should be determined for every profile. It will be proven that this value is the same for all t.

As already mentioned it is essential that the discontinuity may not contradict the law of conservation of mass. This means that the area below the analytical curve must be equal in value to the area below the profile corrected by the discontinuity as shown in Figure 4.3.

The area below the analytical curve is calculated as follows:

$$\int_{S_{1a}}^{S_{1M}} w(S_1)t\,dS_1 = \frac{ut}{\phi}\int_{S_{1a}}^{S_{1M}} \frac{df_1}{dS_1}dS_1 = \frac{ut}{\phi}[f_1(S_{1M}) - f_1(S_{1a})] \tag{4.39}$$

The area below the corrected profile (*Welge* approximation) will be:

$$w(S_{1f})t(S_{1f}-S_{1a})+\int_{S_{1f}}^{S_{1M}} w(S_1)tdS_1 = \frac{ut}{\phi}\left[\left(\frac{df_1}{dS_1}\right)_{S_1=S_{1f}}\cdot(S_{1f}-S_{1a})+f_1(S_{1M})-f_1(S_{1f})\right] \tag{4.40}$$

Eq. 4.39 and Eq. 4.40 though must result in:

$$\left(\frac{df_1}{dS_1}\right)_{S_1=S_{1f}} = \frac{f_1(S_{1f})-f_1(S_{1a})}{S_{1f}-S_{1a}} \tag{4.41}$$

There is only one point that can satisfy Eq. 4.41. This point is the tangency point of the line drawn from point S_{1a} to the curve f_1, which is independent of time. The meaning of Eq. 4.41 is illustrated in Figure 4.4. The tangency point also gives the value of the saturation at the front (S_{1f}).

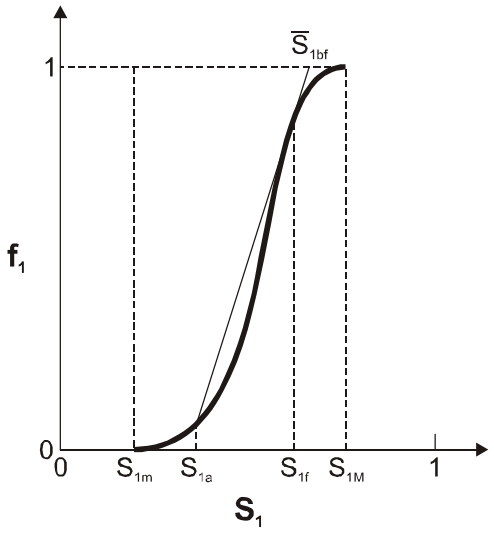

Figure 4.4: Determination of average saturation of the wetting phase after breakthrough (after *Welge*)

In order to calculate the average saturation of phase 1 in the swept zone behind the front ($\bar{S}_{1bf}$), one can write the equation of the tangent of the fractional flow curve as follows:

$$f_1 = \left(\frac{df_1}{dS_1}\right) S_1 + C \tag{4.42}$$

where $\frac{df_1}{dS_1}$ is the slope of the tangent and C is the interception of f_1 axis.

At $f_1 = f_{1f}$; $S_1 = S_{1f}$ (as shown in Figure 4.4) and Eq. 4.42 becomes:

$$C = f_{1f} - \left(\frac{df_1}{dS_1}\right) S_{1f} \tag{4.43}$$

Substituting Eq. 4.43 into Eq. 4.42 yields:

$$f_1 = (S_1 - S_{1f}) \cdot \frac{df_1}{dS_1} + f_{1f} \tag{4.44}$$

At $f_1 = 1.0$; $S_1 = \bar{S}_{1bf}$ and Eq. 4.44 becomes:

$$1 = (\bar{S}_{1bf} - S_{1f}) \cdot \frac{df_1}{dS_1} + f_{1f} \tag{4.45}$$

From Eq. 4.37, $\frac{df_1}{dS_1}$ can be expresses as:

$$\frac{df_1}{dS_1} = \frac{\phi}{u} w = \frac{\phi}{u} \cdot \frac{dx}{dt} = \frac{\phi A}{q} \cdot \frac{dx}{dt} \tag{4.46}$$

After integrating, Eq. 4.46 can be written as:

$$\frac{df_1}{dS_1} = \frac{\phi AL}{Q} \tag{4.47}$$

where Q is the cumulative amount of injected displacing phase (1). Substituting Eq. 4.47 into Eq. 4.45 and solving for $\bar{S}_{1bf}$ yields:

$$\bar{S}_{1bf} = S_{1f} + \frac{Q}{\phi AL}(1 - f_{1f}) \tag{4.48}$$

There also is an alternative derivation of Eq. 4.48, based on material balance, is given in [4.3].

Figure 4.5 shows the cumulative production by a linear displacement. It illustrates that after breakthrough the cumulative production of the displacing fluid (Q_1) will increase rapidly and the cumulative production of the displaced fluid (Q_2) will decrease by the same amount so the total cumulative production (Q) is a linear function.

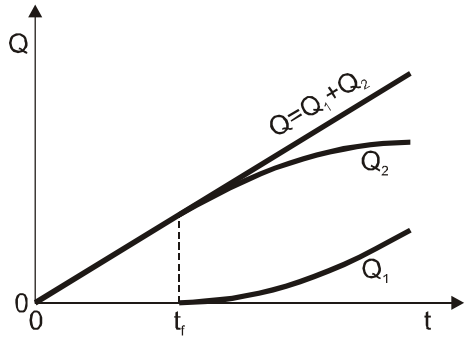

Figure 4.5: Cumulative production by linear displacement (after *Marle*)

Example 4.1:

A cylindrical sandstone core having diameter of 0.05 [m], length of 1 [m] and porosity of 20%. Saturated with oil (35 API) and irreducible water saturation (S_{1m} = 0.2). Water was injected into the core with a steady rate of 0.1 [$cm^3 s^{-1}$] to displace the oil. The fractional flow was calculated and listed below:

Sw:

S_w	f_w
0.20	0.00
0.40	0.30
0.50	0.62
0.55	0.75
0.60	0.85
0.65	0.92
0.70	0.96
0.75	0.99

Calculate the following:

a.) The water saturation at the water front (S_{1f}).
b.) The average oil saturation in the swept area of the core (behind the water front).
c.) The cumulative water injected to reach the average water saturation behind the front determined in part (B).
d.) The velocity of the water front.
e.) Estimate the time of the water breakthrough.

Solution:

a.) From the plot of the fractional flow curve (f_w verses S_w):

b.) The point of tangency represents the water saturation at the front is S_{1f} = 0.55.

c.) Extension of the tangent to f_w=1.0, the average water saturation behind the front is

S_{wbf} = 0.65, Then the average oil saturation behind the front = 1.00 – 0.65 = 0.35.

From Eq. 4.48, the cumulative water injected can be determined from:

$$Q = \phi AL\left[\frac{\bar{S}_{1bf} - S_{1f}}{1 - f_{1f}}\right] = 0.2 \cdot \frac{3.14 \cdot 25}{4} \cdot 100 \cdot \left(\frac{0.65 - 0.55}{1 - 0.775}\right) = 175 \text{ cm}^3$$

d.) The slope of f_w curve at (S_w = 0.55) = 2.17

Then the velocity of the front calculated from:

$$w = \frac{q_1}{A\phi} \cdot \frac{df_1}{dS_1} = \frac{0.1}{\pi(2.5)^2 \cdot 0.2} \cdot 2.17 = 0.055 \text{ cm}/s$$

e.) The time of water breakthrough is:

$$t = \frac{L}{w_f} = \frac{100}{0.055} = 30 \text{ min}$$

4.4 Influence of Gravity and Capillary Force

4.4.1 Influence of Gravity

Eq. 4.26 may be written in the following form:

$$f_1 = \frac{1}{1 + \frac{k_{r2}}{k_{r1}} \cdot \frac{\mu_1}{\mu_2}} \cdot \left[1 - \frac{k k_{r2}}{\mu_2} \cdot \frac{(\rho_1 - \rho_2) g}{u} \right] \tag{4.49}$$

Displacement proceeds in vertical direction from bottom to top. At first the curve f_1 for $\rho_1 = \rho_2$ is drawn. The second term of Eq. 4.49 vanishes and gravity has no more influence.

If $\rho 1 > \rho 2$ the term inside the parenthesis becomes smaller than 1 which means that the fractional curve shifts to the right. The tangent drawn from the initial point $[S_{1i}, f_1(S_{1i})]$ is not so steep but the saturation at the front becomes larger and displacement more effective. The limiting points of the curve f_1 remain unchanged since they only depend on the k_r-functions (see Figure 4.6).

The relation:

$$\frac{k k_{r2}}{\mu_2} \cdot \frac{(\rho_1 - \rho_2) g}{u} \tag{4.50}$$

is simply the relation between the frictional force and gravity. If the velocity of filtration increases the fraction will become smaller and the fractional curve shifts back to the case $\rho_1 = \rho_2$.

The theoretical case of $\rho_1 < \rho_2$ can't be handled by the theory previously discussed. Because this state is not stable and the fluids will exchange their positions in counterflow. A stable frontal displacement is only possible if the heavier fluid is maintained below the lighter fluid.

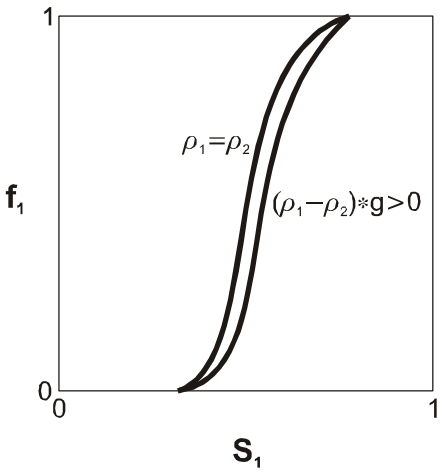

Figure 4.6: The influence of gravity on the fractional curve (after *Marle*)

4.4.2 Influence of the Capillary Force

When considering the capillary force one must regard the fact that Eq. 4.30 is not linear. The solution can only be achieved with help of numerical methods, for example, by the method of finite differences. Discussion of such methods of solution would surpass the objective of this textbook.

The *Buckley-Leverett* solution neglecting the capillary force is illustrated in Figure 4.7 which has been discussed previously. The other profiles were calculated by applying Eq. 4.30 for various rates of filtration with the help of the method of finite differences.

In case of a slow displacement the capillary force is larger than the viscous forces. This is expressed in a rather flat saturation profile. In the case of a fast displacement the profile becomes steeper and tends to the *Buckley-Leverett* solution. It can be observed that when the displacing phase reaches the end of the medium the displacing efficiency is larger at a fast displacement than at a slow displacement.

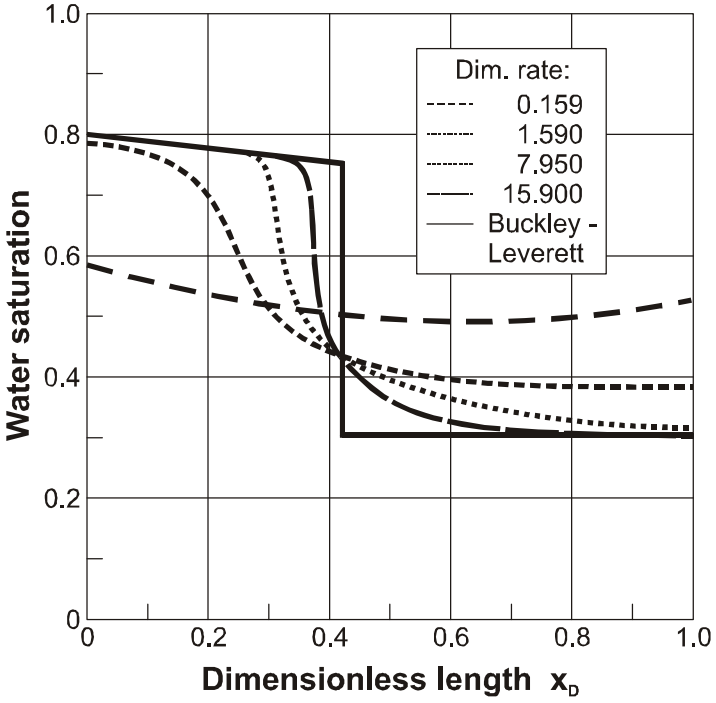

Figure 4.7: Influence of the velocity of displacement on the distribution of saturation regarding the capillary force (by *Douglas et al* 1958)

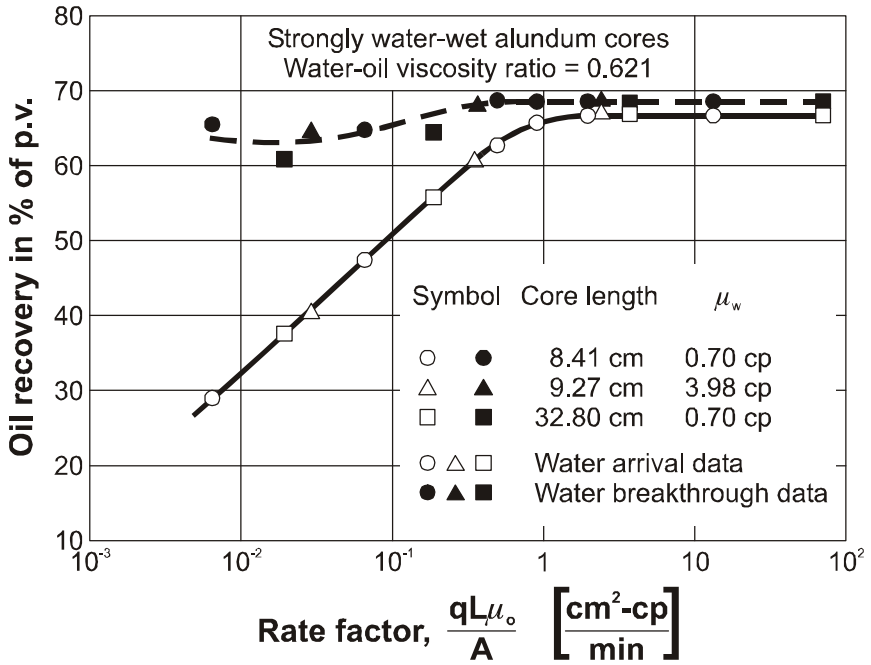

Figure 4.8: The displacing efficiency as a function of velocity (by *Kyte, Rappoport* 1958)

Figure 4.8 shows the oil recovery versus the rate factor for different core lengths and for a strong water-wet system. Two things are of importance: First the efficiency of displacement is at certain values independent of velocity. Second the time period between

the arrival and breakthrough of the displacing phase at a small displacing speed is large.

The point of breakthrough is defined as the moment of first outflow of the displacing phase. The deviation is effected by the capillary end-effect.

4.4.3 The Capillary End-Effect

The end-effect is a phenomenon at which the wetting phase is held back by the capillary force at the boundary of the medium. Until saturation at the boundary has not yet reached the value S_{1M} the capillary force will be larger than zero and the capillary gradient is infinitely large.

In Figure 4.9 the fluid arriving at the boundary of the medium accumulates and causes a peculiar deformation of the saturation profile. Breakthrough takes place at S_{1M} and in the following the saturation profile will tend towards the line of the saturation S_{1M}.

On the other side the displacing phase may be nonwetting. Then the end-effect must be considered in opposite. The saturation of the displacing phase remains S_{1m} and the profile developes as shown in Figure 4.10.

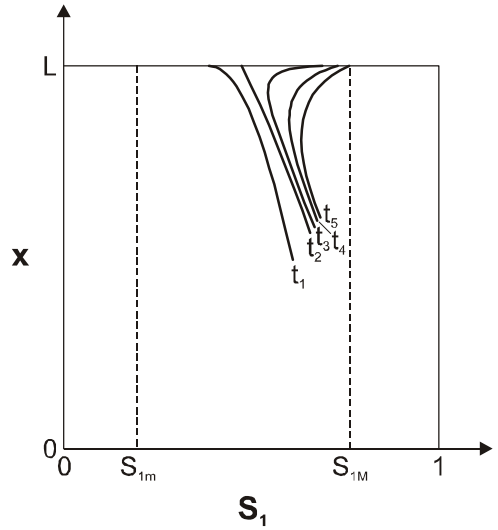

Figure 4.9: "Endeffect" in case of a wetting displacing phase (after *Marle*)

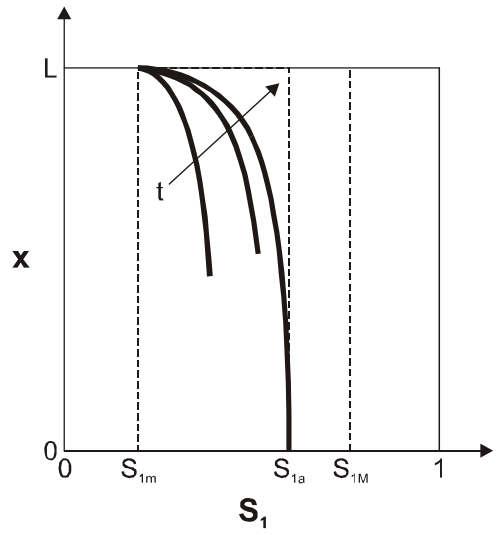

Figure 4.10: Endeffect" in case of a nonwetting displacing phase (after *Marle*)

4.4.4 Imbibition

Let us consider a porous medium contacted with the wetting phase at its bottom surface and all other sides are covered by a impermeable layer. At the initial time $t = 0$ the saturation of the wetting phase is S_{1m}. Due to capillary forces the wetting phase tends to intrude at the bottom side and thus displaces the nonwetting phase in counter flow. It is assumed that the fluids are incompressible.

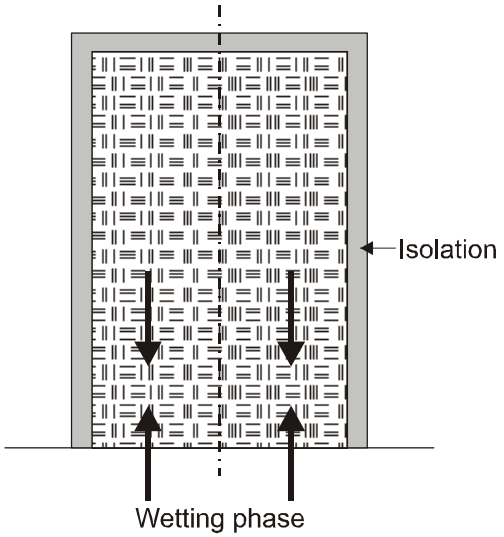

Figure 4.11: Countercurrent imbibition

Therefore:

$$u_1 + u_2 = 0 \tag{4.51}$$

Eq. 4.51 along with Eq. 4.15, Eq. 4.2, Eq. 4.9 – Eq. 4.14 remain further valid. Then Eq. 4.9 is divided by k_{r1}/μ_1 and Eq. 4.10 by k_{r2}/μ_2. Afterwards they are subtracted one from another yields:

$$u_1\left(\frac{\mu_1}{k_{r1}} + \frac{\mu_2}{k_{r2}}\right) = k(\boldsymbol{\rho_1} - \boldsymbol{\rho_2})\boldsymbol{g} + k\frac{dP_c}{dS_1} \cdot \frac{\partial S_1}{\partial x} \tag{4.52}$$

From Eq. 4.51 and Eq. 4.12. Therefore:

$$u_1 = \varphi_1^+ + \psi_1^+ \cdot \frac{\partial S_1}{\partial x} \tag{4.53}$$

where:

$$\varphi_1^+ = \frac{k(\rho_1 - \rho_2)g}{\frac{\mu_1}{k_{r1}} + \frac{\mu_2}{k_{r2}}} \tag{4.54}$$

$$\psi_1^+ = \frac{k}{\frac{\mu_1}{k_{r1}} + \frac{\mu_2}{k_{r2}}} \cdot \frac{dP_c}{dS_1} \tag{4.55}$$

Substituting of Eq. 4.39 into Eq. 4.13 leads to:

$$\frac{\partial}{\partial x}\left[\varphi_1^+ + \psi_1^+\frac{\partial S_1}{\partial x}\right] + \phi\frac{\partial S_1}{\partial t} = 0 \tag{4.56}$$

or

$$\frac{1}{\phi}\left[\frac{\partial \varphi_1^+}{dS_1} \cdot \frac{\partial S_1}{\partial x} + \frac{\partial}{\partial x}\left(\psi_1^+\frac{\partial S_1}{\partial x}\right)\right] + \frac{\partial S_1}{\partial t} = 0 \tag{4.57}$$

Eq. 4.57 is in its form identical with Eq. 4.30. The boundary conditions are:

At the outlet $x = L$:

$$u_1 = \left[\varphi_1^+ + \psi_1^+\frac{\partial S_1}{\partial x}\right]_{x=L} = 0 \tag{4.58}$$

At the inlet $x = 0$, the capillary pressure is zero, thus:

$$(S_1)_{x=0} = S_{1M} \tag{4.59}$$

The boundary value problem Eq. 4.57 – Eq. 4.59 can only be solved numerically.

To illustrate this it is of use to regard the calculations by *Blair* (1960). The result is shown in Figure 4.12 and Figure 4.13. It is appropriate to mention that the pressure gradients of the phases are corresponding to the counterflow opposed to one another. These numerical results were verified by experiments of *Graham* and *Richardson* shown in Figure 4.14.

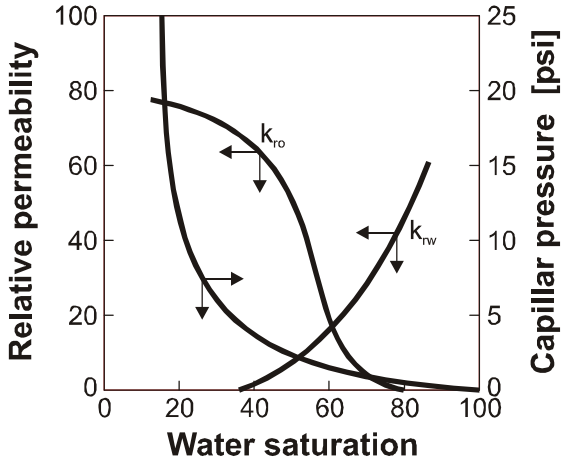

Figure 4.12: Capillary pressure and relative permeability functions used in the calculation by *Blair*

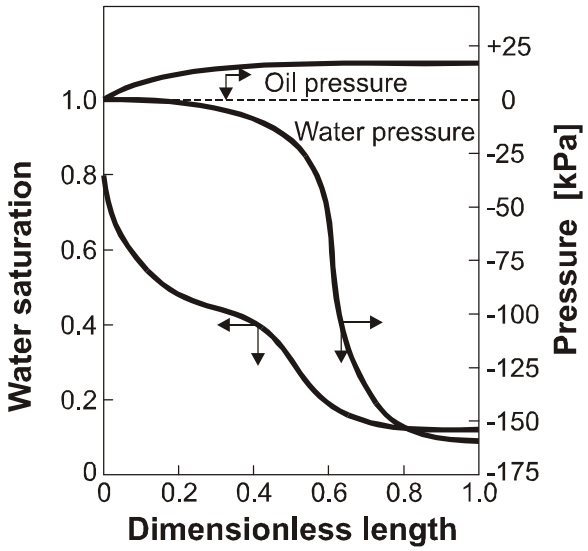

Figure 4.13: Distribution of pressure and saturation in case of linear (counterflowing) imbibition (by *Blair*)

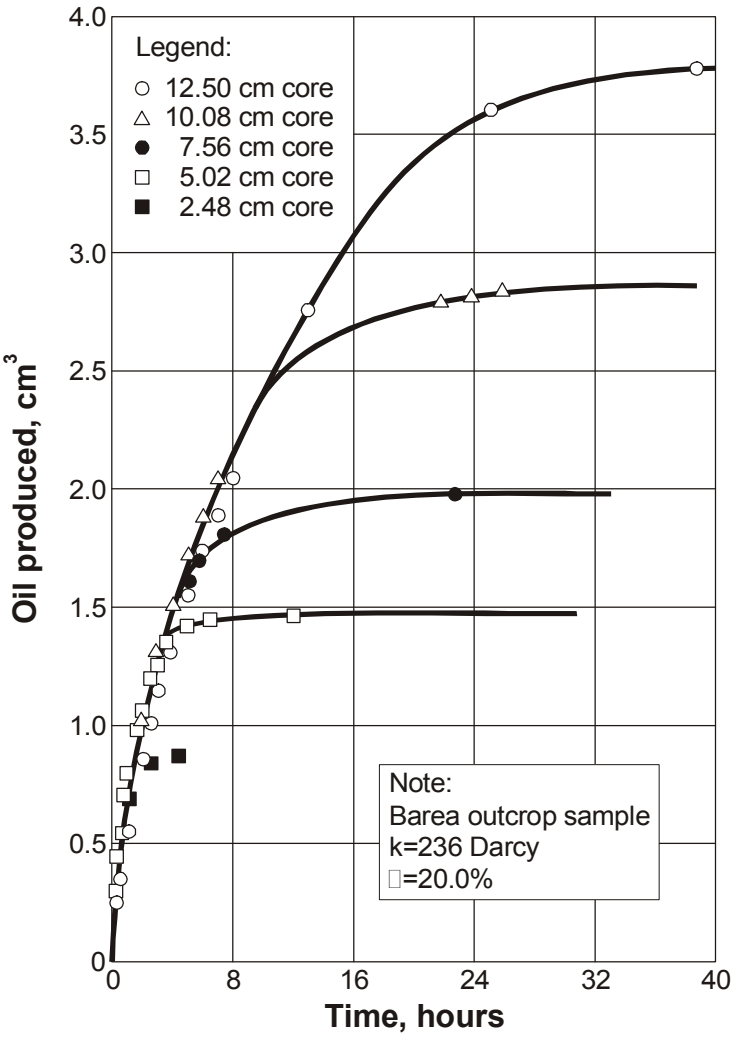

Figure 4.14: Recovery in case of linear counterflowing imbibition and the experimental determination of the influence of a certain in core-length. (by *Graham* and *Richardson*)

4.5 References

4.1 Blair, P.M. paper no. 1475G, *Trans. AIME* secondary Rec. Symp., Wichita Falls, Texas, U.S.A. (May 1960)

4.2 Buckley, J.R. and Leverett, M.C., *Trans. AIME* 146, 107 (1942).

4.3 Craig, F.F., Jr.: "The Reservoir Engineering Aspects of Waterflooding" *Monograph Vol. 3 of the Henry L. Doherty Serie*s N.Y./Dallas (1971).

4.4 Douglas, J.,Jr., Blair, P.M., and Wangner, R.J.: "Calculation of Linear Waterflooding Behavior Including the Effects of Capillary Pressure" *Trans. AIME* 215, 96 (1958).

4.5 Kyte, J.R., and Rappoport, L.A.: *Trans. AIME* 215, 423 (1958).

4.6 Marle, C.M.: "Multiphase Flow in Porous Media" *Institut Francais du Petrole, Gulf Publishing Company* (1981).

4.7 Welge, H. J.: "A Simplified Method for Computing Oil Recovery by Gas or Water Drive" *Trans. AIME*,195, 91 (1952).

Table 4.1: Summary of the Equations of One Phase and Two Phase Filtration.

One Phase	**Two Phase**
Basic Equation of Motion	
$\bar{u} = -\frac{k}{\mu}(\nabla p + \rho g \bar{i}_3)$	$\overline{u_1} = -\frac{k k_{r1}}{\mu_1}(\nabla p_1 + \rho_1 g \bar{i}_3)$
	$\overline{u_2} = -\frac{k k_{r2}}{\mu_2}(\nabla p_2 + \rho_2 g \bar{i}_3)$
	$p_2 - p_1 = P_c(S_1)$
Equation of State	
$\rho = \rho(p)$	$\rho_1 = \rho_1(p_1) \qquad \rho_2 = \rho_2(p_2)$
$\mu = \mu(p)$	$\mu_1 = \mu_1(p_1) \qquad \mu_2 = \mu_2(p_2)$
Equation of Continuity	
	$S_1 + S_2 = 1$
$\nabla(\rho \bar{u}) = -\frac{\partial(\phi\rho)}{\partial t}$	$\nabla(\rho_1 \overline{u_1}) = -\frac{\partial(\phi S_1 \rho_1)}{\partial t}$
	$\nabla(\rho_2 \overline{u_2}) = -\frac{\partial(\phi S_2 \rho_2)}{\partial t}$

Table 4.2: Summary of the Equations of Two Phase Filtration.

Two Phase 1-Dimensional	
$u_1 = -\frac{kk_{r1}}{\mu_1}\left(\frac{\partial p_1}{\partial x} + \rho_1 g\right)$	$\frac{\partial p_1}{\partial x} = -\rho_1 g - \frac{\mu_1 f_1 u}{kk_{r1}}$
$u_2 = -\frac{kk_{r2}}{\mu_2}\left(\frac{\partial p_2}{\partial x} + \rho_2 g\right)$	$\frac{\partial p_2}{\partial x} = -\rho_2 g - \frac{\mu_2 (1-f_1) u}{kk_{r2}}$
$p_2 - p_1 = P_c(S_1)$	$\frac{\partial p_2}{\partial x} - \frac{\partial p_1}{\partial x} = \frac{\partial P_c(S_1)}{\partial x} = \frac{\partial P_c}{\partial S_1}\frac{\partial S_1}{\partial x}$
$\rho_1 = \text{constant}; \quad \rho_2 = \text{constant}$	
$\mu_1 = \text{constant}; \quad \mu_2 = \text{constant}$	
$S_1 + S_2 = 1$	
$u = u_1 + u_2 \qquad f_1 = \frac{u_1}{u}$	$f_1 = \frac{1 + \frac{kk_{r2}}{u\mu_2}\left(\frac{\partial P_c}{\partial S_1}\frac{\partial S_1}{\partial x} - \Delta\rho g\right)}{1 + \frac{\mu_1}{\mu_2}\frac{k_{r2}}{k_{r1}}}$
$\frac{\partial u_1}{\partial x} + \phi\frac{\partial S_1}{\partial t} = 0$	$\frac{u}{\phi}\frac{\partial f_1}{\partial S_1}\frac{\partial S_1}{\partial x} + \frac{\partial S_1}{\partial t} = 0$

5 Piston-Like Displacement

5.1 The Mobility Ratio

It was observed that in case of neglecting the capillary forces between displacing and displaced phases a discontinuity in the saturation will develop which may be presented by a sharp front. It is defined as displacement front. The displaced phase flows ahead of the front and the displacing phase is predominant behind the front.

If the capillary force is not negligible then the saturation profile becomes continuous and a more or less smooth profile. This part is called a transition zone.

If the displacement velocity is not extremely small the *Buckeley-Leverett* discontinuity may be considered as a sufficient good approximation.

It is recommended to introduce further simplification by specifying the displacement as piston-like. The meaning is illustrated in Figure 5.1: It is assumed that ahead of the front:

$$S_1 = S_{1m} \qquad \text{and} \qquad u_1 = 0 \tag{5.1}$$

and behind the front:

$$S_1 = S_{1M} \qquad \text{and} \qquad u_2 = 0 \tag{5.2}$$

The mobilities of the displacing and displaced fluids are:

$$\lambda_1 = \frac{k_{r1M}}{\mu_1} \tag{5.3}$$

and

$$\lambda_2 = \frac{k_{r2M}}{\mu_2} \tag{5.4}$$

respectively.

The mobility ratio (M) is defined as:

$$M = \frac{\lambda_1}{\lambda_2} = \frac{k_{r1M}}{\mu_1} \Big/ \frac{k_{r2M}}{\mu_2} \tag{5.5}$$

The mobility ratio is the ratio between the mobilities of the displaced phase ahead of the front and the displacing phase behind the front and it is a constant for a given rock-fluid system

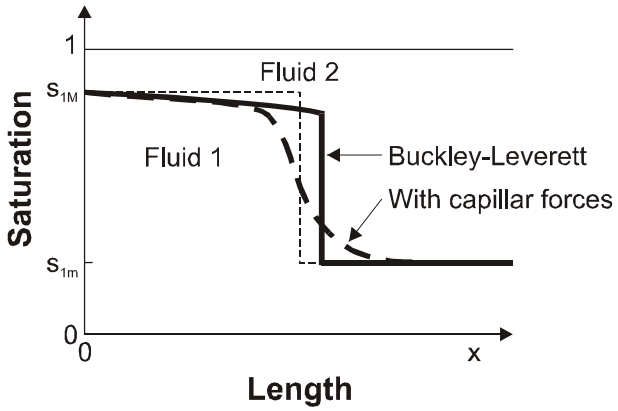

Figure 5.1: Comparison of saturation profiles according to different mathematical models

5.2 Propagation of a Displacement Front

It is assumed that the flow regimes behind the front just as ahead of the front are at steady state and the fluids are incompressible. At time *t* the position of the front may be described by the following function:

$$F(x_1, x_2, x_3, t) = 0 \tag{5.6}$$

The propagation velocity of this surface is $\vec{v} = (v_1, v_2, v_3)$ where $\vec{v}$ is a function of $\vec{x}$ and *t*. The new position of the surface after a time period ∂t can then be described as follows:

$$F(x_1 + v_1 \partial t, x_2 + v_2 \partial t, x_3 + v_3 \partial t, t + \partial t) = 0 \tag{5.7}$$

When differentiating with respect to *t*:

$$\frac{\partial F}{\partial t} + \frac{\partial F}{\partial x_1} v_1 + \frac{\partial F}{\partial x_2} v_2 + \frac{\partial F}{\partial x_3} v_3 = 0 \tag{5.8}$$

or in vector form:

$$\frac{\partial F}{\partial t} + \vec{v}\nabla F = 0 \tag{5.9}$$

The *Darcy*'s law in vector form is given by:

$$\vec{u} = -\frac{k\rho}{\mu}\nabla\psi \tag{5.10}$$

Substituting Eq. 5.10 into Eq. 5.9 we obtained:

$$\frac{\partial F}{\partial t} - \frac{k\rho}{\phi\mu}\nabla\psi\nabla F = 0 \tag{5.11}$$

where the relation between $\vec{u}$ and $\vec{v}$ is:

$$\vec{u} = \phi\vec{v} \tag{5.12}$$

The potential function for a constant density is:

$$\psi = gx_3 + \frac{p}{\rho} \tag{5.13}$$

The problem is now formulated according to *Muskat* (1934): Determine the distribution of the potential Ψ_1 between the border $\Gamma^{(1)}$ and the surface $F(\vec{x}, t) = 0$ and the distribution of the potential Ψ_2 between the surface $F(\vec{x}, t) = 0$ and the border $\Gamma^{(2)}$.

The following boundary conditions are valid:

$$\begin{aligned} \psi_1 &= \psi_1^{(1)} \qquad \vec{x} \in \Gamma^{(1)} \\ \psi_2 &= \psi_2^{(2)} \qquad \vec{x} \in \Gamma^{(2)} \end{aligned} \tag{5.14}$$

If neglecting the capillary force the pressure must be equal at the surface $F(\vec{x}, t)$:

$$p_1 = p_2 \tag{5.15}$$

Then the component of velocity normal to the front must be continuous.

From Eq. 2.89 the equation of motion for the front may be written as follows:

$$\frac{k_1\rho_1}{\mu_1}\frac{\partial\psi_1}{\partial n} = \frac{k_2\rho_2}{\mu_2}\frac{\partial\psi_2}{\partial n} \tag{5.16}$$

or in consequence to Eq. 5.11:

$$\phi\frac{\partial F}{\partial t}-\left(\frac{k\rho}{\mu}\right)_1\nabla\psi_1\nabla F = \phi\frac{\partial F}{\partial t}-\left(\frac{k\rho}{\mu}\right)_2\nabla\psi_2\nabla F = 0 \tag{5.17}$$

5.2.1 Linear Displacement

Let us look upon a horizontal displacement inside a linear medium with length L. The front of displacement has proceeded to x_f during the time period t as shown in Figure 5.2. Just as in region 1 the filtration in region 2 is also a single phase filtration and according to Eq. 3.3:

$$\frac{\partial^2 p_1}{\partial x^2} = 0 \qquad 0 < x < x_f \tag{5.18}$$

$$\frac{\partial^2 p_2}{\partial x^2} = 0 \qquad x_f < x < L \tag{5.19}$$

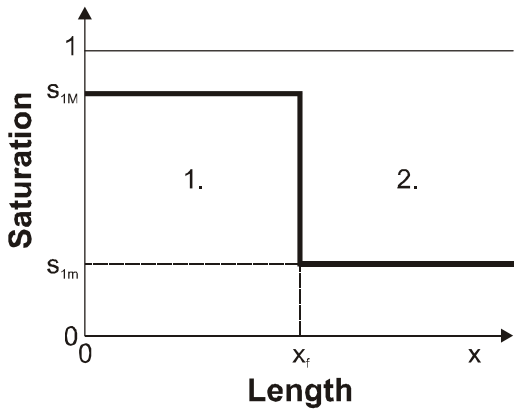

Figure 5.2: Schematic diagram of piston-like displacement

The boundary conditions at x = 0, and x = L are:

$$p_1 = p_{10} \qquad x = 0 \tag{5.20}$$

$$p_2 = p_{2L} \qquad x = L \tag{5.21}$$

At the displacement front:

$$p_1 = p_2 \qquad x = x_f$$
$$\lambda_1 \frac{\partial p_1}{\partial x} = \lambda_2 \frac{\partial p_2}{\partial x} \tag{5.22}$$

Since $\lambda_1/\lambda_2 = M$, then:

$$M\frac{\partial p_1}{\partial x} = \frac{\partial p_2}{\partial x} \tag{5.23}$$

Then the initial condition is given by:

$$x_f = 0 \qquad \text{at} \qquad t = 0 \tag{5.24}$$

After integrating twice Eq. 5.18 and Eq. 5.19 become:

$$p_1 = a_1 x + b_1 \tag{5.25}$$

$$p_2 = a_2 x + b_2 \tag{5.26}$$

a_1, b_1, a_2 and b_2 are all constants of integration which can be determined by the Substitution of Eq. 5.20 - Eq. 5.23 into Eq. 5.25 and Eq. 5.26 leads to:

$$a_1 = \frac{p_{2L} - p_{10}}{x_f + M(L - x_f)} \tag{5.27}$$

$$b_1 = p_{10} \tag{5.28}$$

$$a_2 = \frac{M(p_{2L} - p_{10})}{x_f + M(L - x_f)} \tag{5.29}$$

$$b_2 = p_{2L} - \frac{M(p_{2L} - p_{10})}{x_f + M(L - x_f)} \tag{5.30}$$

The velocity of the front is:

$$v_f = \frac{dx_f}{dt} = \frac{u_1}{\phi_D} \tag{5.31}$$

where ϕ_D is the displaced fraction of the pore volume which is determined by:

$$\phi_D = \phi(S_{1M} - S_{1m}) \tag{5.32}$$

and

$$u_1 = -k\lambda_1 \frac{\partial p_1}{\partial x} = -k\lambda_1 a_1 \tag{5.33}$$

From Eq. 5.27 and Eq. 5.33, the Darcy velocity in Eq. 5.31 can be expressed as:

$$v_f = \frac{dx_f}{dt} = \frac{k\lambda_1}{\phi_D} \frac{(p_{10} - p_{2L})}{x_f + M(L - x_f)} \tag{5.34}$$

Eq. 5.34 is then integrated yields:

$$t = \frac{\phi_D}{k\lambda_1 (p_{10} - p_{2L})} \left[MLx_f + \frac{1}{2}(1 - M)x_f^2 \right] \tag{5.35}$$

where t is the time period in which the front proceeds to x_f. The time t is proportional to x_f if $M = 1$, which means that the two phase mobilities are equal in value.

In order to simplify Eq. 5.35 the dimensionless variables, defined below, were used:

$$x_{Df} = \frac{x_f}{L} \qquad t_D = \frac{k\lambda_1 (p_{10} - p_{2L})}{\phi_D L^2} \tag{5.36}$$

Then Eq. 5.35 becomes:

$$t_D = Mx_{Df} + \frac{1}{2}(1 - M)x_{Df}^2 \tag{5.37}$$

Eq. 5.37 is illustrated graphically in Figure (5.3) which shows the relation between t_D and x_{Df} for different values of M.

5.2.2 Displacement in an Inclined Layer

Let us now regard a non horizontal layer in which both the displaced and displacing phase are in static equilibrium if $\rho_1 > \rho_2$ and the heavier displacing phase is below. During the displacement the boundary of the phases become inclined. Figure 5.4 illustrates three cases: a) the Initial case at t = 0 a static condition is reached. In case b) the displacing phase pushes forwards at the bottom of the layer and affects an unfavorable efficiency of displacement. In case c) the displacement is evenly balanced over the whole thickness. The question arises now is:

When does displacement b) and when does displacement c) takes place?

Same simplifications which has been previously discussed are applied:

- The phases are incompressible.
- Ahead of the front the saturation of the displacing phase is $S_{1m} = 1 - S_{2M}$, where S_{2M} is the initial saturation of the displaced phase. The relative permeability of phase 1 is zero ahead of the front.
- Behind the front the saturation of the displacing phase is $S_{1M} = 1 - S_{2m}$ and the relative permeability of phase 2 is zero.

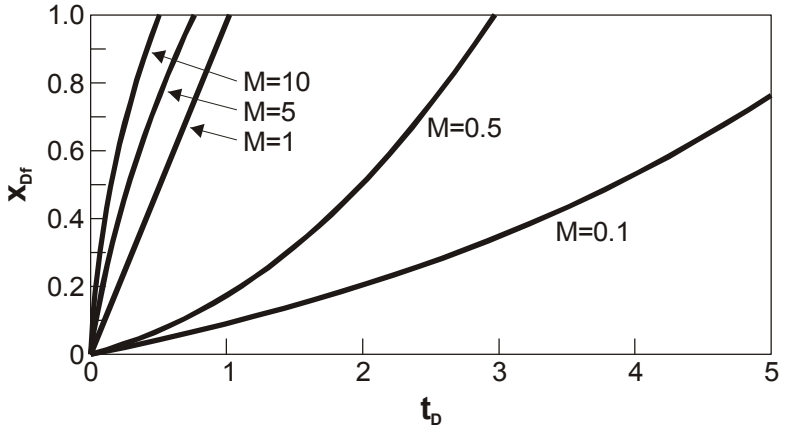

Figure 5.3: Influence of the mobility ratio on front propagations in case of a linear displacement

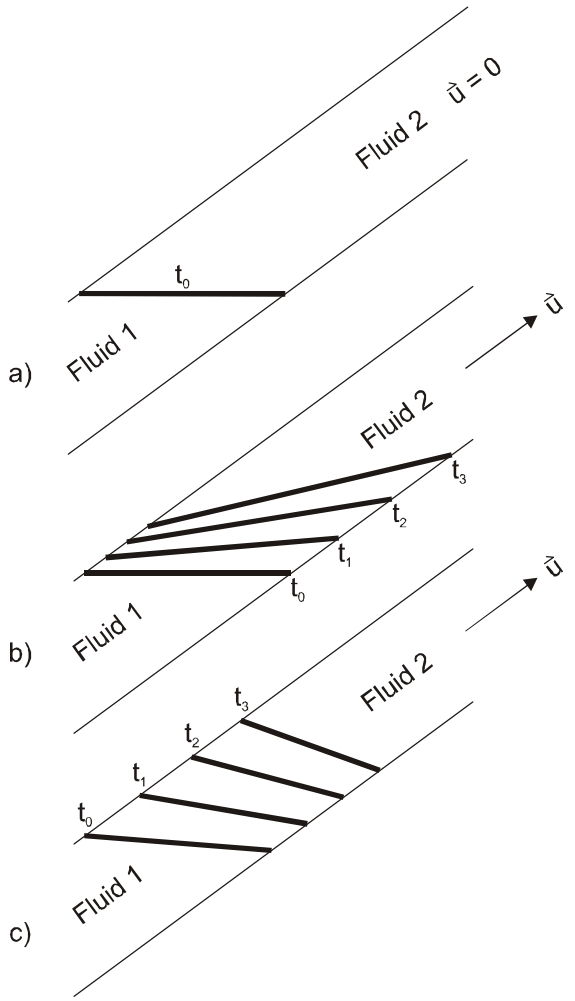

Figure 5.4: Possible positions of the displacing front in inclined layer.

Behind the front:

$$\vec{u_1} = -\frac{kk_{r1M}}{\mu_1}(\nabla p_1 + \rho_1 g\vec{i_3}) \tag{5.38}$$

$$\grave{u}_2 = 0 \tag{5.39}$$

$$\nabla\grave{u}_1 = 0 \tag{5.40}$$

Ahead of the front:

$$\grave{u}_1 = 0 \tag{5.41}$$

$$\grave{u}_2 = -\frac{kk_{r2M}}{\mu_2}(\nabla p_2 + \rho_2 g\vec{i_3}) \tag{5.42}$$

$$\nabla \vec{u}_2 = 0 \tag{5.43}$$

The boundary conditions are as follows:

$$\begin{aligned} \vec{u}_1 &= \vec{u} \quad \text{in infinity behind the front} \\ \vec{u}_2 &= \vec{u} \quad \text{in infinity ahead of the front} \end{aligned} \tag{5.44}$$

$$\left.\begin{aligned} \vec{u}_1 \cdot \vec{n} &= 0 \\ \vec{u}_2 \cdot \vec{n} &= 0 \end{aligned}\right\} \quad \text{at the impermeable boundaries of the layer} \tag{5.45}$$

$$\left.\begin{aligned} p_1 &= p_2 \\ \vec{u}_1 \cdot \vec{n} &= \vec{u}_2 \cdot \vec{n} \end{aligned}\right\} \quad \text{at the front} \tag{5.46}$$

The conditions formulated in Eq. 5.46 neglects the capillary forces and the continuity of filtration velocity at the front.

The general solution was previously discussed. This though is so complicated that solutions are only achieved numerically. In order to answer the original question it is not of importance to know the position and shape of the front at all times. It is satisfactory to know if a stable shape is formed after a certain distance of displacement. This stable shape of the front then proceeds translatorial.

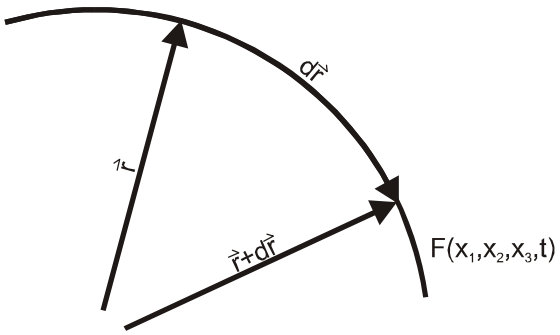

Figure 5.5: Forces acting on the displacing front.

Actually it is essential to know if the boundary value problem Eq. 5.38 - Eq. 5.46 have a semi steady-state solution and in addition which kind? The following idea was provided by *Dietz* (1953).

In the Figure 5.5 two neighboring points at the front are considered. Those are $\vec{r}$ and $(\vec{r} + d\vec{r})$. At both points Eq. 5.46 must be valid:

$$\begin{aligned} p_1(\vec{r}) &= p_2(\vec{r}) \\ p_1(\vec{r} + d\vec{r}) &= p_2(\vec{r} + d\vec{r}) \end{aligned} \tag{5.47}$$

Since:

$$p_1(\vec{r}+d\vec{r})-p_1(\vec{r}) = \nabla p_1 d\vec{r} \tag{5.48}$$

$$p_2(\vec{r}+d\vec{r})-p_2(\vec{r}) = \nabla p_2 d\vec{r} \tag{5.49}$$

from Eq. 5.47:

$$(\nabla p_1 - \nabla p_2)d\vec{r} = 0 \tag{5.50}$$

Substitution of ∇p_1 and ∇p_2 from Eq. 5.38 and Eq. 5.42 into Eq. 5.50 leads to:

$$\left[(\rho_1-\rho_2)g\vec{i}_3+\left(\frac{\mu_1}{kk_{r1M}}-\frac{\mu_2}{kk_{r2M}}\right)\vec{u}\right]d\vec{r} = 0 \tag{5.51}$$

This equation indicates that if a stationary solution for the fluid phase exists it must be perpendicular to the vector:

$$\vec{w} = (\rho_1-\rho_2)g\vec{i}_3+\frac{\vec{u}}{k}\frac{\mu_1}{k_{r1M}}(1-M) \tag{5.52}$$

where M is the Mobility Ratio:

$$M = \left(\frac{k_{r1}}{\mu_1}\right)\Big/\left(\frac{k_{r2}}{\mu_2}\right) \tag{5.53}$$

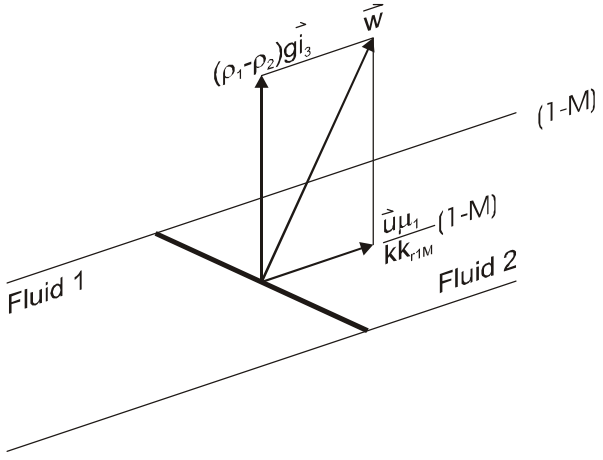

Figure 5.6: Position of the displacing front by favorite mobility ratio (after *Marle*)

Figure 5.6 illustrates the position of the front. The heavier fluid 1 displaces the lighter fluid 2 from bottom to top. The mobility of the displaced fluid is superior. In this case

$M < 1$. Both terms of the right side of Eq. 5.52 become positive. With increasing displacement velocity the vector $\vec{w}$ turns to the direction of $\vec{u}$. This position is semi steady-state and stable. If the velocity of filtration is reduced to zero the front will turn to the horizontal position and maintain this position.

Now let us see the case where $M > 1$:

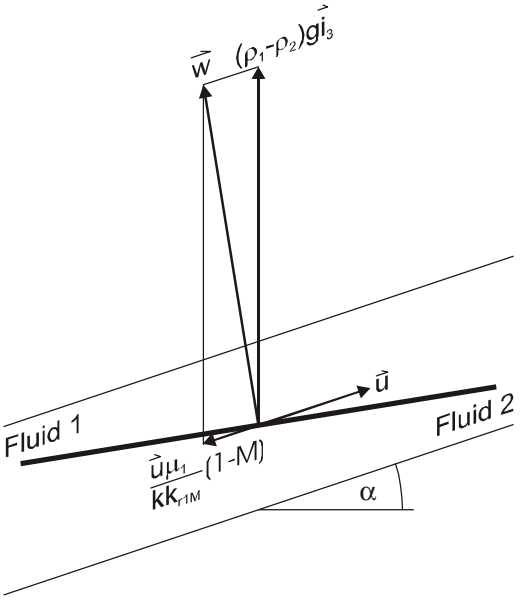

Figure 5.7: Position of the displacing front by unfavorable mobility ratio.

The displacement proceeds from bottom to top. The heavier but more mobile phase displaces the lighter and less mobile phase. Figure 5.7 states that again a stationary and stable front will exist. This front though becomes more and more flattered as front velocity increases.

If the velocity exceeds a certain critical value a stationary position of the front becomes impossible to maintain. This critical velocity may be calculated using Eq. 5.52. At the critical velocity the vector $\vec{w}$ is perpendicular to the axis of symmetry of the layer. In consequence the scalar multiplication with $\vec{u}$ becomes zero:

$$\vec{w} \cdot \vec{u} = \left[(\rho_1 - \rho_2) g \vec{i}_3 + \frac{\vec{u}}{k} \frac{\mu_1}{k_{r1M}} (1 - M) \right] \vec{u} = 0 \tag{5.54}$$

Since $\vec{i}_3 \cdot \vec{u} = |\vec{u}| \cdot \sin\alpha$ and $\vec{u} \cdot \vec{u} = |\vec{u}|^2$ Eq. 5.54 becomes:

$$u_k = -\frac{k(\rho_1 - \rho_2) g \sin\alpha}{\frac{\mu_1}{k_{r1M}} (1 - M)} \tag{5.55}$$

u_k is the critical velocity of filtrations. A filtration with velocity higher then u_k is called supercritical.

A case of $\rho_1 < \rho_2$ will not be discussed. In this case though the heavier fluid is on top of the lighter fluid which makes the front unstable.

5.2.3 Supercritical Displacement

If the velocity of displacement is larger than the critical velocity the interface will become more and more extended Figure 5.8. This displacement is called supercritical. The theories of *Le Fur* and *Sourieau* are used for explanation purposes in this work.

At first it is assumed that displacement is at an advanced stage. The front has travelled a considerably far distance and the state is to be referred to as practically stable. That means, the rate of changes is everywhere moderate.

In this case the *Dupuit*-assumption is valid which states that the equipotentials are perpendicular to the layer. In this case u_1 is the same at every point of the layer which contains the fluid 1 (section $h_1(x,t)$).

The same is valid for u_2 in the layer section $h_2(x,t)$. The relation between h_1 and h_2 is:

$$h = h_1(x, t) + h_2(x, t) \tag{5.56}$$

and

$$u = \frac{1}{h}[h_1 u_1 + h_2 u_2] \tag{5.57}$$

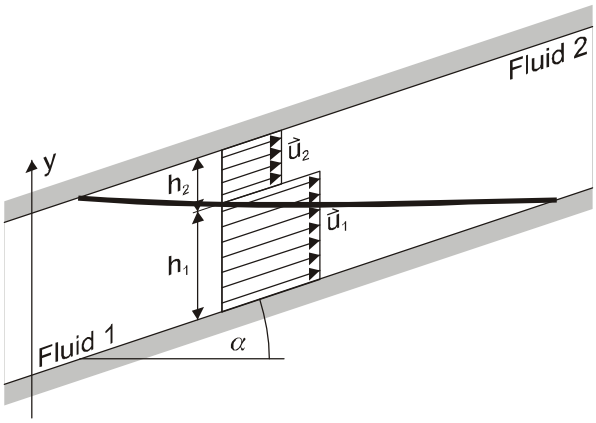

Figure 5.8: Supercritical displacement in inclined layer (after *Marle*)

If $\rho_1 > \rho_2$ the displacing fluid takes the lower part of the layer and $h_1(x,t)$ is referred to as the distance between the bottom of the layer and the front. In an arbitrary but fixed point x_a the value $h_1(x,t)$ will monotonously increase with time.

The velocity of filtration in direction of the *x*-axis is:

$$\grave{u}_1 = -\frac{kk_{r1M}}{\mu_1}\left(\frac{\partial p_1}{\partial x} + \rho_1 g \sin\alpha\right) \tag{5.58}$$

$$\grave{u}_2 = -\frac{kk_{r2M}}{\mu_2}\left(\frac{\partial p_2}{\partial x} + \rho_2 g \sin\alpha\right) \tag{5.59}$$

Since filtration is parallel to the axis of the layer at every point (a consequence of the *Dupuit*-assumption) the following equations are valid:

$$\frac{\partial p_1}{\partial y} + \rho_1 g \cos\alpha = 0 \tag{5.60}$$

$$\frac{\partial p_2}{\partial y} + \rho_2 g \cos\alpha = 0 \tag{5.61}$$

The equation of continuity is set up for the whole layer as:

$$\frac{\partial (u_1 h_1)}{\partial x} + \phi (S_{1M} - S_{1m}) \frac{\partial h_1}{\partial x} = 0 \tag{5.62}$$

and the following average values are defined as:

$$\overline{S_1} = \frac{h_1 S_{1M} + h_2 S_{1m}}{h} \tag{5.63}$$

$$\overline{S_2} = \frac{h_1 S_{2m} + h_2 S_{2M}}{h} = 1 - \overline{S_1} \tag{5.64}$$

$$w_1 = \frac{h_1}{h} u_1 \tag{5.65}$$

$$w_2 = \frac{h_2}{h} u_2 \tag{5.66}$$

$$p_1^*(x, t) = p_1(x, 0, t) \tag{5.67}$$

$$p_2^*(x, t) = p_2(x, 0, t) \tag{5.68}$$

$$\gamma = g \sin\alpha \tag{5.69}$$

$$k_{r1}^{*}(\overline{S_1}) = k_{r1M}\frac{\overline{S_1} - S_{1m}}{S_{1M} - S_{1m}} \tag{5.70}$$

$$k_{r2}^{*}(\overline{S_2}) = k_{r2M}\frac{\overline{S_1} - S_{1m}}{S_{1M} - S_{1m}} \tag{5.71}$$

As before the capillary force is neglected and the pressures of the phases must be equal at the front, then:

$$p_1(x, h_1, t) = p_2(x, h_2, t) \tag{5.72}$$

and from Eq. 5.67 and Eq. 5.68:

$$p_1^{*}(x, t) + h_1\rho_1 g\cos\alpha = p_2^{*}(x, t) + h_2\rho_2 g\cos\alpha \tag{5.73}$$

Since:

$$h_1 = h\frac{\overline{S_1} - S_{1m}}{S_{1M} - S_{1m}} \tag{5.74}$$

and from Eq. 5.73:

$$P_c^{*}(S_1) = p_2^{*}(x, t) - p_1^{*}(x, t) = h\frac{\overline{S_1} - S_{1m}}{S_{1M} - S_{1m}}(\rho_1 - \rho_2)g\sin\alpha \tag{5.75}$$

Substitution of Eq. 5.63 - Eq. 5.75 into Eq. 5.58, Eq. 5.59 and Eq. 5.62 leads to:

$$w_1 = -\frac{kk_{r1}^{*}}{\mu_1}\left(\frac{\partial p_1^{*}}{\partial x} + \rho_1\gamma\right) \tag{5.76}$$

$$w_2 = -\frac{kk_{r2}^{*}}{\mu_2}\left(\frac{\partial p_2^{*}}{\partial x} + \rho_2\gamma\right) \tag{5.77}$$

$$\overline{S_1} + \overline{S_2} = 1 \tag{5.78}$$

$$\frac{\partial w_1}{\partial x} + \phi\frac{\partial \overline{S_1}}{\partial t} = 0 \tag{5.79}$$

$$w_1 + w_2 = 0 \tag{5.80}$$

$$p_2^* - p_1^* = P_c^*(\overline{S_1}) \tag{5.81}$$

Eq. 5.76 - Eq. 5.81 may be considered identical with the equations of *Buckley - Leverett* Eq. 4.9 - Eq. 4.14. The two dimensional approximation of the supercritical displacement corresponds with a one dimensional displacement where

γ	is the fictitious gravity,
$\overline{S_1}, \overline{S_1}$	the average saturations,
p_1^*, p_2^*	are the fictitious phase pressures
w_1, w_2	are the fictitious fractional velocity,
$k_{r1}^*(\overline{S_1}), k_{r2}^*(\overline{S_2})$	are the pseudo relative permeabilities
$P_c^*(\overline{S_1})$	is the pseudo capillary pressure.

All factors, except P_c, are physically corresponds to the actual factors. Therefore the fictive saturation is the average saturation the fictive pressure is the pressure at any select point, etc. Only the function $P_c^*(\overline{S_1})$ has nothing to do with capillary pressure, because the capillary forces were neglected due to precondition Eq. 5.72.

5.3 References

5.1 Dietz, D.N.: "A theoretical approach to the problem of encroaching and by-passing edge water" *Koninkl, Ned., Akad., Wetenschap*, Proc. B56,83 (1953).

5.2 Marle, C.M.: "Multiphase Flow in Porous Media" *Institut du Petrole. Gulf Publishing Company* (1981).

5.3 Muskat, M.: "Flow of Homogeneous Fluids through Porous Media". *McGraw Hill Book Co*., N.Y. (1937).

6 References

1 Aavatsmark, I., Barkve, T., Boe, O. and Mannseth, T.: "Discretisation on Unstructured Grid for Inhomogeneous, Anisotropic Media, Part I: Derivation of the Methods," SIAM J.Sci. Comput. **19** (1998), 1700-1716.

2 Aavatsmark, I., Barkve, T., Boe, O. and Mannseth, T.: "Discretisation on Unstructured Grid for Inhomogeneous, Anisotropic Media, Part II: Discussion and Numerical Results," SIAM J.Sci. Comput. **19** (1998), 1717-1736.

3 Aavatsmark, I., Barkve, T., Boe, O. and Mannseth, T.: "A Class of Discretisation Methods for Structured and Unstructured Grids for Anisotropic, Inhomogeneous Media," Proc. 5th European Conference on the Mathematics of Oil Recovery, Leoben/Austria, Sept. 3-6, 1996.

4 Aavatsmark, I., Reiso, E. and Teigland, R.: "MPFA for Faults and Local Refinements in 3D Quadrilatereal Grids With Application to Field Simulation," paper SPE 66356, presented at the SPE 16th Reservoir Simulation Symposium held in Houston,TX, 11-14 February 2001.

5 Abbas, H. and Neda, J: "Rock Mechanics in Wellbore Construction," Chap. **6** in Economides,M.J. at al. "Petroleum Well Construction," J.Wiley & Sons, Chichester (1998).

6 Abdelmawla A.M.: "Numerical Well Test Modeling in a Full-Field Simulator Offers New Opportunities for Reservoir Characterization", paper presented at the 6th European Conference on Mathematics of Oil Recovery (ECMOR VI), Peebles, Scotland, September 7-11, 1998.

7 Abdelmawla, A. and Heinemann, Z.:”Numerical Well Test Modelling in a Full-field Simulator Offers New Opportunities for Reservoir Characterization,” Paper presented at the 6th European Conference on Mathematics of Oil Recovery (ECMOR VI), Peebles, Scotland, September 7-11, 1998.

8 Abdou,M.K., Pham,H.D. and Al-Aqueeli,A.S.:"Impact of Grid Selection on Reservoir Simulation,"JPT(July 1993) 664-69.

9 Abou-Kassem J.H., Aziz K.: "Analytical Well Models for Reservoir Simulation", paper SPE 11719, presented at 1985 SPE California Regional Meeting held in Ventura.

10 Abou-Kassem, J.H. and Aziz, K.:”Analytical Well Models for Reservoir Simulation,” SPEJ, August 1985, 573-579.

11 Afilaka, J. and Deimbacher, F.: ”Numerical Well Testing in Complex Reservoirs,” Petroleum Engineer International, June 1997, 21-28.

12 Agarwal, R.G.:”A New Method to Account for Producing Time Effect when Drawdown Type Curves are Used to Analyze Pressure Buildup and Other Test Data,” SPE 9289, paper presented at the 1980 Annual Technical Conference and Exhibition, Dallas, September 21-24.

13 Akbar, A.M., Arnold, M.D. and Harvey, A.H.:”Numerical Simulation of Individual Wells in a

Field Simulation Model," Paper presented at the 1972 SPE Annual meeting, San Antonio, October 8-11.

14 Amado, L.C.N, Ganzer, L. and Heinemann, Z.E.: "Finite Volume Discretization of the Fluid Flow Equations on General Perpendicular Bisection Grids", paper presented at the 1994 Fifth Intl. Forum on Reservoir Simulation, Muscat, Oman, Dec. 10-14.

15 Anderson,W.G.: "Wettability Literature Survay-Part 1: Rock/Oil/Brine interactions and the effects of Core Handling on Wettability," JPT, Oct.1986, p.1125-44.

16 Anderson,W.G.: "Wettability Literature Survay-Part 2: Wettability Massurements," JPT, Nov.1986, p.12425-62.

17 Aziz, K. and Settari, A.: Petroleum Reservoir Simulation, Applied Science Publishers, 1979.

18 Babu, D.K., Odeh, A.S., Al-Khalifa, A.J.A. and McCann, R.C.:"The Relation between Wellblock and Wellbore Pressures in Numerical Simulation of Horizontal Wells," SPERE, August 1991, 324-328.

19 Babu, D.K. and Odeh, A.S.:"Productivity of a Horizontal Well," SPERE, November 1989, 417-421.

20 Beckner, B.L., Mutfilz, J.M., Ray, M.B. and Tomich, J.F.: "EM^{power}: New Reservoir Simulation System," paper SPE 68116 presented at 2001 SPE Middle East Oil Show held in Bahrain, 17-20 March 2001.

21 Blair, P.M. paper no. 1475G, *Trans. AIME* secondary Rec. Symp., Wichita Falls, Texas, U.S.A. (May 1960)

22 Bourdet, D., Ayoub, J. and Pirard, Y.:"Use of Pressure Derivative in Well Test Interpretation," SPE Formation Evaluation, June 1989, 293-302.

23 Brand, C.W. and Heinemann, Z.E.: "A New Iterative Solution Technique for Reservoir Simulation Equations on Locally refined Grids," SPE Reservoir Engineering, Nov.1990, p.555-560.

24 Brand, C.W. and Heinemann, Z.E.: "Fundamentals of Gridding Techniques in Reservoir Simulation," paper presented at the Forth Intl. Forum on Reservoir Simulation, Salzburg/Austria, Aug. 31-Sept. 4, 1992.

25 Buckley, S.E. and Leverett, M.C.: "Machanism of Fluid Displacement in Sands," Trans.AIME **146** (1942), p.107-116.

26 Chikhliwala, E.D. and Huang, A.B.: "Investigation on Viscous Fingering by Linear and Weakly Nonlinear Stability Analysis," SPERE (Nov.1988) p.1268-1278.

27 Chouke, R.L., van Meurs, P. and van der Poel, C.: "The Instability of Slow, Immiscible, Viscous Liquid-Liquid Displacements in Permeable Media," *Trans*.AIME **216**, (1959) p.188-194.

28 Coats, K.H. and Modine, A.D.: "A Consistent Method for Calculating Transmissibilities in Nine-Point Difference Equations," paper SPE 12248 presented at the 1983 SPE Symposium on Reservoir Simulation, San Francisco

29 Collins D.A., Mourits F.M.: "Multigrid Methods Applied to Near-Wellbore Modeling in Reservoir Simulation", unconsolitied paper, SPE 23607, 1991.

30 Craft, B.C. and Hawkins, M.F.:"Applied Petroleum Reservoir Engineering," Prentice Hall, November 1964, 314.

31 Deimbacher, F.,X. and Heinemann, Z.E.: "Time Dependent Incorporation of Locally Irregular Grids in Large Reservoir Simulation Models," Paper presented at the 12th SPE Symposium on Reservoir Simulation, New Orleans, February 28 - March 3, 1993.

32 Deimbacher F.X., Komlosi F. and Heinemann Z.E.: "Fundamental Concepts and Potential Applications of the Windowing Technique in Reservoir Simulation", SPE 29851, presented at 1995 SPE Middle East Oil Show held in Bahrain, 17-20 March 1995.

33 Ding Y., (1996): "Well Modeling in Reservoir Simulation", paper presented at the 5th European Conference on the Mathematics of Oil Recovery, Leoben.

34 Ding., Y.:"A Generalized 3D Well Model for Reservoir Simulation" Paper presented at SPE Annual Technical Conference, Dallas, October 1995, 227-242.

35 Douglas, Peacemen and Rachford:

36 Durlofsky, J.L.: "Numerical calculation of Equivalent Grid Block Permeability Tensor for Heterogeneous Media," Water Resources Research, Vol.27, No.5, (May 1991) 699-708.

37 Earlougher, R.:"Advances in Well Test Analysis," SPE Monograph Series No. 5, 1977, 22-23,42-45.

38 El-Mandouh, M.S., Betté, S., Heinemann, R.F., Ogiamien, E.B., Bhatia, S.K.: "An Integrated, Full-Field Compositional Simulation of the OSO Reservoir, Nigeria", paper presented at the Forth Intl. Forum on Reservoir Simulation, Salzburg/Austria, Aug. 31-Sept. 4, 1992.

39 Ewing, R.E., Lazarov, R.D. and Vassilevski, P.S.: "Finite Difference Schemes on Grids with Local Refinement in Time and Space for Parabolic Problems I.Derivation, Stability, and Error Analysis," *Computing* **45**, 193-215.

40 Fleming,G.C.:"Modeling the Performance of Fractured Wells in Pattern Floods Using Orthogonal Curvilinear Grids", paper SPE 20744 presented at the 1990 Annual Technical Conference and Exhibition, New Orleans, Sept. 23-26.

41 Forsyth P.A. and Sammon P.H.: "Local Mesh Refinement and Modeling of Faults and Pinchouts", SPE 13524, SPEFE (June 1986) 275-85.

42 Forsyth, P.A.: "A Control Volume Finite Element Method for Local Mesh Refinement," paper SPE 18415 presented at 1989 SPE Symposium on Reservoir Simulation, Houston, TX, Feb. 6-8.

43 Fung, L.S.K., Hiebert, A.D. and Nghiem, L.: "Reservoir Simulation with a Control-Volume Finite-Element Method," paper SPE 21224 presented at 1991 SPE Symposium on Reservoir Simulation, Anaheim, CA, Feb 17-20.

44 Ganzer, L.:"A Novel Approach for Multi-Purpose Reservoir Simulators Using Mixed Models," Paper presented at the 6th European Conference on Mathematics of Oil Recovery (ECMOR VI), Peebles, Scotland, September 7-11, 1998.

45 Ganzer, L.:"Petroleum Reservoir Simulation Using Mixed Models," PhD. Dissertation at Mining University Leoben, September 1997.

46 Geoquest: "FlowGrid User Manual, Geoquest", Abingdon U.K. (1998).

47 Geoquest: “Welltest 200 User Manual”, Geoquest, Abingdon U.K. (1997).

48 Gunasekera, D., Cox, J and Lindsey, P.: “The Generation and Application of K-Orhogonal Grid Systems,” paper SPE 37998, presented at the SPE 14th Reservoir Simulation Symposium held in Dallas,TX,, Jun. 8-11, 1997.

49 Gosselin, O. and Thomas, J.H.: “Domain Decomposition Methods in Reservoir Simulation Coupling Well and Full-Field Models,” paper presented at the 1990 Second European Conference on the Mathematics of Oil Recovery, Arles, France, Sept. 11-14.

50 Graham,J.W. and Richardson, J.G: Note not published, Referenced in Collins,R.E.: "Flow of Fluids through porous materials, Reinhold Publishing Coorporation, Yew York, 1961, p.166.

51 Gunasekara,D., Herring,J. and Cox,J.: “Segmented Coordinate Line Based Unstructured Grids”, 6th European Conference on the Mathematics of Oil Recovery, Peebles, 8-11 Sept.1998.

52 Gunasekera, D., Childs, P., Herring, J. and Cox, J.: “A Multi-Point Flux Discretization Scheme for General Polyhedral Grids,” paper SPE 48855, presented at the SPE 6th International Oil&Gas Conference and Exhibition held in China, Beijing, Nov. 2-6, 1998.

53 Hall, K.R. and Yarborough, L.: “New, Simple Correlation for Predicting Critical Volume,” Chem. Eng. (Nov. 1971) 76-77.

54 Hegre, T.M., Dalen, V. and Henriquez, A.: "Generalized Transmissibilities for Distored Grids in Reservoir Simulation",paper SPE 15622 presented at 1986 SPE 61st Annual Technical Conference and Exhibition held in New Orleans, LA October 5-8.

55 Heinemann Z.E., Gerken G., and Meister, S.: “Anwendung der localen Netzverfeinerung bei Lagerstättensimulation” paper presented at the 1982 27th DGMK Annual Meeting held 8. Oct.1982 in Achen, Erdöl-Erdgas 6. (Jun.1983), 199-204.

56 Heinemann Z.E., Gerken G. and vonHantelmann G.: “Using Grid Refinement in a Multiple-Application Reservoir Simulator”, SPE 12255, presented at the 1983 SPE Symposium on Reservoir Simulation, San Francisco, Nov. 15-18.

57 Heinemann, Z. E., Brand, C. W.: “Gridding techniques in reservoir simulation, Proc. First Intl. Forum on Reservoir Simulation, Alpbach 1988, pp. 339-425.

58 Z.E.Heinemann et *al.*:”Modeling Reservoir Geometry with Irregular Grids,” Paper presented at the SPE Symposium on Reservoir Simulation, Houston, TX, February 6-8, 1989, 37-54.

59 Heinemann, Z.E. and Brand, C.W.: “Gridding Techniques in Reservoir Simulation,” paper presented at the Second Intl. Forum on Reservoir Simulation, Alpbach/Austria, Sept. 4-8, 1989.

60 Heinemann, Z.E. and Deimbacher, F.X.: “Advances in Reservoir Simulation Gridding,” paper presented at the Forth Intl. Forum on Reservoir Simulation, Salzburg/Austria, Aug. 31-Sept. 4, 1992.

61 Heinemann, Z.E.: “Interactive Generation of Irregular Simulation Grids and its Practical Applications” paper SPE paper SPE 27998 presented at the University of Tulsa Centennial Petroleum Engineering Symposium, Tulsa, OK, Aug. 29-31,1994.

62 Heinemann,Z.E.: “Advances in Gridding Techniques,” paper presented at the Fifth Intl. Forum on Reservoir Simulation, Muscat/Oman, Dec. 10-14, 1994.

63 Heinemann, Z.E., Heinemann, G.F. and Tranta B.M: “Modeling Heavily Faulted Reservoirs,”

paper SPE 48998, presented at the SPE Annual Technical Conference and Exhibition held in New Orleans, Louisiana.,Dallas,TX, Sept. 27-30, 1998.

64 Heinemann G.F., Brockhauser S.: ”Implementation of Three-Dimensional KPEBI Grids for Slanted Wells in a Field-scale Reservoir Model,” Paper presented at the 6th European Conference on Mathematics of Oil Recovery (ECMOR VI), Peebles, Scotland, September 7-11, 1998.

65 Heinemann, G. and Abdelmawla, A.:”Comparison of ***SURE*** Simulator 3D Window Horizontal Well to Horizontal Well Analytical Solutions,” Internal report, HOT Engineering, April 1998.

66 Heinemann, G.F., Ahmed Abdelmawla and Brockhauser, S.: “Modeling of Fluid Flow around and within Highly Deviated Horizontal Wells,” Proc. 7th European Conference on the Mathematics of Oil Recovery, Baveno/Italy, Sept. 5-8, 2000.

67 Heinrich, B.: "Finite Difference Methods on Irregular Networks," Verlag Birkhäuser, Basel, Boston, Stuttgart. 1987, p.206.

68 Herweijer, J.C. and Durbule, O.R.F.: ”Screening of Geostatistical Reservoir Models with Pressure Transients,” JPT, November 1995, 973-979.

69 Higgins and Leighton

70 Hickernell, F.J. and Yortsos, Y.C.: "Linear Stability of Miscible Process in Porous Media in Absence of Dispersion," Stud.Appl.Math.. **74**, (1986) p.93-115.

71 Hirasaki, G.J. and O’Dell, P.M.: “Representation of Reservoir Geometry for Numerical Simulation,” Trans.AIME, 249,(1970), 393-404.

72 Homsy, G.M.: "Viscous Fingering in Porous Media," Ann.Rev.Fluid Mech.. **19** (1987), p.271-311.

73 Horner, D.R.:” Pressure Buildup in Wells,” Proceedings of Third World Petroleum Congress, The Hague, 1951, 503-523.

74 http://www.posc.org/rescue/Rescue980615_doc/WhatsInRescue.htm, August 16, 2001.

75 Jahveri, B.S. and Youngren, G.K.: “Three-Parameter Modification of the Peng-Robinson Equation of State to Improve Volumetric Predictions,” paper SPE 13118 presented at the 1984 Annual Meeting, Houston, Sept. 16-19.

76 Kamal, M., Freyder, D.G. and Murray, M.A.: ”Use of Transient Testing in Reservoir Management,” JPT, November 1995, 992-999.

77 Kesler, M.G. and Lee, B.I.: “Improve Predictions of Enthalpy of Fractions,” Hydro. Proc. (March 1976) 55, 153-158.

78 Kocberber, Sait.: “An Automatic, Unstructured Control Volume Generation System for Geologically Complex Reservoirs”, paper presented at the 1997 Reservoir Symposium held in Dallas, Texas, 8-11 June 1997.

79 Komlosi, F.:”Use of the Windowing Technique and a New Radial Grid for the Accurate Simulation of Transient Well Tests in a Field Scale Reservoir Model,” Master Thesis, Mining University Leoben, June 1994.

80 Krysl, P. and Oritz, M.: “Variational Delaunay Approach to the Generation of Tetrahedral Finite

Element Meshes". submitted on January 21, 1999 to the International Journal for Numerical Methods in Engineering.

81 Kunianski, J. and Hillestad, J.G.:"Reservoir Simulation using Bottomhole Pressure Boundary Conditions," SPEJ, December 1980, 473-486.

82 Lee, J.:"Well Testing," SPE Textbook Series, Vol. 1, 1982, 44.

83 Lee, S.H. and Milliken, W.J.:"The Productivity Index of an Inclined Well in Finite-Difference Reservoir Simulation," Paper presented at the 12th SPE Symposium on Reservoir Simulation, New Orleans, February 28 - March 3, 1993.

84 Li, K. and Horne, R.N.: "Wettability Evaluation Method for both Gas-Liquid-Rock and Luiqued-Liqued-Rock Systems," paper SPE 80233, presented at the SPE International Symposium on Oilfield Chemistry, Houston,TX. 5-7 February 2003.

85 Lohrenz, J., Bray, B.G. and Clark, C.R.: "Calculating Viscosities of Reservoir Fluids From Their Compositions," JPT (Oct. 1964) 1171-1176.

86 Manzocchi, T., Walsh, J.J., Nell, P. and Yielding, G.: "Fault Transmissibility Multiplier for Flow Simulation Models," Petroleum Geoscience, Vol.5 1999, pp.53-63.

87 Matijevic, P. and Deimbacher, F.X.: "Modeling Faults in Reservoir Simulation", Proc. 4th European Conference on the Mathematics of Oil Recovery, Rørøs, Norway, June 7-10. 1994.

88 Matthews, C.S., Brons, F. and Hazebroek, P.:"A Method for Determination of Average Pressure in Bounded Reservoir," Trans. AIME, 1954, 182-191.

89 Martin and Wegner

90 Miller, C.C., Dyes, A.B. and Hutchinson, C.A., Jr.:"The Estimation of Permeability and Reservoir Pressure from Bottom Hole Pressure Build-up Characteristics," Trans. AIME, 1950, 189, 91-104.

91 Mlacnik M.J. and Heinemann Z.E. (2001): "Using Well Windows in Full Field Reservoir Simulation". SPE 66371, paper presented at the SPE Reservoir Simulation Symposium held in Houston, Texas, 11-14 February 2001.

92 Mlacnik M.J., Harrer A. and Heinemann G.F. (2001): "State-of-the-Art in the Windowing Technique". PAPER 2001-03, paper presented at the Petroleum Society's Canadian International Petroleum Conference 2001, Calgary, Alberta, June 12 - 14, 2001.

93 Mrosovsky, I. and Ridings, R.L.:"Two-Dimensional Radial Treatment of Wells within a Three-Dimensional Reservoir Model," SPEJ, April 1974, 127-131.

94 Muskat, M.:"The Flow of Homogeneous Fluids through Porous Media," McGraw-Hill Book Co., New York City (1937); reprint edition, International Human Resources Development Corp., Boston (1982).

95 Nacul E.C., Lepretre C. et al., (1990): "Efficient Use of Domain Decomposition and Local Grid Refinement in Reservoir Simulation", SPE 20740, 65th Annual Conference and Exhibition of the Society of Petroleum Engineers, New Orleans.

96 Nghiem, L.X.: "An Integral Approach for Discretizing the Reservoir Fluid Equations," SPERE (May 1988) 685-690.

97 Odeh,A. and Babu,D.:"Transient Flow Behavior of Horizontal Wells: Pressure Drawdown and Buildup Analysis," SPE Formation Evaluation, March 1990, pp. 7-15.

98 Palagi, C. and Aziz, K.:"A Dual Timestepping Technique for Simulating Tracer Flow," Unsolicited Paper, SPE 24220, September 1991.

99 Palagi, C.L., Aziz, K.:"The Modelling of Vertical and Horizontal Wells with Voronoi Grid," Paper presented at Western Regional Meeting, California, March 1992, 435-452.

100 Patgawkar, A., Shinkhare, D., Mahapatra, S., Gopalsamy, S. and Mudur, S.P.: "Tetrahedral Discretization of Complex Volumetric Spaces". National Center for Software Technology, India.

101 Peaceman, D.W.: Fundamentals of Numerical Reservoir Simulation, Elsevier Scientific Publishing Company, 1977.

102 Peaceman, D.W.:"Interpretation of Well-block Pressures in Numerical Reservoir Simulation," SPEJ, June 1978, 183-194.

103 Peaceman, D.W.: "Interpretation of Well-Block Pressures in Numerical Reservoir Simulation. Part 3: Some Additional Well Geometries" paper SPE 16976 presented at SPE Annual Technical Conference, Dallas, TX.,27-30 Sept. 1987.

104 Peaceman, D.W.:"Interpretation of Well-block Pressures in Numerical Reservoir Simulation with Nonsquare Grid Blocks and Anisotropic Permeability," SPEJ, June 1983, 531-543.

105 Peaceman, D.W.:"Representation of a Horizontal Well in Numerical Reservoir Simulation," Paper presented at 11th. SPE Symposium on Reservoir Simulation, California, February 1991, 153-162.

106 Pedrosa, Jr., O.A. and Aziz, K. "Use of Hybrid Grid in Reservoir Simulation," SPERE (Nov. 1986) 611-621.

107 Peery, J.H. and Herron, E.H.: "Three-Phase Reservoir Simulation," JPT **21** (1969), p.211-220., Trans AIME **246**, p.211-220.

108 Peneloux, A., Rauzy, E. and Freze R.: "A Consistent Correction for Redlich-Kwong-Soave Volumes," Fluid Phase Equilibria (1982) 7-23.

109 Peng, D.Y. and Robinson, D.B.: "A New Two-Constant Equation of State," Ind. Eng. Chem. Fund. (1976) 59-64.

110 Perrine, R.L.: "The Development of Stability Theory for Miscible Liquid-Liquid Displacement," SPEJ, March 1961, p.17-25.

111 Petterson, O.: "Building, Mapping, and History Matching very large and Complex Grids - with examples from the Gullfaks Field", paper presented at the 1994 Fourth European Conference on the Mathematics of Oil Recovery, Rørøs, Norway, June 7-10.

112 Pointing, D.K.: "Corner Point Geometry in Reservoir Simulation," Mathematics of Oil Recovery, King, P.R.(ed) Oxford, 1992.

113 Puchyr, P.J.:"A Numerical Well Test Model," Paper presented at the SPE Rocky Mountain Regional Meeting held in Denver, Colorado, April 1991, 125-139.

114 Quandalle P., Besset P.: "The Use of Flexible Gridding for Improved Reservoir Modeling", SPE

12238, presented at the 1983 SPE Symposium on Reservoir Simulation, San Francisco, Nov. 15-18.

115 Reid, R.C., Prausnitz, J.M. and Poling, B.E.: The Properties of Gases and Liquids, 4th Edition, McGraw-Hill Inc., New York (1987).

116 Rozon, B.J.:"A Generalized Finite Volume Discretization Method for Reservoir Simulation", paper SPE 20744 presented 1989 at the 10th SPE Symposium on Reservoir Simulation, Huston, Feb.6-8.

117 Schwarz, H.A.: “Über einige Abbildungsaufgaben,” Gesammelte Mathematische Abhandlungen (Nov. 1889) 65-83.

118 Sharpe, H.N. and Ramesh, B.A.:”Development and Validation of a Modified Well Model Equation for Nonuniform Grids with Application to Horizontal Well and Coning Problems,” Paper presented at the 67th Annual Technical Conference and Exhibition of SPE held in Washington, DC, October 4-7, 1992.

119 Shiralkar, G.S.:”Calculating of Flowing Well Pressures in Reservoir Simulation Using Nine-point Differencing,” Journal of Canadian Petroleum Technology, November-December 1989, 73-82.

120 Snyder, L.J.: "two-Phase Reservoir Flow Calculation," SPEJ 9. (1969) p.170-182.

121 Soave, G.: “Equilibrium Constants from a Modified Redlich-Kwong Equation of State,” Chem. Eng. Sci. (1972) 1197-1203.

122 Søreide,I.: “Improved Phase Behavior Prediction of Petroleum Reservoir Fluids From a Cubic Equation of State,” Dr.Ing. thesis, IPT Report 1989:4, Norwegian Institute of Technology, Department of Petroleum Engineering and Applied Geophysics (1989).

123 Stiel, L.I. and Thodos G.: “The Viscosity of Polar Substances in the Dense Gaseous and Liquid Regions,” AIChE J. (Mar. 1964) 275-277.

124 Van Poolen, H.K., Breitenbach, E.A. and Thurnau, D.H.:”Treatment of Individual Wells and Grids in Reservoir Modelling,” SPEJ, December 1968, 341-346.

125 Verma, S.: "Flexible Grids for Reservoir Simulation," Ph.D. Dissertation, Departement of petroleum Engineering,Stanford University, Palo Alto, California, USA, June 1996.

126 Verma, S. and Aziz, K.: “A Control Volume Schema for Flexible Grids is Reservoir Simulation,” paper SPE 37999 presented at 1997 SPE Symposium on Reservoir Simulation, Dallas, TX, June 6-8.

127 von Rosenberg D.W.: “Local Grid Refinement for Finite Difference Networks”, SPE 10974, presented at the 1982 SPE Technical Conference and Exhibition, New Orleans, Sept. 26-29.

128 Wadsley

129 Watson, D.F.: “Computing the N-dimensional Delaunay Tesselation with Application to Voronoi Polytopes”, Computer Journal, **24**, 167-172,1981.

130 Williamson, A.S. and Chappelear, J.E.:”Representing Wells in Numerical Reservoir Simulation: Part 1- Theory, Part 2- Implementation,” SPEJ, June 1981.

131 Whitson, C.H., and Michelsen, M.L.: "The Negative Flash," Fluid Phase Equilibria, 53 (1989)

51-71.

132 Yanosik, L.J. and McCracken, T.A.: "A Nine-Point, Finite Difference Reservoir Simulator for Realistic Prediction of Adverse Mobility Ratio Displacements," SPEJ (Aug.1979) 253-62; Trans., AIME, **267**.

133 Yielding,G., Freeman, B. and Needham, D.T.: “Quantitative Fault Seal Prediction,” American Association of Petroleum Geologists Bulletin, **81**, 897-917 (1997).

134 Yortsos, Y.C. and Huang, A.B.. Linear Stability Analysis of Immiscible Displacement," SPERE, (July 1986), p.378-390.

135 Young, L.C.: " Rigorous Treatment of Distorted Grids in 3D", paper SPE 51899 presented at 1999 SPE Symposium on Reservoir Simulation, Huston, TX, Febr. 14-17.